

**AES/TGP/10-44 Exergy analysis of the use of geothermal energy and carbon capture, transportation and storage in underground aquifers**

**23-12-2010 J.W.C. de Mooij**

# Exergy analysis of the use of geothermal energy and carbon capture, transportation and storage in underground aquifers

Jonathan W.C. de Mooij

1250388

M.Sc. Thesis

December 2010

Faculty of Civil Engineering and Geosciences  
Department of Applied Earth Sciences  
Section for Applied Geophysics and Petrophysics



#### Disclaimer

The results and maps in this report are based on local and regional geological mapping of the West Netherlands Basin. The results and maps in this report have been carefully compiled. Nonetheless the presented results may contain incomplete, incorrect information. The results and maps were generated by a modelling study of geological parameters of the studied aquifers. Therefore, the results and maps of this report should only be used for regional geological evaluations and optimization discussion. The results and maps in this report should not be used for local geothermal studies and commercial purposes. Furthermore, advances in knowledge and new data may cause some results and maps to become out of date. TU Delft and DAP claim to be not responsible for any eventual errors or other consequences resulting from the use of the results, model and maps in this report.

Title : Exergy analysis of the use of geothermal energy and carbon capture, transportation and storage in underground aquifers

Author : J.W.C. de Mooij

Date : 23rd of December 2010

Supervisor(s) : Dr. K.H.A.A. Wolf  
Ali Akbar Eftekhari  
Prof. Dr. J. Bruining

TA Report Number : AES/TGP/10-44

Postal Address : Section for Applied Geophysics and Petrophysics  
Department of Applied Earth Sciences  
Delft University of Technology  
P.O. Box 5028  
The Netherlands

Telephone : (+31) 15 2781328 (secretary)

Telefax : (+31) 15 2781189

Copyright ©2010 Section for Applied Geophysics and Petrophysics

All rights reserved.  
No parts of this publication may be reproduced,  
Stored in a retrieval system, or transmitted,  
In any form or by any means, electronic,  
Mechanical, photocopying, recording, or otherwise,  
Without the prior written permission of the  
Section for Applied Geophysics and Petrophysics

## Abstract

At the moment global climate change is one of the most prominent environmental and energy issues of our life time. Currently CO<sub>2</sub> levels in the atmosphere stand at 387 ppm, almost 40% higher since the start of the industrial revolution and the highest for at least the last 650,000 years. About 96% of these carbon emissions are the result of using fossil fuels. Another problem is that the fossil fuel reserves will be exhausted within 200 years and the nuclear energy within 260 years. Something has to be done to stop the addition of fossil fuels and carbon dioxide emissions! However investing in renewable energy is still expensive but high energy prices, CO<sub>2</sub> emissions, rising temperatures, fossil fuels depletion and the demand to be less dependent on other countries makes it more and more attractive to invest in renewable energy, like solar energy, wind energy, biomass, geothermal energy, tidal power and hydro power. Not all renewable energy sources are suitable in the Netherlands. Geothermal energy, still unknown by a lot of people, has a very good potential to succeed in the Netherlands. The average temperature of the Dutch subsurface at a depth of 2,000 meters is around 75 – 80 °C. This energy is very suitable to heat houses, afterwards the rest heat can be used to heat low heat demanding facilities like swimming pools and greenhouses. In spite of the good potential, geothermal energy is still used on a small time scale in the Netherlands. Hopefully DAP can make a change in this by making more people aware that geothermal energy has a great potential for the Netherlands. The Netherlands has a geothermal potential of 90,000 PJ in heat. The benefits of geothermal energy are that it is clean and available 24 hours a day, 365 days a year. Also geothermal power plants have average availabilities of 90% or higher, compared to 75% for coal power plants. The greenhouse gas emissions of the geothermal plants are only 91 gCO<sub>2</sub>/kWh, this is very low compared to other fuels.

The annual Dutch CO<sub>2</sub> emission is nearly 180 Mt CO<sub>2</sub> at present, of which approximately 100 Mt CO<sub>2</sub>/year emitted by the energy and manufacturing industry. The biggest emitters are large point sources like the power generation sector and large energy-consuming industries like oil and gas processing, iron and steel, cement and chemicals production. CCS can lower the emissions from the large point sources by capturing the carbon dioxide. CCS is not a new technology, this proven technique is already used for nearly 100 years for industrial purposes or to increase oil or gas production. CCS technology can reduce carbon dioxide emissions from large industrial sources and coal-fired power stations by approximately 85 - 90% depending on the used type of capture technology. Also transportation of CO<sub>2</sub> is not a new technology in the Netherlands because there is already a pipeline of 85 km from the Shell refinery in Pernis to greenhouses in the Westland area. However, large-scale CCS will require a new transportation infrastructure to link sources and sinks. In densely populated countries such as the Netherlands this can become a considerable challenge, think of Barendrecht. Even though the Netherlands has a very good storage potential there is a spatial mismatch between CO<sub>2</sub> sources and sinks.

When a new energy source is discovered the first and most important thing to know is how much energy (quantity) can be extracted from this source. But what we really need to know is the work potential (quality) of this energy source, in our case a geothermal well beneath the TU Delft. Work potential is the amount of energy which can be extracted as useful work, this property is called exergy. The maximum available power from the DAP geothermal reservoir is 0.66 MW and is obtained at a flow rate of 180 m<sup>3</sup>. It is not smart to increase the production rate above 200 m<sup>3</sup> because the losses are increasing faster than the extra gained exergy. The invested energy in materials and drilling are minor compared to the energy needed for capture and compression. Over 94% of the total energy demand is needed to capture the CO<sub>2</sub> over a life-time of 30 years.

## Acknowledgements

This report is the result of a 10 month master thesis project concluding my masters program 'Sustainable Energy Technology' at the Delft University of Technology. I chose to specialize in geothermal energy combined with carbon capture and storage, because this combination could be an important sustainable energy technology. These two subjects were relatively new to me because there were no core courses about these topics in my masters program. This made the project in the beginning sometimes very tough due to my lack of knowledge in geology, drilling etc. I was given a lot of freedom to work on my own and do other things, like already following some courses of my second master and also being a member of the Faculty Student Council of Applied Sciences. That is why it took me 16 months to finish this project. However, it goes without saying that I could not perform this work without help from others.

In the first place I would like to thank Karl-Heinz Wolf for giving me the opportunity to perform my master thesis in the Department of Geotechnology. Also I would like to thank Professor Hans Bruining for being my supervisor. Special thanks goes to Ali Akbar Eftekhari for the discussions we had and the calculations we did. Finally I want to thank Douglas Gilding and other people from DAP helping me when I had questions.

The Delft Geothermal Project (DAP) was started in 2007 by students, alumni and staff of the Department of Applied Earth Sciences. The basic idea is to develop an innovative geothermal system, with the objectives to provide sustainable heating for the Delft University of Technology, to demonstrate novel technologies reducing the cost of geothermal systems, to investigate options for co-injection of CO<sub>2</sub>, and to generate new research opportunities. Contributing to this project was a great honour and I would like to thank everybody for the pleasant cooperation.

DAP is under performance with the financial support of the Ministry of Economic Affairs, Energiebeheer Nederland (EBN), Eneco Energy, Dutch State Mines (DSM), Wintershall Noordzee, Nederlandse Aardolie Maatschappij (NAM), PGMI, WEP, Acquit, IF Technology, Panterra, the Province of Zuid-Holland and TNO, and is hosted and supported by Delft University of Technology.

DAP is one of the participants in the CATO-2 program. CATO-2 is a Dutch national R&D program for CO<sub>2</sub> capture, transportation and storage. CATO-2 gave me financial support to write a paper with Karl-Heinz Wolf about geothermal energy and CCS. I am proud that this topic of research is a contribution to the CATO-2 program, work package 3.5.

At last I want to thank my family and close friends who always supported me. In the end it resulted in a thesis I can be really proud of.

## Content

<b>ABSTRACT</b> .....	<b>4</b>
<b>ACKNOWLEDGEMENTS</b> .....	<b>5</b>
<b>LIST OF FIGURES</b> .....	<b>9</b>
<b>LIST OF TABLES</b> .....	<b>10</b>
<b>LIST OF ABBREVIATIONS</b> .....	<b>11</b>
<b>NOMENCLATURE</b> .....	<b>12</b>
<b>1 INTRODUCTION</b> .....	<b>13</b>
<b>2 GEOTHERMAL ENERGY</b> .....	<b>16</b>
2.1 Geological background.....	17
2.2 Utilization of geothermal resources.....	18
2.3 CO <sub>2</sub> emission Geothermal Energy.....	18
2.4 Geothermal Energy in The Netherlands .....	19
2.5 Delft University of Technology location .....	20
2.6 Geological setting.....	20
2.7 Temperature Gradient.....	20
2.8 Reservoir Properties .....	20
<b>3 CARBON CAPTURE AND STORAGE (CCS)</b> .....	<b>22</b>
3.1 What is CCS?.....	22
3.2 Environmental effects .....	22
3.3 Risk of CCS .....	22
<b>4 CO<sub>2</sub> SOURCES</b> .....	<b>23</b>
<b>5 CO<sub>2</sub> CAPTURE</b> .....	<b>24</b>
5.1 CO <sub>2</sub> capture systems.....	24
5.2 CO <sub>2</sub> Capture Technologies .....	24
5.3 Energy Penalty / Emission factor.....	24
<b>6 CO<sub>2</sub> TRANSPORT</b> .....	<b>25</b>
6.1 Pipeline.....	25
6.2 Ship.....	25
<b>7 CO<sub>2</sub> STORAGE</b> .....	<b>26</b>
7.1 Potential storage sites within the Netherlands .....	27
<b>8 EXERGY ANALYSIS</b> .....	<b>28</b>
8.1 Energy invested into materials for the wells .....	29
8.1.1 Energy invested to produce the steel casing.....	29
8.1.2 Energy invested to produce cement.....	30
8.2 Energy invested in drilling the geothermal doublet .....	31
8.3 Energy demand for CO <sub>2</sub> capture.....	32

8.4	Energy demand for CO <sub>2</sub> compression .....	32
8.5	Energy invested in CO <sub>2</sub> transportation .....	33
8.6	Total invested energy .....	33
8.7	Exergy production by geothermal well.....	34
8.8	Power loss along the wells .....	35
8.9	Power loss in the reservoir .....	36
8.10	Determination of the optimal flow rate .....	38
8.11	Energy payback time .....	40
<b>9</b>	<b>CO<sub>2</sub> EMISSION .....</b>	<b>41</b>
9.1	CO <sub>2</sub> Emission during the production of steel pipes.....	41
9.1.1	Total CO <sub>2</sub> emission for the production and placing of steel pipes.....	42
9.2	CO <sub>2</sub> Emission during the production of cement.....	42
9.3	CO <sub>2</sub> Emission during drilling .....	43
9.4	CO <sub>2</sub> Emission during CO <sub>2</sub> capture .....	43
9.5	CO <sub>2</sub> Emission during CO <sub>2</sub> compression .....	43
9.6	CO <sub>2</sub> Emission avoided by geothermal energy.....	43
9.7	Total CO <sub>2</sub> emission over 30 years of operation .....	43
<b>10</b>	<b>CONCLUSION .....</b>	<b>45</b>
<b>11</b>	<b>RECOMMENDATIONS AND FUTURE WORK .....</b>	<b>46</b>
	<b>REFERENCES.....</b>	<b>47</b>
	<b>APPENDIX .....</b>	<b>53</b>
	<b>LIST OF FIGURES APPENDIX.....</b>	<b>54</b>
	<b>LIST OF TABLES APPENDIX.....</b>	<b>55</b>
<b>APPENDIX A:</b>	<b>ARTICLE GUARDIAN .....</b>	<b>56</b>
<b>APPENDIX B:</b>	<b>CHAPTER 3: CARBON CAPTURE AND STORAGE (CCS).....</b>	<b>57</b>
<b>APPENDIX C:</b>	<b>CHAPTER 4: CO<sub>2</sub> SOURCES .....</b>	<b>60</b>
<b>APPENDIX D:</b>	<b>CHAPTER 5: CO<sub>2</sub> CAPTURE .....</b>	<b>63</b>
<b>APPENDIX E:</b>	<b>CHAPTER 6: CO<sub>2</sub> TRANSPORT.....</b>	<b>73</b>
<b>APPENDIX F:</b>	<b>CHAPTER 7: CO<sub>2</sub> STORAGE.....</b>	<b>77</b>
<b>APPENDIX G:</b>	<b>EXERGY PRODUCTION (ALL STEPS) .....</b>	<b>84</b>
<b>APPENDIX H:</b>	<b>PARAGRAPH 9.1 AND 9.2 .....</b>	<b>87</b>
<b>APPENDIX I:</b>	<b>CONVERSION FACTORS .....</b>	<b>97</b>
<b>APPENDIX J:</b>	<b>ENERGY DENSITY .....</b>	<b>98</b>
<b>APPENDIX K:</b>	<b>CO<sub>2</sub> EMISSION FACTORS.....</b>	<b>99</b>
<b>APPENDIX L:</b>	<b>ELECTRICITY EMISSION FACTORS.....</b>	<b>101</b>
<b>APPENDIX M:</b>	<b>LAY-OUT DRILLING RIG (OIL RIG NT8).....</b>	<b>102</b>
<b>APPENDIX N:</b>	<b>CALCULATION OF THE WALL THICKNESS OF THE PIPE .....</b>	<b>103</b>

---

<b>APPENDIX O:</b>	<b>DRILLING FORMULAS .....</b>	<b>105</b>
<b>APPENDIX P:</b>	<b>COMPLETE EXERGY TABLE.....</b>	<b>107</b>
<b>APPENDIX Q:</b>	<b>FLOW CHART .....</b>	<b>109</b>

## List of Figures

Figure 1.1: Past and future CO <sub>2</sub> concentrations in the atmosphere .....	13
Figure 1.2: Demographic distribution and R/P-ratio of fossil fuels ( BP, June 2010) .....	13
Figure 1.3: World population prospects between 1950 – 2050 (Worldwatch Institute, 1992) .....	14
Figure 1.4: Relation between temperature and CO <sub>2</sub> over the past 450.000 years (UNEP GRIDA, 2008) .....	14
Figure 1.5: Schematic plan of combined geothermal heat production and CO <sub>2</sub> injection.....	15
Figure 2.1: Geothermal field (Dickson and Fanelli, 2004) .....	16
Figure 2.2: The Earth's crust, mantle, and core (Dickson and Fanelli, 2004) .....	17
Figure 2.3: Diagram showing the utilization of geothermal fluids (derived from Lindal, 1973).....	18
Figure 2.4: Comparison of CO <sub>2</sub> emissions from electricity generation (Bloomfield, 2003).....	18
Figure 2.5: Temperature map at a depth of 2000 meters (Lokhorst and Wong, 2007) .....	19
Figure 2.6: Graph of the porosity of the Delft Sandstone Member (Gilding, 2010) .....	21
Figure 2.7: Temperature map of the Delft subsurface (DAP website).....	21
Figure 3.1: CO <sub>2</sub> capture and storage from power plants.....	22
Figure 4.1: Emissions of CO <sub>2</sub> from fossil fuel use (2010) .....	23
Figure 5.1: Technology options for CO <sub>2</sub> separation and capture (Rao, A. and Rubin, E., 2002).....	24
Figure 7.1: Different types of storage options (Frost, 2008) .....	26
Figure 7.2: Storage availability in time (Damen et al., 2009).....	27
Figure 8.1: Classification of resources (Wall, 1987) .....	28
Figure 8.2: Casing drilling sequence with steel pipe (Leijnse, 2008) .....	29
Figure 8.3: Solubility CO <sub>2</sub> into water (Duan and Sun, 2003/2006) .....	32
Figure 8.4: Solubility of CO <sub>2</sub> into water @ 40 °C (Duan and Sun, 2003/2006) .....	32
Figure 8.5: Schematic overview how to extract heat from the geothermal reservoir.....	34
Figure 8.6: Friction factor - Reynolds number (Janssen and Warmoeskerken, 2001) .....	35
Figure 8.7: Effect of diameter on the power loss along the walls of the wells.....	36
Figure 8.8: Effect of permeability on the power loss in the reservoir.....	37
Figure 8.9: Available Exergy .....	38
Figure 8.10: Annual heat production compared with exergy. The pumping power is needed to generate .....	39
Figure 8.11: Energy Consumption (years) .....	40
Figure 8.12: Energy Consumption (months).....	40
Figure 9.1: Total CO <sub>2</sub> emissions for laying a pipeline .....	42
Figure 9.2: Total CO <sub>2</sub> emission over 30 years of operation .....	43
Figure 9.3: CO <sub>2</sub> emission within the first year of operation .....	44
Figure 9.4: CO <sub>2</sub> emission within the first year of operation (basic) .....	44

## List of Tables

Table 1.1: <i>Nomenclature</i> .....	12
Table 2.1: <i>Data of Delft subsurface (Gilding, 2010; Den Boer, 2008 and Smits, 2008)</i> .....	20
Table 4.1: <i>Purity of CO<sub>2</sub> sources (CO<sub>2</sub>NET, 2009)</i> .....	23
Table 7.1: <i>The worldwide capacity of potential CO<sub>2</sub> storage reservoirs (Herzog, 2004)</i> .....	26
Table 7.2: <i>Properties of CO<sub>2</sub> storage site (IPCC, 2005)</i> .....	27
Table 7.3: <i>Technical CO<sub>2</sub> storage potential in the Netherlands (Damen et al., 2009))</i> .....	27
Table 8.1: <i>The quality of some common energy forms (Wall, 1987)</i> .....	28
Table 8.2: <i>Steel Demand of injection pipe</i> .....	29
Table 8.3: <i>Steel Demand of production pipe</i> .....	29
Table 8.4: <i>Portland Cement Content</i> .....	30
Table 8.5: <i>Chemical exergy of Portland Cement</i> .....	30
Table 8.6: <i>Demand of cement for injection pipe</i> .....	31
Table 8.7: <i>Demand of cement for production pipe</i> .....	31
Table 8.8: <i>Power demand during CO<sub>2</sub> compression</i> .....	33
Table 8.9: <i>Total energy consumption over 10, 20 and 30 years life-time</i> .....	33
Table 8.10: <i>Parameters exergy calculations</i> .....	34
Table 8.11: <i>Available Exergy</i> .....	38
Table 8.12: <i>Exergy and heat production (thermal MW) as a function of flow rate (without losses)</i> .....	39
Table 9.1: <i>Energy consumption and CO<sub>2</sub> emissions in the steel industry in 1986 and 1994 (Kim et al, 2002)</i> .....	41
Table 9.2: <i>Total primary energy consumption and CO<sub>2</sub> emissions (global average) per ton of steel</i> .....	41
Table 9.3: <i>Total CO<sub>2</sub> emissions for laying a pipeline</i> .....	42

## List of Abbreviations

CCS	Carbon Capture and Storage
CH <sub>4</sub>	Methane
CO <sub>2</sub>	Carbon Dioxide
CO	Carbon Monoxide
DAP	Delft Aardwarmte Project
DEA	Diethanolamine
DGA	Diglycolamine
DIPA	Diisopropanolamine
ECBM	Enhanced Coal Bed Methane recovery
EOR	Enhanced Oil Recovery
Fe	Iron
GHG	Greenhouse Gas
H <sub>2</sub>	Hydrogen
H <sub>2</sub> S	Hydrogen Sulfide
IEA	International Energy Agency
IGCC	Integrated Gasification Combined Cycle
IPCC	Intergovernmental Panel on Climate Change
LCA	Life Cycle Analysis
MDEA	Methyldiethanolamine
MEA	Monoethanolamine
Mg	Magnesium
MJ	Mega Joule
N <sub>2</sub>	Nitrogen
NGCC	Natural Gas fired Combined Cycles
O <sub>2</sub>	Oxygen
PC	Pulverized Coal plants
PJ	Peta Joule
PPM	Parts Per Million
PPMV	Parts Per Million Volume
PPB	Parts Per Billion
SOFC	Solid Oxide Fuel Cells
TEA	Triethanolamine
TNO	Toegepast Natuurwetenschappelijk Onderzoek
TU Delft	University of Technology Delft

## Nomenclature

Table 1.1 shows a list of the nomenclature which is used within this thesis.

**Table 1.1: Nomenclature**

Symbol	Name	Unit
<b>C</b>	Specific heat capacity	J/(kg·K)
<b>C<sub>p</sub></b>	Water heat capacity at constant pressure	J/(kg·K)
<b>D</b>	Tubing inner diameter	m
<b>E</b>	Energy	J
<b>Ex</b>	Exergy	J
<b>G</b>	Gravity	m/s <sup>2</sup>
<b>K</b>	Permeability	mD
<b>K<sub>D</sub></b>	Absolute permeability of Delft formation	mD (10 <sup>-15</sup> m <sup>2</sup> )
<b>L<sub>t</sub></b>	Tubing length	m
<b>L<sub>w</sub></b>	Distance between production and injection well	m
<b>P</b>	Density	kg/m <sup>3</sup>
<b>Q</b>	Flow rate	m <sup>3</sup> /hour
<b>t</b>	Time	s
<b>T</b>	Temperature	K or °C
<b>T<sub>0</sub></b>	Ambient temperature	K
<b>T<sub>1</sub></b>	Injected water temperature	K
<b>T<sub>2</sub></b>	Produced water temperature	K
<b>U</b>	Darcy velocity	m/s
<b>V</b>	Velocity	m/s
<b>W</b>	Reservoir width	m
<b>δ</b>	Thickness of the production interval	m
<b>δ<sub>D</sub></b>	Thickness of Delft formation	m
<b>f</b>	Friction factor	-
<b>η</b>	Efficiency	-
<b>Φ</b>	Porosity	-
<b>μ</b>	Viscosity	Pa·s
<b>μ<sub>w</sub></b>	Viscosity (Water)	Pa·s
<b>ρ<sub>w</sub></b>	Density (Water)	kg/m <sup>3</sup>
<b>ρ<sub>s</sub></b>	Density (Steel)	kg/m <sup>3</sup>
<b>ρ<sub>c</sub></b>	Density (Cement)	kg/m <sup>3</sup>
<b>Subscripts</b>		
<b>Eq</b>	Equivalent	
<b>I</b>	Injected	
<b>O</b>	Initial / virgin	
<b>R</b>	Rock	
<b>W</b>	Water	

# 1 Introduction

At the moment global climate change is one of the most prominent environmental and energy issues of our life time (Anderson, 2004). Since the start of the industrial revolution the CO<sub>2</sub> content in de atmosphere increased rapidly, see Figure 1.1 (Left: Earth System Research Laboratory, Right: United Nations Environment Programme (UNEP)). The increasing use of fossil fuels to meet energy needs has led to higher carbon dioxide (CO<sub>2</sub>) emissions into the atmosphere. It is widely accepted that, whereas the CO<sub>2</sub> concentration was about 280 ppm before the industrial revolution, it increased from 315 ppmv in 1950 to 355 ppmv in 1990 (Gupta and Fran, 2002). Scientists at the Mauna Loa observatory in the US state of Hawaii say that CO<sub>2</sub> levels in the atmosphere now stand at 387 parts per million (ppm), up almost 40% since the industrial revolution and the highest for at least the last 650,000 years (Guardian, 2008). About 96% of these carbon emissions resulted from using fossil fuels (US Environmental Protection Agency, 2002).

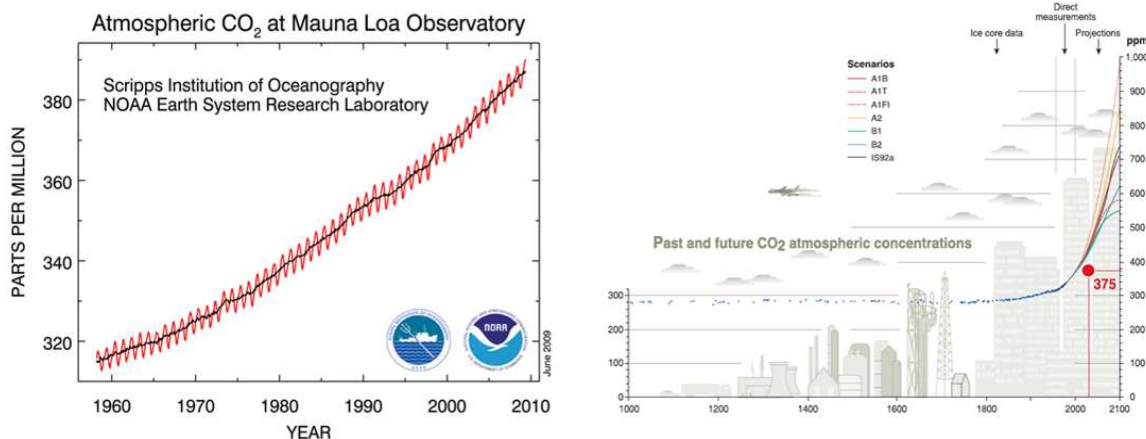


Figure 1.1: Past and future CO<sub>2</sub> concentrations in the atmosphere

This is mainly caused by the growth of the world population and its associated economic growth. People are becoming richer and richer which causes an increasing demand in primary energy sources. Fossil fuels and nuclear power are the main sources of energy in today's energy system and they supply round 80% of the energy demand (BP, 2009). Under the assumption that the population of mankind does not change drastically and that they will consume energy at the current level, the fossil fuel reserves will be exhausted within 200 years and the nuclear energy within 260 years (Zeeman, 2009). According to BP Statistical Review of World Energy 2010 the R/P-ratio of oil is 45.7, natural gas 62.8 and coal 119. These numbers carry an uncertainty factor of two, i.e., the true reserves may be twice as large and we also learned that the real reserves of coal are probably considerably larger than the proved reserves of 150 years, most likely more than 200 years and possibly closer to 300 years. This will look like a very long time, but when we compare this period of time to the time span of existence of the earth or human civilization, it is a negligible fraction of time. We have to be aware that the reserves of fossil fuels on the earth are limited and will be exhausted.

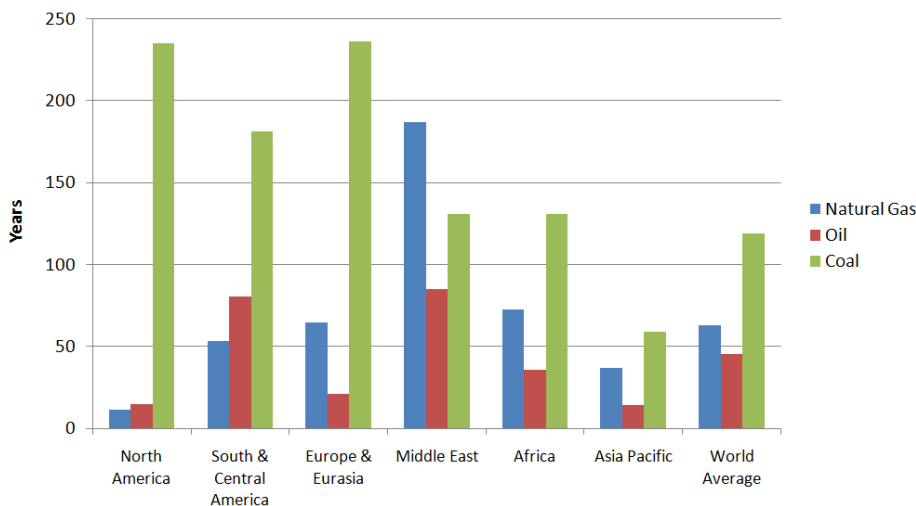


Figure 1.2: Demographic distribution and R/P-ratio of fossil fuels (BP, June 2010)

It is expected that the world population will grow and will reach 10 billion in 2050 with medium growth (see Figure 1.3). In order to provide the growing population with high living standards, further economic development is essential. Economic development requires more energy, this extra demand of energy has to come from additional energy sources next to the traditional ones.

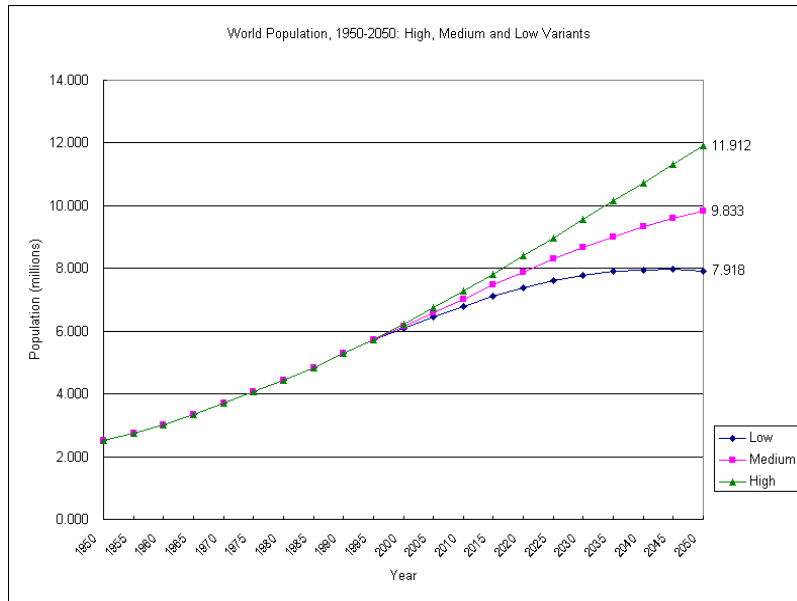


Figure 1.3: World population prospects between 1950 – 2050 (Worldwatch Institute, 1992)

Already today most of countries have not enough installed capacity to keep up with the daily demand. For example the energy demand in China and India is growing so fast that they have an energy problem during peak demands. The increase in the world-wide demand for energy, in combination with other oil-related events, like the Iraq crisis and the Gulf Hurricane, made the oil price rise to around 140 Dollar per barrel Brent light in July 2008. In addition, the gas price is coupled to the oil price.

Even though it is still a subject for discussion, it is widely believed that the human contribution to the increase of CO<sub>2</sub> in the atmosphere is one of the main causes of temperature rise (Figure 1.4). Climate change model projections summarized in the latest IPCC report indicate that global surface temperature will probably rise a further 1.1 to 6.4 °C during the twenty-first century (IPCC, 2007). Increase in temperature will cause sea-level rise, change of vegetation, increase of deserts, more droughts and flooding etc. A solution is to use less fossil fuels and more renewables. But before we have enough installed capacity in renewables to provided the world energy demand, we have to find other ways to get enough energy and minimize the CO<sub>2</sub> emission. One way is to improve the power plants to get higher efficiencies but this still doesn't solve the CO<sub>2</sub> emission problem. Since a few years governments introduced CO<sub>2</sub> emission rights and opened an emission trade to stimulate the reduction of CO<sub>2</sub> emission. A way to reduce the emission is to capture, transport and store the CO<sub>2</sub> underground in empty gas fields and aquifers.

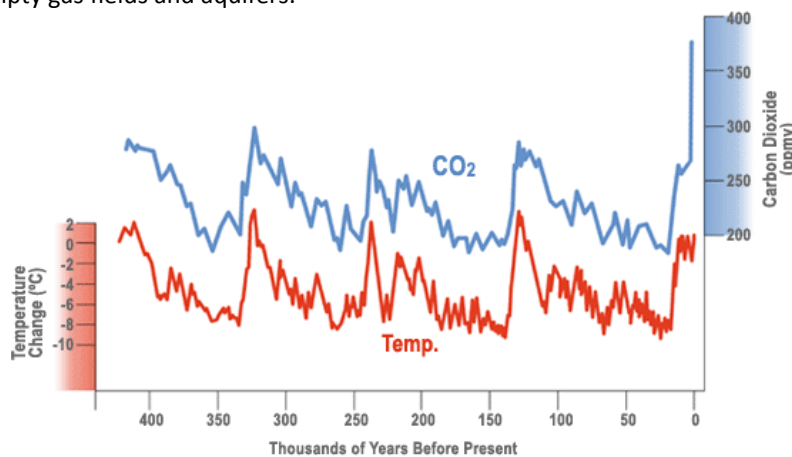


Figure 1.4: Relation between temperature and CO<sub>2</sub> over the past 450.000 years (UNEP GRIDA, 2008)

High energy prices, CO<sub>2</sub> emissions, rising temperatures, fossil fuels depletion and the feeling to be less dependent on other countries make it more and more attractive to invest in renewable energy, like solar energy, wind energy, biomass, geothermal energy, tidal power and hydro power. At the moment the price of these renewables are too high and are not yet competitive with fossil fuels. But this will change in the future when fossil fuels are becoming more expensive and/or renewables are becoming cheaper and have a higher efficiency. Also severe fluctuations of the oil price can be an important factor to switch over to renewables. In 2006, about 18% of global final energy consumption came from renewables, with 13% coming from traditional biomass, such as wood-burning (REN21, 2007). Investing in renewables is a very important issue at the moment because of the environmental concern of global warming.

These conditions motivated Students of Delft University, Department of Applied Earth Sciences to launch a project that combines the production of geothermal energy and CO<sub>2</sub> storage. The project is called “Delft Aardwarmte Project” (DAP). Geothermal energy is an effective way to improve sustainability and diversification of energy production. Comparing geothermal energy with other sustainable energy sources, geothermal energy has some advantages. Geothermal energy is always available and this source is not affected by external factors like for example clouds. Without wind a windmill will not produce energy and at night a PV solar cell will not generate electricity. Furthermore, it is 100 % clean (excluding production); i.e. there is no emission of CO<sub>2</sub> during usage or skyline destruction. Geothermal energy is providing a source of “unlimited” energy, since the earth is constantly releasing heat to its crust (Beardsmore, 2001).

The objective of the Delft Geothermal Project (DAP) is to produce geothermal energy from hot water from the subsurface. The system consists of two wells and is called a geothermal doublet. One well is used to produce hot water (75 – 80 °C) from a depth of approximately 2.5 kilometers. This water is transported to the surface and pumped through a heat exchanger, after which the extracted energy is used for heating purposes. After passing the heat exchanger, CO<sub>2</sub> is dissolved in the now “cold” water (40°C) and is reinjected through a second well. Figure 1.5 shows a schematic overview of the situation. The hot water is going to be recovered from the Delft Sandstone Formation, which is present in the underground of the TU Delft campus (DAP, 2008).

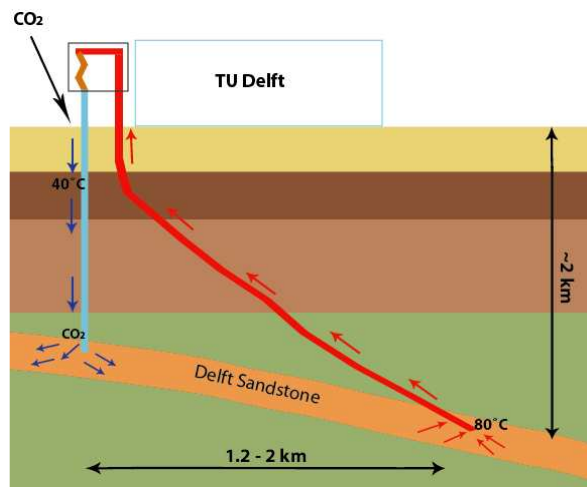


Figure 1.5: Schematic plan of combined geothermal heat production and CO<sub>2</sub> injection

The objectives of this study are:

- (1) to make an exergy analysis of the whole geothermal system with co-injection of CO<sub>2</sub>,
- (2) to find the optimal flow rate of the produced heat and minimize the losses,
- (3) to estimate CO<sub>2</sub> injection scenarios
- (4) to find the “energy pay-back time”.

This study will result in new insights and a better understanding of geothermal energy, carbon capture and storage (CCS) and exergy analysis. The first chapters describe what geothermal energy, CCS, CO<sub>2</sub> sources, CO<sub>2</sub> capture, CO<sub>2</sub> transport and CO<sub>2</sub> storage is and explain the basics. The following two chapters (8 and 9) will discuss the performed calculations. Chapter 8 shows the exergy analysis, chapter 9 shows the calculation of the total emitted CO<sub>2</sub> during the construction process and production process of geothermal heat. This report ends with a conclusion and recommendations. Note that this thesis does not contain financial calculations, all investments are in energy terms.

## 2 Geothermal Energy

Geothermal energy is the energy contained as heat in the earth's interior. The benefits of geothermal energy are that it is clean and available 24 hours a day, 365 days a year. Also geothermal power plants have average availabilities of 90% or higher, compared to 75% for coal power plants (US Department of Energy, 2006). Geothermal energy originates from the original formation of the planet, from radioactive decay of minerals, and from solar energy absorbed at the surface. The earth contains huge amounts of this heat but this heat source is not evenly distributed, seldom concentrated and often too deep to be exploited industrially (Barbier, 2002). The heat dissipates from the earth's interior towards the surface, the average geothermal gradient is 2.5 to 3°C/100 meters of depth (Dickson and Fanelli, 2004). According to Ecofys the average geothermal gradient in the Netherlands is 31°C/km (3.1°C/100 meters). This average is also supported by studies of Smits (2008), Grobbelen et al., (2009), and Simmelink et al., (2007). The temperature within the first few meters below ground level is around 10°C. This temperature corresponds to the mean external air temperature. So the temperature at a depth of 2000 meters will be around 75°C. (Dickson and Fanelli, 2004). But there are areas where the thermal gradient is much bigger, one of the reasons for this higher gradient occurs when there is a magma body very near the surface releasing heat. A carrier is needed for the extraction and utilization of heat and to transfer this heat towards accessible depths. Initially heat is transferred from depth to sub-surface regions by conduction and finally by convection with geothermal fluids (mainly rainwater). These fluids that penetrated into the Earth's crust from the recharge areas, have been heated on contact with the hot rocks, and have accumulated in aquifers. These aquifers (reservoirs) are the essential parts of most geothermal fields (Barbier, 2002). Figure 2.1 shows a geothermal field.

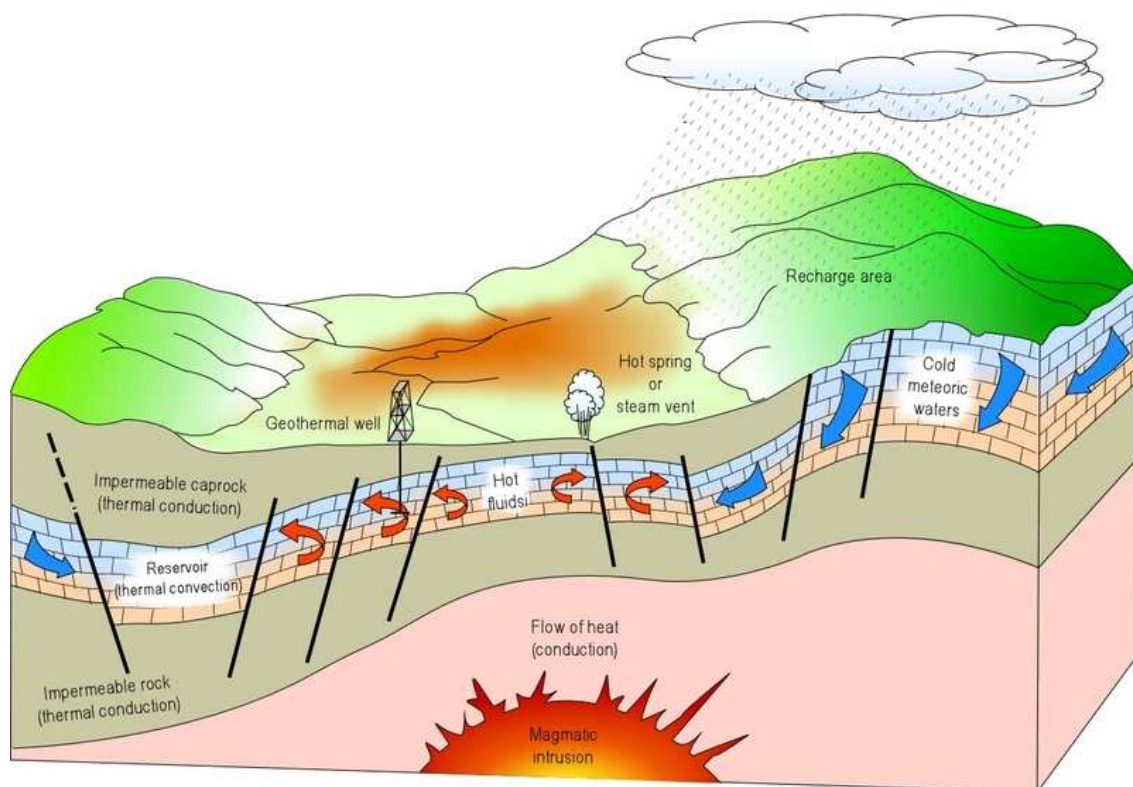


Figure 2.1: Geothermal field (Dickson and Fanelli, 2004)

As can be seen from Figure 2.1 the reservoir is situated between two impermeable rock plates. These plates prevent loss of heat and pressure. Depending on the hydrogeological situation and the temperature of the rocks present at the field, the field can produce superheated steam or steam mixed with liquid water, or only hot water. Wells are needed to extract the hot fluids from the reservoir (Barbier, 2002). The usage of these fluids depends on the temperature and pressure:

- Electricity generation (high-temperature fluids)
- Space heating, for example houses, and industrial processes (low-temperature fluids)

## 2.1 Geological background

From Figure 2.2 it can be seen that the earth consists of three concentric zones: crust, mantle and core. The top right of the figure shows a section through the crust and the uppermost mantle. The crust of the earth is relatively thin. The average thickness of the crust is about 20 – 65 km, under continents, and 7 km under the ocean. This is only a fraction compared to the total radius of the earth of 6370 km. The mantle lies between the core and crust of the earth and has a thickness of 2900 km. It is assumed that the mantle consists of ultrabasic rock such as peridotite, which is a heavy igneous rock made up chiefly of ferromagnesian silicate minerals. The earth's core extends from 2900 to 6370 km, so the thickness is 3470 km. The temperature in the core should be around 4000°C and the pressure at the earth's centre 3.6 million bar (360,000 MPa).

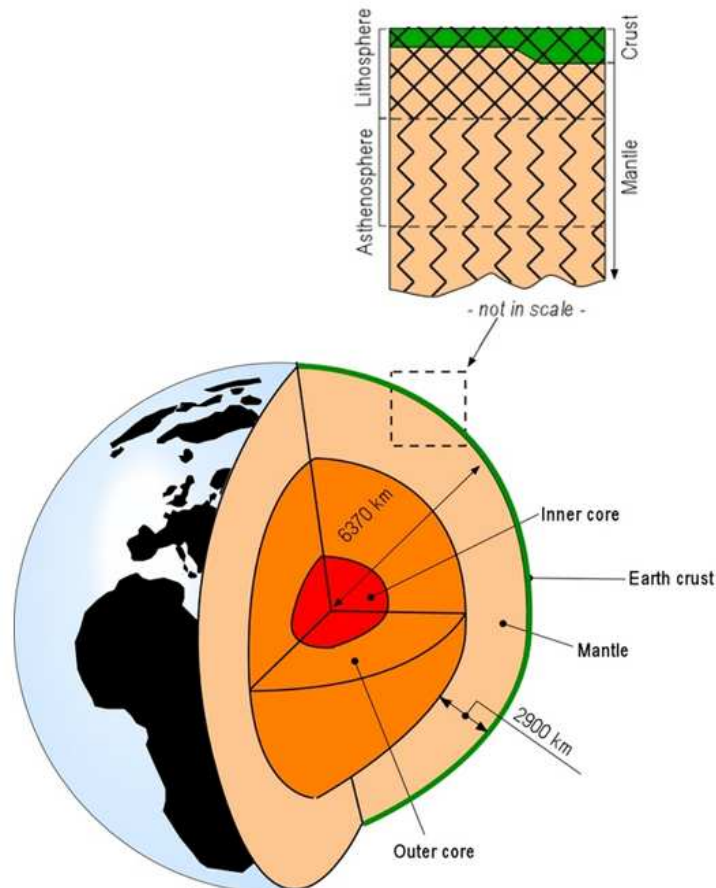


Figure 2.2: The Earth's crust, mantle, and core (Dickson and Fanelli, 2004)

According to Barbier (2002) and the US Department of Energy geothermal energy is generally cost-competitive with conventional sources of energy. With the present technology and economic factors geothermal wells have a depth usually up to a depth of 5 km. Once a geothermal region has been identified, a series of resource assessments will be made during the exploration and development process. As more data become available the resource assessment will become more certain. The main requirements for a good geothermal resource are:

- a high temperature for good power plant efficiency;
- a large quantity of stored heat for resource longevity;
- a low rate of liquid production per unit of energy (in case of electricity generation);
- reinjection well sites available;
- produced fluids with a near-neutral pH for low corrosion rates in wells and plants;
- adequate permeability to ensure adequate outputs from individual wells;
- a low tendency for scaling in pipelines and wells;
- low elevation and easy terrain for access roads;
- a low risk of vulcanicity and hydrothermal eruptions;
- proximity to electrical load or transmission lines.

## 2.2 Utilization of geothermal resources

Electricity generation is the most important form of utilization of high-temperature geothermal resources (> 150 °C). The medium-to-low temperature resources (< 150 °C) are suited for many different types of application. The classical Lindal diagram (Lindal, 1973), which shows the possible uses of geothermal fluids at different temperatures, still holds valid. Figure 2.3 is derived from the original Lindal diagram, with the addition of electricity generation from binary cycles. Fluids at temperatures below 20 °C are rarely used and in very particular conditions, or in heat pump applications. In the case of DAP and Ammerlaan (Ammerlaan is a greenhouse farmer situated at Pijnacker), the extracted heat can be used to heat a municipal swimming pool, for which a water temperature of 30 – 50 °C is required, or greenhouses, for which a temperature between 35 – 80 °C is required, see the Lindal diagram. The Lindal diagram emphasises two important aspects of the utilization of geothermal resources (Gudmundsson, 1988): (a) with cascading and combined uses it is possible to enhance the feasibility of geothermal projects and (b) the resource temperature may limit the possible uses. Existing designs for thermal processes can, however, be modified for geothermal fluid utilization in certain cases, thus widening its field of application.

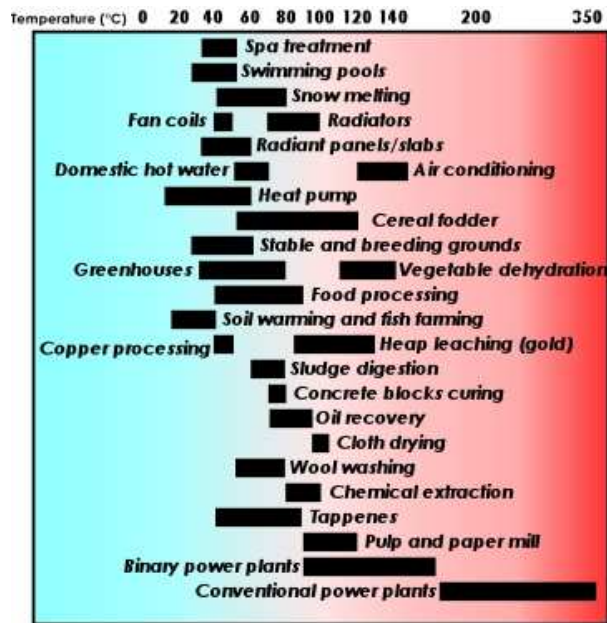


Figure 2.3: Diagram showing the utilization of geothermal fluids (derived from Lindal, 1973)

## 2.3 CO<sub>2</sub> emission Geothermal Energy

Figure 2.4 compares the CO<sub>2</sub> emissions from geothermal power plants to those from fossil fuel plants. Bloomfield calculated the CO<sub>2</sub> emission values for coal, oil and natural gas plants using data from the US DOE's Energy Information Administration (EIA). The greenhouse gas emissions of the geothermal plants are: carbon dioxide 91 g/kWh, hydrogen sulphide 85 g/kWh, methane 750 g/kWh and ammonia 599 g/kWh (Bloomfield, et al., 2003). Bertani and Thain (2002) investigated the emissions from 85 geothermal plants currently operating in 11 countries and found a weighted average of 122 g CO<sub>2</sub>/kWh, which compares fairly well with the value of 91 g/kWh reported for the USA plants by Bloomfield, et al. (2003).

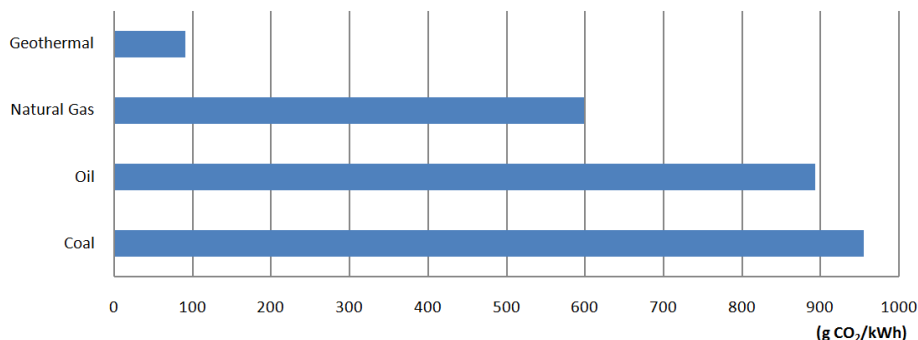


Figure 2.4: Comparison of CO<sub>2</sub> emissions from electricity generation (Bloomfield, 2003)

## 2.4 Geothermal Energy in The Netherlands

Figure 2.5 shows the geothermal energy potential of The Netherlands at a depth of 2000 meters. The natural heat flux in the Dutch underground is around  $0.063\text{W/m}^2$ . The Netherlands has a geothermal potential of 90.000 PJ in heat. The geothermal potential in electricity is in the order of a few GWe capacity (Ecofys, 2009). According to Gilding (2010) geothermal energy is a hot topic and resulted in a rush for geothermal exploration licenses started in The Netherlands by glasshouse farmers and energy companies. From 2008 to 2010, 400 km<sup>2</sup> of exploration license applications were received by the Dutch Ministry of Economic Affairs for areas in the Netherlands with a goal to drill for geothermal energy (Vis et al., 2010). This geothermal heat can be used to heat buildings and businesses in a sustainable way. Geothermal energy is a nearly CO<sub>2</sub> emission free solution for heat production. Because of the geothermal gradient in the Netherlands only two types of geothermal systems are currently used. System 1: Shallow geothermal systems targeting shallow groundwater for seasonal heat and cold storage of a single building. System 2: A deep geothermal system producing heat from aquifers 1500 up to 5000 meters deep for large glasshouses and district heating networks. No enhanced geothermal system (EGS) or ultra deep geothermal systems, system to 5000 meters deep or more, have been realized in the Netherlands (Gilding, 2010).

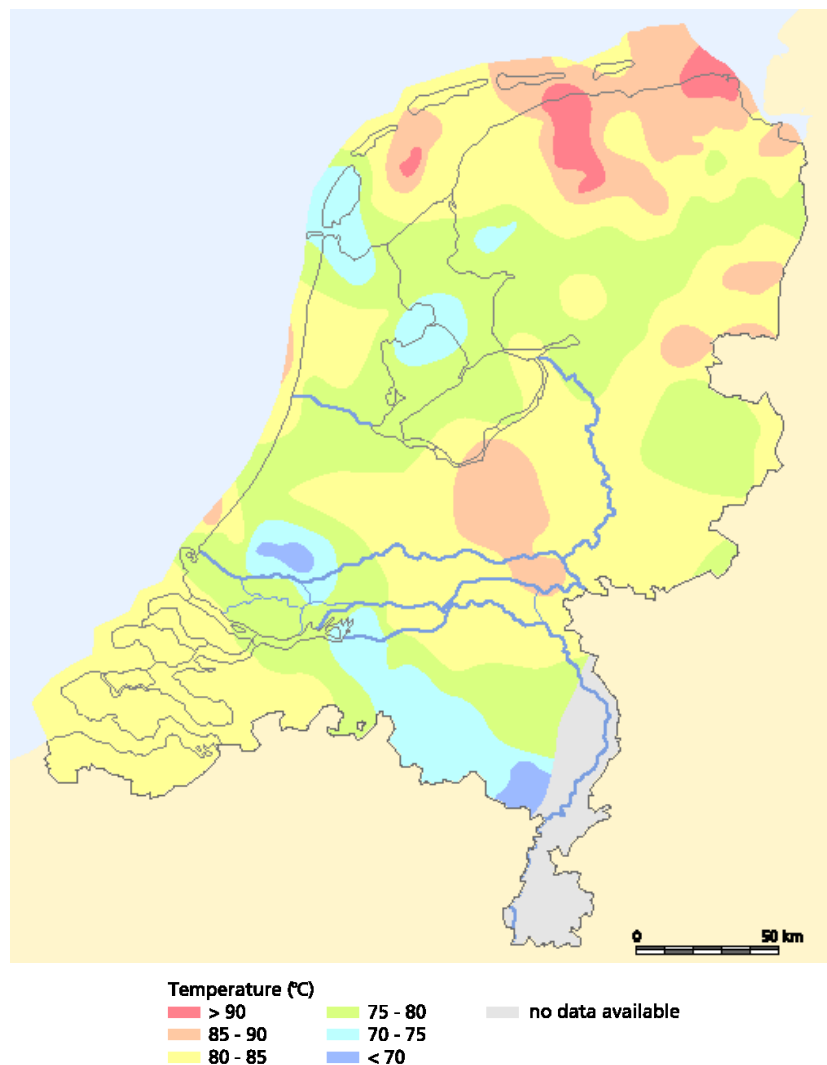


Figure 2.5: Temperature map at a depth of 2000 meters (Lokhorst and Wong, 2007)

## 2.5 Delft University of Technology location

In august 2009 the University of Technology Delft has received a permit from the Ministry of Economic Affairs to perform a geothermal exploration. This permit will pave the way for research into the use of geothermal energy on the campus and in the Delft region, and for developing teaching programmes on the subject. There is a twofold advantage to this permit. It will contribute to the development and transfer of new knowledge and expertise, but it will eventually make it possible to provide sustainable heating for campus buildings. This development chimes with the university's ambition of creating a climate-neutral campus. TU Delft is the first university in the Netherlands to receive a geothermal exploration permit (TU Delft, 31 august 2009).

Paragraphs 2.6, 2.7 and 2.8 are based on the bachelor Thesis of Chris den Boer (2008).

## 2.6 Geological setting

Knowledge of the geology is of great importance for successful implementation of the geothermal system. The subsurface of the TU Delft region is sited in the West Netherlands Basin, which has been an area of oil production since 1954. (De Jager et al, 1996) The basin existed from the Late Jurassic to the Early Cretaceous and opened in a series of NW-SE trending rift basins forming half-graben structures. While being formed these rifts were filled with fluvial sediments. (den Hartog Jager, 1996). During the Late Cretaceous compression occurred leading to the reactivation of the earlier faults. This resulted in the formation of complex inversion structures and NNW-SSE fault structures. (De Jager, 2007)

For geothermal heat purposes there are two intervals of interest in Zuid-Holland: the Lower Triassic and the Lower Cretaceous sandstones (Lokhorst & Wong, 2007). Research within DAP looked at the Lower Cretaceous sandstones. There are three formations which are potentially interesting: the Berkel sandstone, the Rijswijk sandstone and the Delft sandstone. The shallowest of the three is the Berkel sandstone. The Rijswijk sandstone is formed during coastal transgression sand and has good lateral continuity. The Delft Sandstone, the deepest of those three, is a stacked distributary-channel deposit with massive sandstone sequences (Van Adrichem Boogaardt & Kouwe, 1993).

The Delft Sandstone Formation is chosen to be the target zone for the geothermal system of DAP because it is situated below the Rijswijk sandstone, which means higher aquifer temperature and because of the potentially high reservoir qualities of the Delft sandstone. In an ongoing study within DAP the target horizon, the Delft sandstone, was interpreted with the use of seismic data provided by the NAM. An anticlinal structure was found. Data from 45 wells from the surrounding of Delft supported the interpretation (Smits, 2008).

## 2.7 Temperature Gradient

In the Netherlands the geothermal gradient is about 3°C per 100 meters. For verification of this gradient a TNO study (Simmelink et al, 2007) was performed for the Den Haag Geothermal project resulting in a specific temperature gradient. The reservoir temperature for the DAP target zone is estimated using this Den Haag relation (Smits, 2008). If we look at this target zone for DAP we see that the Delft Sandstone goes to a depth of around 2100 to 2500 meters. This corresponds to an in-situ temperature of 75°C to 80 °C.

## 2.8 Reservoir Properties

Unfortunately the wells drilled in the TU Delft area do not provide enough information about the reservoir properties of the Delft Sandstone. To make a good prediction of the porosity and the permeability data from an analogue field is used. This field is the Moerkapelle field located about 15 kilometers north-east of the TU Delft area. The Moerkapelle field is a heavy oil field with the Delft Sandstone at a depth of about 800-1000 meter. Petrophysical analysis of the logs from the Moerkappelle wells provided average properties for the Delft Sandstone:

**Table 2.1:** Data of Delft subsurface (Gilding, 2010; Den Boer, 2008 and Smits, 2008)

Average porosity:	0.21
Average Permeability:	495 mD
Average Thickness:	60-115 m

The average porosity can be determined from Figure 2.6 on the next page. An average permeability of 495 mD was found in the thesis of Den Boer, 2008. The thickness of the well is supported by all three writers.

Figure 2.6 shows the porosity of the Delft Sandstone Member from all available well log porosity data points. The horizontal axis shows the porosity and the vertical axis gives the percentage of the total data points (Gilding, 2010).

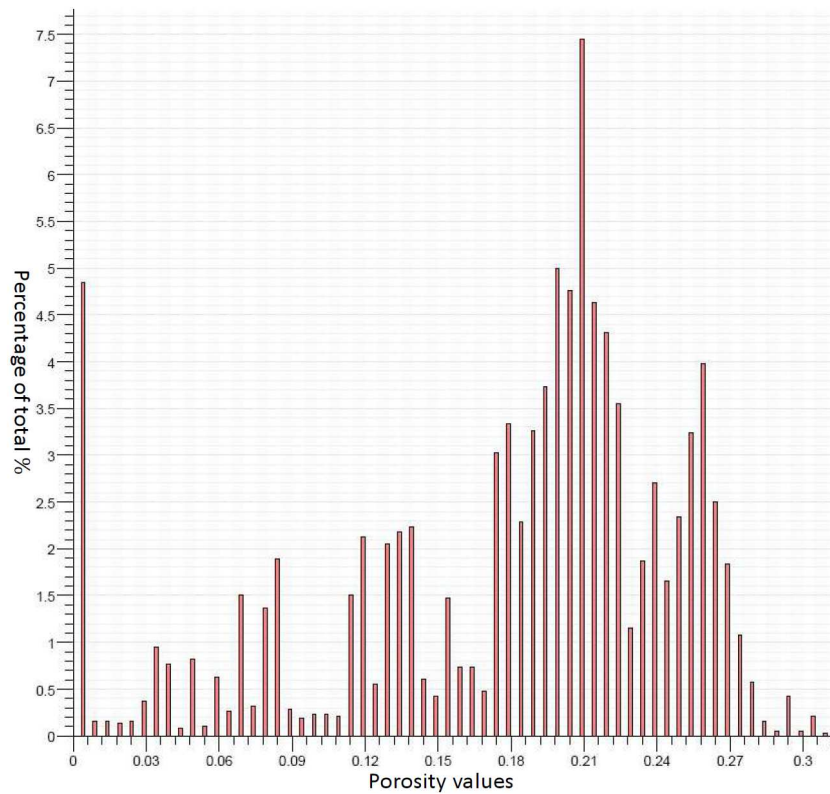


Figure 2.6: Graph of the porosity of the Delft Sandstone Member (Gilding, 2010)

Figure 2.7 shows the subsurface of the Delft area, the red lines represent the production wells and the blue lines the injection wells. The space between the production and injection well will be around 2000 meters in the case of the Delft Aardwarmte Project (DAP). The yellow line represent the exploration well on the top of the structure. This figure is prepared by the software programs Petrel and Eclipse, the use of the software was made possible thanks to Schlumberger.

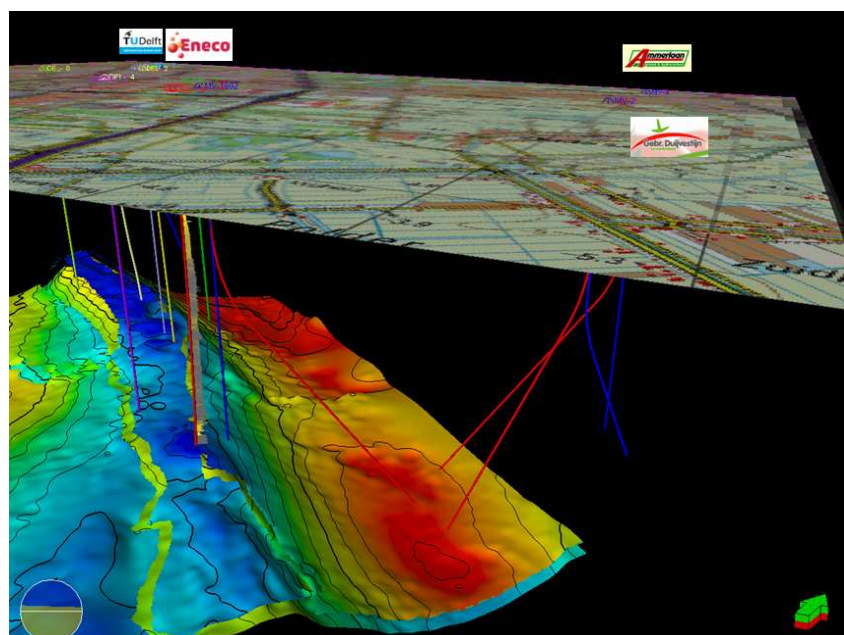


Figure 2.7: Temperature map of the Delft subsurface (DAP website)

### 3 Carbon Capture and Storage (CCS)

This chapter describes carbon capture and storage (CCS). The chapter is divided into four paragraphs. The first paragraph describes what CCS is. After this the following paragraphs describe the environmental effects, risks and maturity of CCS.

#### 3.1 What is CCS?

Carbon capture and storage is a set of technologies aimed at capturing carbon dioxide emitted from industrial and energy-related processes before it enters the atmosphere, compressing the CO<sub>2</sub>, and storing it for long-term (indefinitely) in formations such as depleted natural gas fields, deep saline aquifers and unmineable coal seams. CCS is not a new technology. CO<sub>2</sub> has been captured for nearly 100 years for industrial purposes or to increase oil or gas production. CCS technology can reduce carbon dioxide emissions from large industrial sources and coal-fired power stations by approximately 85 - 90% depending on the type of capture technology used (Undrum et al, 2000). CCS has the potential to be an essential technology to significantly reduce greenhouse gas emissions and allow the continued use of fossil fuels for energy security, without further damaging climate security. According to Koornneef (2009) carbon capture and storage is often considered in literature as one of the temporary technological solutions to control CO<sub>2</sub> emissions from large point sources.

#### 3.2 Environmental effects

The merit of CCS systems is the reduction of CO<sub>2</sub> emissions by up to 85 – 90%, depending on plant type. Generally, environmental effects from use of CCS arise during power production, CO<sub>2</sub> capture, transport and storage. Additional energy is required for CO<sub>2</sub> capture, and this means that substantially more fuel has to be used, depending on the plant type.

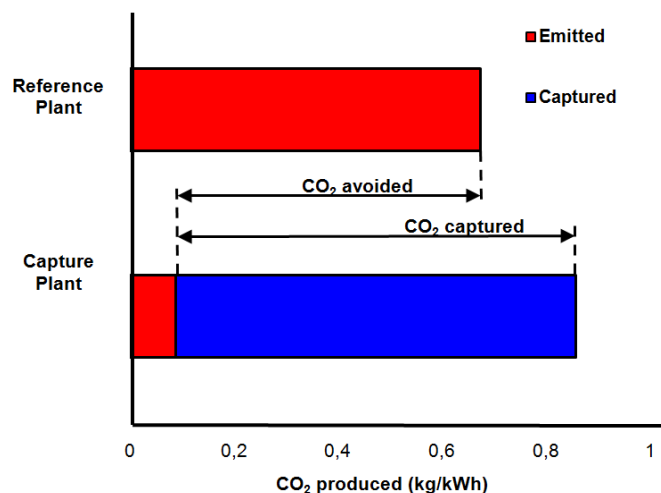


Figure 3.1: CO<sub>2</sub> capture and storage from power plants

Figure 3.1 shows the CO<sub>2</sub> emission of a power plant with and without capture plant. The capture plant causes a loss in overall efficiency for the power plant. Additional energy is required for capture, transport and storage and any leakage from transport. This results in a larger amount of “CO<sub>2</sub> produced per unit of product” (lower bar) relative to the reference plant (upper bar) without capture (IPCC, 2005).

#### 3.3 Risk of CCS

A major concern with CCS is whether leakage of stored CO<sub>2</sub> will compromise CCS as a climate change mitigation option. For well-selected geological storage sites, IPCC (Intergovernmental Panel on Climate Change) estimates that risks are comparable to those associated with current hydrocarbon activity. CO<sub>2</sub> could be trapped for millions of years, and well selected stores are likely to retain over 99% of the injected CO<sub>2</sub> over 1000 years. For ocean storage, the retention of CO<sub>2</sub> would depend on the depth; IPCC estimates 30–85% would be retained after 500 years for depths 1000 – 3000 m. Mineral storage is not regarded as having any risks of leakage. The IPCC recommends that limits be set to the amount of leakage that can take place. The IPCC is a scientific intergovernmental body tasked with reviewing and assessing the most recent scientific, technical and socio-economic information produced worldwide relevant to the understanding of climate change.

## 4 CO<sub>2</sub> sources

The main sources of CO<sub>2</sub> emission are power generation, industrial processes, transportation and residential and commercial buildings. Figure 4.1 shows a pie chart of the CO<sub>2</sub> emissions per sector in 2010. The total world emission of CO<sub>2</sub> in 2001 was 23,684 Mt/year (Davison, 2007). According to CO<sub>2</sub>Net (2007) the total CO<sub>2</sub> emissions are much higher because Davison does not include the emission caused by land use (deforestation). The emission caused by land use are 1.6 Gt C/year (6 Gt CO<sub>2</sub>/year), the emission caused by fossil fuels consumption are 6 Gt C/year (23.625 Gt CO<sub>2</sub>/year). Hence the total emission of anthropogenic CO<sub>2</sub> will be around 30 Gt CO<sub>2</sub>/year of which 80% is caused by the use of fossil fuels and 20% caused by the use of land.

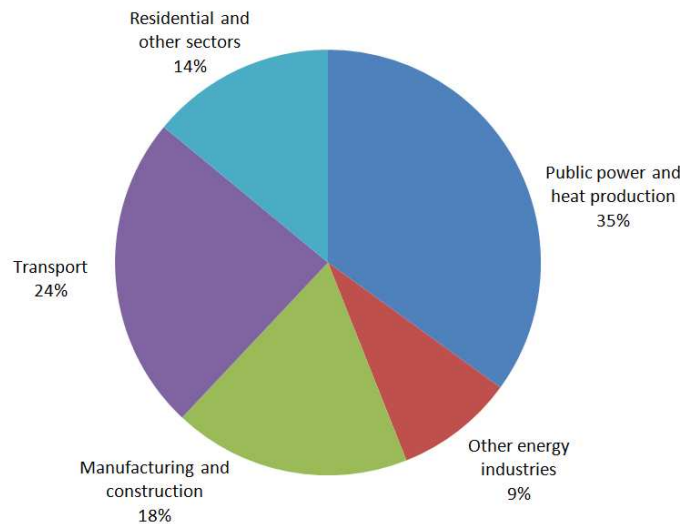


Figure 4.1: Emissions of CO<sub>2</sub> from fossil fuel use (2010)

The annual Dutch CO<sub>2</sub> emission is nearly 180 Mt CO<sub>2</sub> at present, of which approximately 100 Mt CO<sub>2</sub>/year emitted by the energy and manufacturing industry (Klein Goldewijk et al., 2005). The purity of the CO<sub>2</sub> exit stream is very important, high purity emitters are preferable because the CO<sub>2</sub> can be captured at relatively low costs (EIGA, 2008 and IEA GHG, 2002). Table 4.1 shows a list of CO<sub>2</sub> producers and the purity of their CO<sub>2</sub> stream.

Table 4.1: Purity of CO<sub>2</sub> sources (CO<sub>2</sub>NET, 2009)

Sources	Purity
Ammonia	100%
Ethylene oxide	100%
Gas processing	100%
Hydrogen	10 – 100%
Cement	15 – 30%
Iron and steel	15%
Ethylene	10 – 15%
Power	3 – 15%
Refineries	3 – 13%

In Appendix C the extended version of this chapter can be found. In this appendix more information about CO<sub>2</sub> sources and their purity and also a world map with black dots, representing large point sources, can be found.

## 5 CO<sub>2</sub> capture

Currently the best opportunity to optimize the capturing process of CO<sub>2</sub> can be applied to large point sources, such as large fossil fuel or biomass energy facilities, industries with major CO<sub>2</sub> emissions, natural gas processing, synthetic fuel plants and fossil fuel-based hydrogen production plants (Herzog and Golomb, 2004).

### 5.1 CO<sub>2</sub> capture systems

Currently there are three different types of CO<sub>2</sub> capture systems: post-combustion, pre-combustion and oxyfuel combustion. Important factors of selecting these different types of capture systems are the concentration of CO<sub>2</sub> in the gas stream, the pressure of the gas stream and the fuel type (solid or gas). In Appendix D more information about each of these capture systems can be found.

### 5.2 CO<sub>2</sub> Capture Technologies

In this paragraph several different carbon capture technologies which are available at the moment are being treated. Figure 5.1 shows that a wide range of different technology options for CO<sub>2</sub> separation and capture from gas streams exist. The choice of a suitable technology depends on the characteristics of the flue gas stream, which depends on the power plant technology (Rao, A. and Rubin, E., 2002).

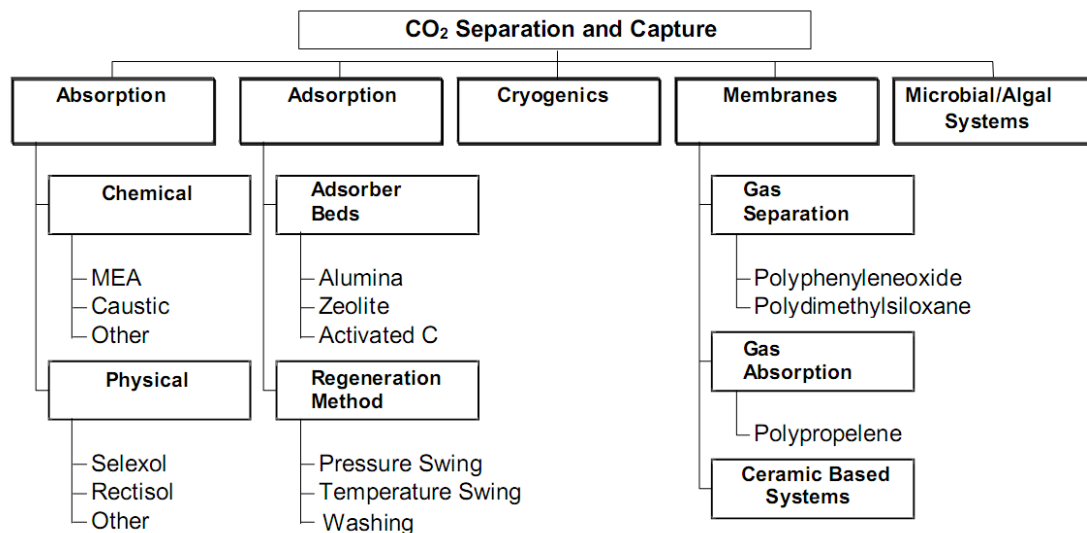


Figure 5.1: Technology options for CO<sub>2</sub> separation and capture (Rao, A. and Rubin, E., 2002)

CO<sub>2</sub> can be separated from other components on the basis of difference in physical and chemical features such as molecular weight, boiling point, solubility and reactivity. The most used separation technologies (CO<sub>2</sub> from other flue gasses) are:

- Absorption: Dissolution/permeation into matrix
- Adsorption: Attachment to surface
- Cryogenic: Separation based on the difference in boiling points
- Membranes: Separation based on the difference in physical/chemical interaction with membrane

Each of the four separation technologies mentioned above are treated more in depth in Appendix D.

### 5.3 Energy Penalty / Emission factor

When doing an exergy analysis it is very important to keep in mind that for the whole carbon capture and storage process also energy is needed. For every m<sup>3</sup> of natural gas or oil and every kg of coal used for the CCS process CO<sub>2</sub> is being emitted. Hence it is important to keep in mind the capture efficiency of the process. The formula below show how to calculate the efficiency of the CO<sub>2</sub> capture facility. Again more information can be found in the appendix.

$$\text{Capture efficiency} = \frac{CO_2 \text{ avoided}}{CO_2 \text{ captured}} = \frac{CO_2 \text{ captured} - CO_2 \text{ released CCS}}{CO_2 \text{ captured}}$$

## 6 CO<sub>2</sub> transport

After CO<sub>2</sub> has been captured at a large point source it has to be transported to a place where it can be stored. Between the capture and storage facility, the CO<sub>2</sub> has to be transported by one or a combination of several transport media like truck, train, ship or pipeline with possible intermediate storage (Koornneef et al, 2009). In this chapter transportation by pipeline and ship are being highlighted. In Appendix E the extended version of this chapter can be found.

### 6.1 Pipeline

CO<sub>2</sub> can be transported through pipelines in three ways: in the form of a gas, a supercritical fluid or in the subcooled liquid state (Zang et al, 2006). Only two methods can be used to transport CO<sub>2</sub> over long distances: a supercritical fluid or a subcooled liquid (McCoy and Rubin, 2008). Transportation in the gas phase is disadvantaged because of the low density and consequently the large pipe diameter and high pressure drop. Most CO<sub>2</sub> pipelines are used for enhanced oil recovery, the CO<sub>2</sub> is transported as a supercritical fluid (Zang et al, 2006).

According to Black & Veatch power plant engineering (1996) it is well established, for the quantities and distances required for CO<sub>2</sub> sequestration, that pipeline transport is the most economical. Pipelines are used all over the world for transportation in the energy sector, e.g. for natural gas, refined products, coal slurry and also CO<sub>2</sub> (Zang et al, 2006). Carrying CO<sub>2</sub> in pipelines onshore is not a new concept (Gale, 2004). Currently there is over 6000 km of CO<sub>2</sub> pipelines in operation in the USA, mainly for enhanced oil recovery (EOR). These pipelines are mainly situated in remote areas with low population densities. When CCS in the future will be implemented on a large scale, a large network of CO<sub>2</sub> pipelines will be needed. Part of this infrastructure will be located near densely populated areas, so safety issues are much more complex (Koornneef, 2009).

In the Netherlands an existing pipeline of 85 km is being used to transport CO<sub>2</sub> – at low pressure – from the Shell refinery in Pernis to greenhouses in the Westland area. *“A total CO<sub>2</sub> supply capacity of 160 tonne per hour (44 kg/s) can be obtained. The CO<sub>2</sub> produced in Pernis is available at atmospheric pressure and is compressed to about 20 bar to allow the dry and gaseous CO<sub>2</sub> to flow from Pernis to the greenhouses.”* (Ecofys, 2006). However, large-scale CCS will require a new transportation infrastructure to link sources and sinks. In densely populated countries such as the Netherlands this can become a considerable challenge (booklet Cato2). In the appendix a blueprint for a CO<sub>2</sub> pipeline infrastructure for the Netherlands can be found.

### 6.2 Ship

After the CO<sub>2</sub> has been captured, it has to be transported to a storage site. In chapter 7 we describe different ways of storing CO<sub>2</sub>. Due to the scattered CO<sub>2</sub> sources and the uncertainty in the growth of the CO<sub>2</sub> market, a cost effective and flexible transport system is required. In this paragraph transportation by ship is being discussed. Transport by ship is not a new concept because transportation of LNG and ethylene already exist. The use of ships for transporting CO<sub>2</sub> across the sea is today in an embryonic stage. Worldwide there are only four small ships used for this purpose (IPCC, 2005). The transported CO<sub>2</sub> can be used for EOR, which is done at several places onshore in the United States (Heggum et al., 2005). Although the potential for increased oil recovery is likely, CO<sub>2</sub> is currently not used for EOR in any offshore oilfield. The main source for this paragraph (paragraph 6.2) is Aspelund et al., 2006.

Both investments and operational costs for the liquefaction process are affected by the composition and purity of these CO<sub>2</sub> sources. It is assumed that the sources have to deliver CO<sub>2</sub> at 1.1 bar and 15 °C (298 K). In order to transport CO<sub>2</sub> in large amounts, the gas must be transformed into a form with higher density. In the appendix a figure can be found which shows the typical arrangements for a CO<sub>2</sub> ship. There are three types of tank structures for liquid gas transport ships: pressure type, low temperature type and semi-refrigerated (IPCC, 2005). In Appendix E Figure 6.3 can be found which shows the optimal transport conditions for CO<sub>2</sub>, also the lay-out of a CO<sub>2</sub> transport ship (Figure 6.4) and the main process steps (Figure 6.2) in the transport system of the ship are included.

## 7 CO<sub>2</sub> storage

The extended version of this chapter, which goes more in depth, can be found in Appendix F. After the CO<sub>2</sub> has been captured it needs to be stored so that it will not be emitted into the atmosphere. The captured CO<sub>2</sub> can be transported to different sites where it will be stored. This permanent storage of CO<sub>2</sub> can be done in various forms. There are two potential storage options, which are (IEA, 2009):

- Storage in the oceans
- Storage in geological formations

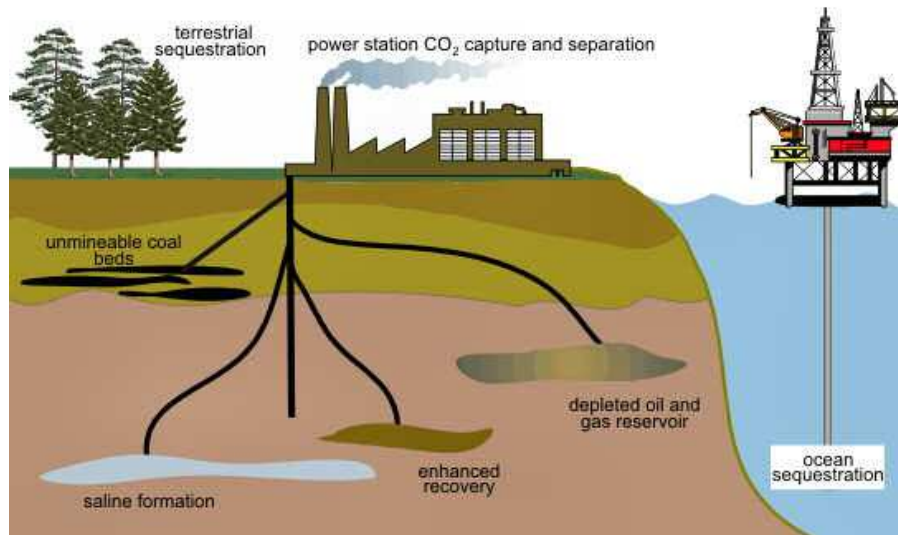


Figure 7.1: Different types of storage options (Frost, 2008)

There are a number of potential geological formations that can be used to store captured CO<sub>2</sub>. These include (Herzog, 2004):

- Depleted gas and oil fields
- Deep saline aquifers
- Deep unminable coal seams
- Formations for enhanced oil recovery

Together, these formations can hold for hundreds to thousands of gigatons of carbon. Figure 7.1 shows the worldwide capacity of potential CO<sub>2</sub> storage reservoirs.

Table 7.1: The worldwide capacity of potential CO<sub>2</sub> storage reservoirs (Herzog, 2004)

Sequestration option	Worldwide capacity (Gt C)
Ocean	1000 – 10,000
Deep saline formations	100 – 10,000
Depleted oil and gas reservoirs	100 – 1000
Coal seams	10 – 1000
Terrestrial	10 – 100
Utilization	Currently < 0.1 Gt C/year

Paragraphs 7.1 and 7.2 explain the storage in oceans and geological formations more thoroughly. Several key criteria must be applied to the storage method (Herzog, 2004):

- The storage period should be prolonged (>100 – 1000 years).
- Cost of storage, including the cost of transportation from source to storage site, should be minimized.
- Risk of accidents should be eliminated.
- The environmental impact should be minimal.
- The storage method should not violate any national or international laws and regulations.

A storage site has to fulfill several properties to be a good CO<sub>2</sub> storage site. Table 7.2 shows some site selection criteria (IPCC, 2005).

**Table 7.2: Properties of CO<sub>2</sub> storage site (IPCC, 2005)**

High storage capacity:	High porosity
	Large reservoir
Efficient injectivity:	High permeability
Safe and secure storage:	Low geothermal gradient & high pressure
	Adequate sealing
	Geological & hydrodynamic stability
Low costs:	Good accessibility, infrastructure
	Source close to storage reservoir

### 7.1 Potential storage sites within the Netherlands

The annual Dutch CO<sub>2</sub> emission is nearly 180 Mt CO<sub>2</sub> at present, of which approximately 100 Mt CO<sub>2</sub>/year emitted by the energy and manufacturing industry (Klein Goldewijk et al., 2005). Around 15 Mt CO<sub>2</sub> can be avoided every year by 2020, when some of the larger gas fields, that become available in the coming decade, are used for storage of CO<sub>2</sub> (Daniëls and Farla, 2006). Table 7.3 shows the technical capacity for CO<sub>2</sub> storage in the Netherlands and the continental shelf. Gas fields represent the major storage potential. The Dutch oil fields represent a relatively low storage potential. Aquifers and coal seams are not that well studied, which causes a relatively large uncertainty in storage capacity (Damen et al., 2009).

**Table 7.3: Technical CO<sub>2</sub> storage potential in the Netherlands (Damen et al., 2009)**

Reservoir	Storage capacity (Mt CO <sub>2</sub> )
Gas fields	
Groningen gas field	7350
Other gas field (onshore)	1600
Other gas field (offshore)	1150
Oil fields	40
Coal seams	170 (40 – 600)
Aquifer trap prospects	
Onshore	400
Offshore	350 (90 – 1100)

Figure 7.2 shows the storage capacity in the Netherlands is gradually increasing in the coming two decades, this is caused by the lifetime of the gas fields. Possibly, the lifetime of gas fields may be extended a few years with rising gas prices.

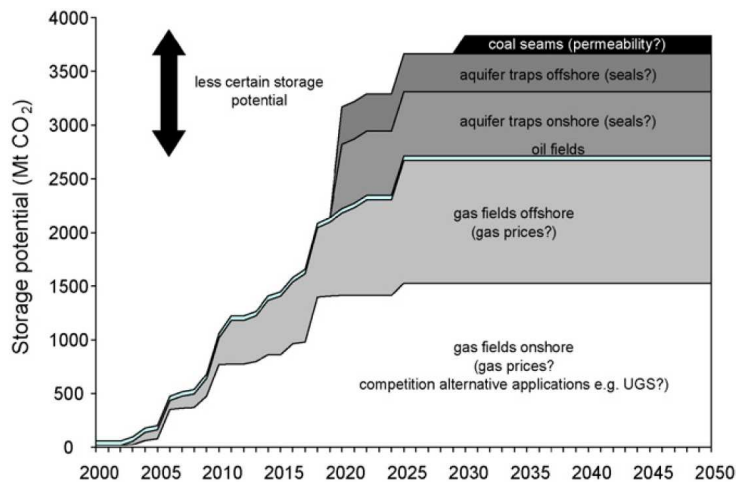


**Figure 7.2: Storage availability in time (Damen et al., 2009)**

## 8 Exergy Analysis

According to Wall (1987): “Natural resources, such as energy and material resources, appear partly as flows and partly as stocks, see Figure 8.1. We regard constantly flowing solar energy, wind energy and water flows as natural flows. A natural flow has a limited size but usually lasts for a very long time. An ecosystem, such as a forest, forms a valuable stock. It is built up of natural flows of sunlight, water, carbon dioxide, and mineral substances. It gives rise to a flow of new biological matter and part of this flow (the yield) can be taken out of the system without decreasing the stock. Other stocks, such as oil deposits, have quite different qualities. A deposit can only yield a flow if it is gradually depleted. Among stocks we therefore differentiate dead stocks or deposits from living stocks or funds. This is a time based classification because the time of reproduction is the physical concept that is of interest here. Deposits and funds are defined with regard to the difference in the time of reproduction. Natural flows and flows from funds are often called renewable flows.”

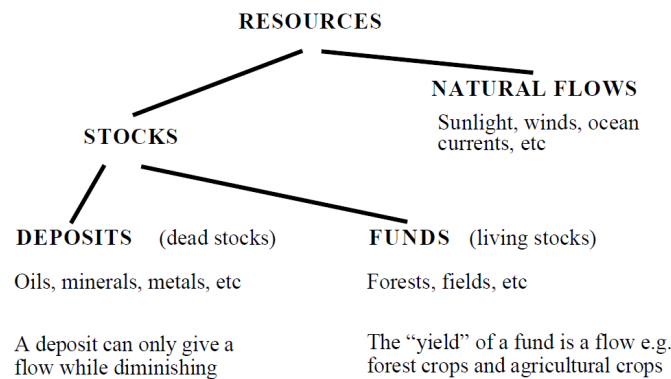


Figure 8.1: Classification of resources (Wall, 1987)

The exergy of a system is the maximum useful work possible during a process that brings the system into equilibrium with a heat reservoir. So exergy is the energy that is available to be used; when a system and surroundings reach equilibrium, the exergy is zero. In other words, an exergy analysis takes into account the quality as well as the quantity of energy (Karakus et al, 2002). Stated by the first law of thermodynamics energy cannot be created or destroyed. The second law of thermodynamics states that energy appears in many forms and different qualities and the quality of energy can increase locally or be destroyed (Hepbasli, 2008). Table 8.1 shows different energy forms and their quality based on a Carnot cycle. The maximum quality factor is 1,0 which means that all the energy can be converted into work. In the TU Delft case we estimate a quality factor less than 0.3.

Table 8.1: The quality of some common energy forms (Wall, 1987)

Energy form	Quality factor
Mechanical energy	1.0
Electrical energy	1.0
Chemical energy	1.0
Nuclear energy	0.95
Sunlight	0.9
Hot steam (600°C)	0.6
District heat (90°C)	0.2 - 0.3
Heat at room temperature (20°C)	0 - 0.2
Thermal radiation from earth	0

When a new energy source is discovered the first and most important thing to know is how much energy can be extracted from this new source. However this information alone is not enough to decide whether or not to build an energy plant. What we really need to know is the work potential (quality) of the new energy source, in our case a geothermal well beneath the TU Delft. Work potential is the amount of energy which can be extracted as useful work, this property is called exergy. The rest of the energy is eventually discarded as waste energy called *anergy* (Szargut, 2003).

## 8.1 Energy invested into materials for the wells

This paragraph considers the energy invested to produce the materials needed for the whole system. The well consist of steel and cement. They are the two most important materials used during drilling and well completion. In paragraph 8.1.1 and 8.1.2 the exergy per kg steel or cement is calculated. Figure 8.2 shows the conventional drilling sequence.

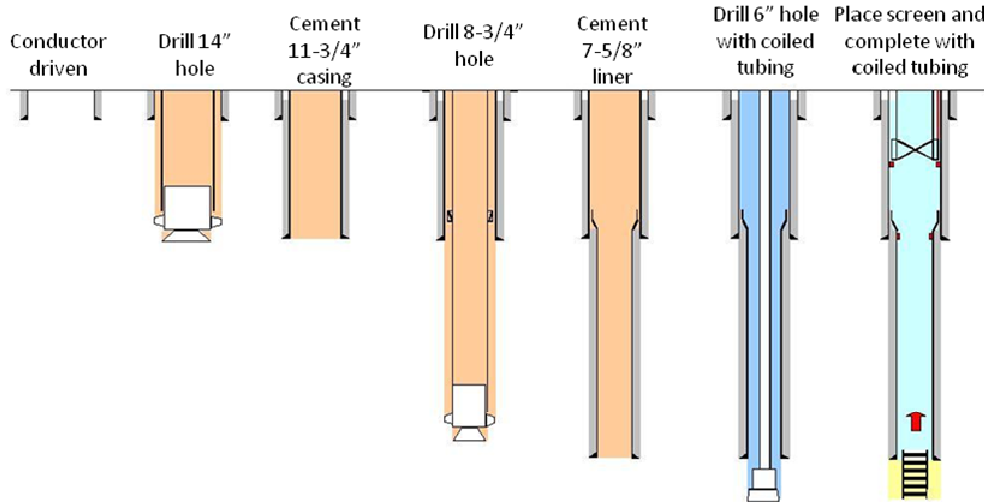


Figure 8.2: Casing drilling sequence with steel pipe (Leijnse, 2008)

### 8.1.1 Energy invested to produce the steel casing

Figure 8.2 shows the lay-out of a geothermal well. As can be seen from the figure the casing of the well consist of 3 segments, with 3 different diameters. There also exists a difference between the production pipe and injection pipe, in the casing length. In Table 8.2 the volume and length of each segment of the injection pipe is being calculated.

Table 8.2: Steel Demand of injection pipe

Casing OD (in.)	Casing ID (in.)	Interval (m)	Casing length (m)	Steel Volume (m <sup>3</sup> )	Casing Weight (kg)
13 3/8	12.459	0 - 60	60	1.10	8,930
10 3/4	9.794	60 - 700	640	12.21	99,415
7	6.331	700 - 1790	1290	17.22	140,227
5.812	4.767	1790 - 1850	60		
<b>Total:</b>				<b>30.52</b>	<b>248,572</b>

Because the lay-out of the injection and production pipe is completely different, the same calculation with different values for the production pipe is done in Table 8.3.

Table 8.3: Steel Demand of production pipe

Casing OD (in.)	Casing ID (in.)	Interval (m)	Casing length (m)	Steel Volume (m <sup>3</sup> )	Casing Weight (kg)
13 3/8	12.459	0 - 60	60	1.10	8,910
10 3/4	9.794	60 - 1200	1140	21.74	177,083
7	6.331	1200 - 3100	1900	25.36	206,535
5.812	4.767	3100 - 3300	200		
<b>Total:</b>				<b>48.20</b>	<b>392,549</b>

The energy figures for a composite well have not been found. Hence, the injection and production well are considered to be steel/cement wells. The amount of steel needed for each all segments result in a total weight of **248,572 kg** steel casing for the injection well and **392,549 kg** steel for the production well. The total weight of both wells is **641,121 kg**. Note that the production interval is completed with a sand screen and no casing is needed; the screen energy figures have been neglected in this calculation but cost a lot of energy to produce.

According to Costa (2001) the chemical exergy needed to produce steel is

$$Ex_{steel}^{ch} = 18.000 \text{ kJ} / \text{kg}$$

The chemical (exergetic) efficiency of the process is 30%, which results in the exergy of steel of

$$Ex_{steel} = 60.000 \text{ kJ} / \text{kg} = 60 \text{ MJ} / \text{kg}$$

Several other sources confirmed the calculation of Costa (2001):

Handbook of Delucchi	58.09 MJ/kg
US Department of Energy	58.22 MJ/kg
Lenzen and Dey (2000)	61.54 MJ/kg

As a consequence, the total exergy consumed for the steel tubing is  $60 \text{ MJ/kg} \times 641,121 \text{ kg} = 38,467,260 \text{ MJ} = \mathbf{38,467 \text{ GJ}}$ .

### 8.1.2 Energy invested to produce cement

In Table 5 all the interval length are measured along the hole. It is assumed to have a 2" annulus between the hole and the casing. The cement density is taken  $1440 \text{ kg/m}^3$ . Cement (Portland Cement as reference) is a mixture of many compounds. Four of these make up 90% or more of the weight of portland cement: tricalcium silicate, dicalcium silicate, tricalcium aluminate, and tetracalcium aluminoferrite. Different types of cement contain the same four major compounds, but in different proportions (Portland Cement Association, 2009).

**Table 8.4: Portland Cement Content**

Name	Percent by weight	Chemical Formula
Tricalcium silicate	50%	$3 \text{ CaO SiO}_2$
Dicalcium silicate	25%	$2 \text{ CaO SiO}_2$
Tricalcium aluminate	10%	$3 \text{ CaO Al}_2 \text{ O}_3$
Tetracalcium aluminoferrite	10%	$4 \text{ CaO Al}_2 \text{ Fe}_2 \text{ O}_3$
Gypsum	5%	$\text{CaSO}_4 \text{ H}_2\text{O}$

Using the chemical formula's of Table 8.5 and the weight ratio of these substances into Portland Cement, the molar mass, molar ratio and chemical exergy of each substance can be calculated. Also the chemical exergy of Portland Cement is calculated by adding up all the chemical exergies of each substance.

**Table 8.5: Chemical exergy of Portland Cement**

Name	Chemical Exergy (kJ/kg)	Molar Mass (g/mol)	Mass ratio	Mole	Chemical Exergy (kJ/kg)
Tricalcium silicate	1019.00	232.30	0.5	2.15	509.5
Dicalcium silicate	601.89	172.24	0.25	1.45	150.5
Tricalcium aluminate	1332.91	270.19	0.1	0.37	133.3
Tetracalcium aluminoferrite	914.27	437.96	0.1	0.23	91.4
Gypsum	24.30	153.15	0.05	0.33	1.2
<b>Chemical Exergy</b>					<b>885.9</b>

Table 8.5 shows that the chemical exergy of Portland Cement is around:

$$Ex_{cement}^{ch} = 886 \text{ kJ / kg}$$

The exergetic efficiency of the whole production process is

$$\eta_e = 0,30$$

which results in the total exergy of cement of,

$$Ex_{cement} = 2950 \text{ kJ / kg}$$

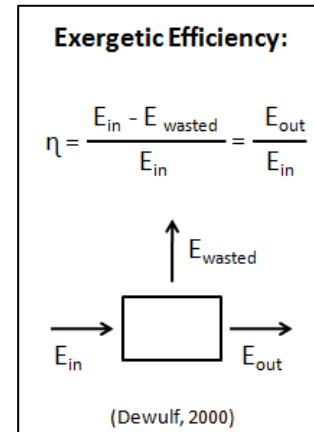


Table 8.6 shows the amount of cement needed for the injection pipe. The total amount of cement needed for the injection pipe is 60.89 m<sup>3</sup>. The density of cement is 1440 kg/m<sup>3</sup> so 87.688 kg of cement is used.

**Table 8.6: Demand of cement for injection pipe**

Hole Diameter (in.)	Casing Outer Diameter (in.)	Interval at depth (m)	Casing length (m)	Cement Volume (m <sup>3</sup> )	Cement Weight (kg)
16	13 3/8	0 – 60	60	3.14	4,524
12 1/4	10 3/4	60 – 700	640	19.15	27,578
8 1/2	7	700 – 1790	1290	38.60	55,586
<b>Total:</b>				<b>60.89</b>	<b>87,688</b>

Table 8.7 shows the amount of cement needed for the injection pipe. The total amount of cement needed for the injection pipe is 94.11 m<sup>3</sup>. The density of cement is 1440 kg/m<sup>3</sup> so 135,518 kg of cement is used.

**Table 8.7: Demand of cement for production pipe**

Hole Diameter (in.)	Casing Outer Diameter (in.)	Interval at depth (m)	Casing length (m)	Cement Volume (m <sup>3</sup> )	Cement Weight (kg)
16	13 3/8	0 – 60	60	3.14	4,524
12 1/4	10 3/4	60 – 1200	1140	34.11	49,123
8 1/2	7	1200 – 3100	1900	56.85	81,871
<b>Total:</b>				<b>94.11</b>	<b>135,518</b>

The amount of cement needed for the injection and production well is respectively **87,688 kg** and **135,518 kg**. The total amount of cement needed for both wells is **223,207 kg**. Note that the excess volume of cement used in any cement job has been ignored. The exergy needed to produce cement is 2950 KJ/kg. Hence, the total energy consumption for production of cement for two wells is 223,207 kg x 2950 kJ/kg = **658 GJ**.

## 8.2 Energy invested in drilling the geothermal doublet

In Appendix O the most important formulas about drilling can be found. These formula's are from SPE (Society of Petroleum Engineers), a paper by Samuel G. and McColpin G., (2001). For this calculation I used real numbers instead of formulas.

The drilling activities at the Ammerlaan geothermal plant are considered to be an analogue for the Delft case. Personal communications with K. Boersma (Petrogas Minerals International B.V) provided information regarding the energy consumption for drilling a well up to 2000 meters. In the case of Ammerlaan it takes around 40 days, drilling with diesel engines, which consume around 3000 liters of diesel per day. For a doublet it takes 2 wells x 40 days/well x 3000 l diesel/day = 240,000 l diesel. Having a diesel heating value of 36.3 MJ/litre, **8712 GJ** is needed, or 9208 Watts over a lifetime of 30 years for the system. The amount of energy used for drilling in the case of DAP can be much lower when composite pipes are used because a completely

different drilling rig can be used, which is much lighter and consumes less energy. In Appendix M the lay-out of a drilling can be found. Another advantage of composite piping is that is less corrosive compared to steel piping. At Ammerlaan the geothermal doublet is only used to produce hot water, DAP wants to co-inject CO<sub>2</sub> with the returning water. Concluding: the amount of energy consumed for composite drilling will be considerably lower, figures have to be found in a follow up of this study.

### 8.3 Energy demand for CO<sub>2</sub> capture

According to Statoil and the Norwegian University of Science and Technology the energy consumption of a CO<sub>2</sub>-capture unit is approximately 1.3-1.7 kWh/kg CO<sub>2</sub> of which 90 % is heat (about 130 °C). An average of 1.5 kWh/kg CO<sub>2</sub> (5400 kJ/kg) is used for the performed calculations. Annually Delft University consumes about 11 million cubic meters of natural gas in the combined heat and power plant. With a heating value (HV) for natural gas of 31.65 MJ/Nm<sup>3</sup>, it gives an energy consumption of ca. 350,000 GJ/year (=11.04 MW), which results in an emission of 19740 ton/year or 54.08 ton/day (emission factor for natural gas is 56.7 kg CO<sub>2</sub>/GJ).

### 8.4 Energy demand for CO<sub>2</sub> compression

After CO<sub>2</sub> capturing, it is compressed and co-injected with the cold return water into the aquifer. The heat is used to heat the campus of the University of Technology Delft. Not all the energy will come from the aquifer, still natural gas will be used to heat the campus. During the combustion the emitted CO<sub>2</sub> will be captured and finally stored in the aquifer. The intention is to inject CO<sub>2</sub> at 40 bar, or at a depth of 400 m water pressure. The CO<sub>2</sub> has to be saturated in the water and be stable under in-situ conditions. De solubility of CO<sub>2</sub> in water is a function of temperature and pressure and already dissolved particles (ions). Figure 8.3 and Figure 8.4 are prepared with data from Duan and Sun (2003) and Duan et al. (2006). Figure 8.3 shows the solubility of CO<sub>2</sub> as a function of pressure at temperatures between 30 °C and 80 °C. The maximum solubility of 1 mol CO<sub>2</sub>/kg H<sub>2</sub>O is equivalent to 44 kg CO<sub>2</sub> / m<sup>3</sup> water. The solubility of CO<sub>2</sub> into H<sub>2</sub>O will decrease with increasing water temperature. Also the curve shows that at pressures above 100 bar the solubility is not increasing that much anymore. The temperature of the water will be around 40°C after heat is extracted by the heat exchanger.

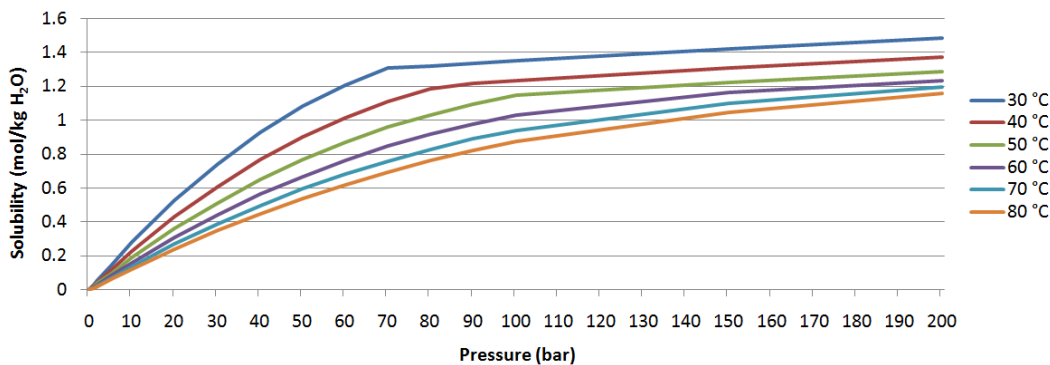


Figure 8.3: Solubility CO<sub>2</sub> into water (Duan and Sun, 2003/2006)

Not only the temperature and pressure are very important, also the salinity of the water is very important. When the salinity of the water increases the solubility of CO<sub>2</sub> decreases, see Figure 8.4. This figure shows the solubility at 40 °C for 0 mol (mol NaCl/kg water), 0.5 mol, 1.0 mol NaCl and seawater (3.5 Wt. % NaCl). As can be seen from the figure the salinity is of minor influence on the solubility.

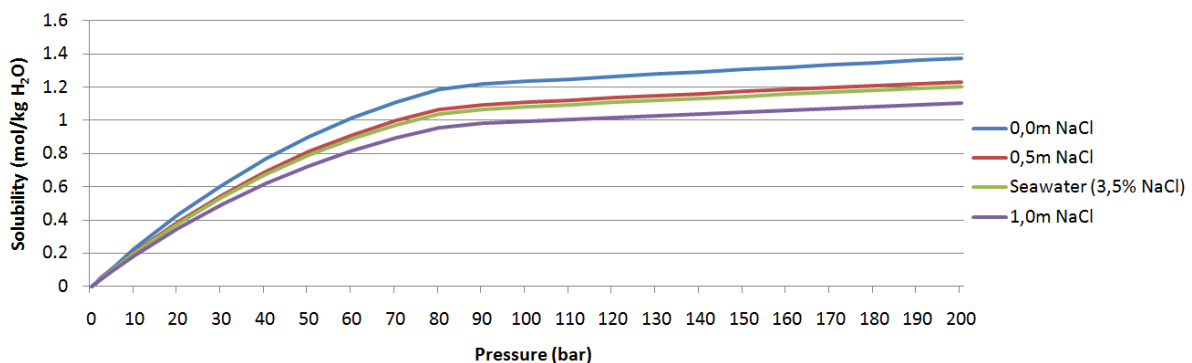


Figure 8.4: Solubility of CO<sub>2</sub> into water @ 40 °C (Duan and Sun, 2003/2006)

For the DAP-situation it is proposed to compress the CO<sub>2</sub> up to 40 bar, before co-injection with the return water. Currently the Delft University of technology emits around 55 tons of carbon dioxide, which is produced by the combined heat and power plant. The plant consumes 11 million cubic meters of natural gas. The captured CO<sub>2</sub> has to be compressed in four compression stages. Table 8.8 shows the power demand at each stage. The equation used for the calculation comes from the book of Walas (2010):

$$THP(\text{theoretical adiabatic horsepower}) = \left[ \frac{(SCFM) T_1}{8130a} \right] \left[ \left( \frac{P_2}{P_1} \right)^a - 1 \right], \text{ where } a = \frac{(k-1)}{k} \text{ and } k = \frac{C_p}{C_v}$$

**Table 8.8: Power demand during CO<sub>2</sub> compression**

Stage [-]	Input pressure [Bar]	Exit pressure [Bar]	Power [HP]
1	1	3	34.67
2	3	9	34.67
3	9	27	34.67
4	27	40	11.32
<b>Total power:</b>			<b>115.33</b>

As can be seen from the table the total power demand for compression is 115 horsepower (when 100% is captured), this is 84,828 Watt (1 HP = 735.4988 Watt).

## 8.5 Energy invested in CO<sub>2</sub> transportation

In the case of DAP transportation between the capture facility and injection site is expected to be less than 200 meters and therefore disregarded as being a contribution to the energy input for this analysis. But in most cases the CO<sub>2</sub> from large point sources cannot be stored on the same location where the CO<sub>2</sub> is been produced because there is no storage medium. The CO<sub>2</sub> has to be transported to a storage facility by pipeline. The Netherlands has many storage options (see chapter 7) and a wide natural gas distribution network, some of these pipes can be used in the future for CO<sub>2</sub> transport. Still a calculation is important to show how much energy is needed to produce the pipes needed for this transport because it can be a very important factor for other countries with no wide natural gas distribution system. In most cases transportation of CO<sub>2</sub> will be over short distances, between 100 – 250 km, in Holland these distances will be even smaller. In the United States CO<sub>2</sub> is already transported 6000 km of CO<sub>2</sub> pipelines in operation, mainly for enhanced oil recovery (EOR).

## 8.6 Total invested energy

Table 8.9 shows the total energy consumption for the CCS facility for a life-time (LT) of 10, 20 and 30 years. The energy invested in materials and drilling stays the same over the 10, 20 and 30 years because it is a one time investment.

**Table 8.9: Total energy consumption over 10, 20 and 30 years life-time**

Energy:	LT 10 years (J)	%	LT 20 years (J)	%	LT 30 years (J)	%
Drilling	8.71E+12	1.4%	8.71E+12	0.7%	8.71E+12	0.5%
Steel	3.85E+13	6.0%	3.85E+13	3.1%	3.85E+13	2.1%
Cement	6.58E+11	0.1%	6.58E+11	0.1%	6.58E+11	0.0%
<b>Materials &amp; Drilling</b>	<b>4.78E+13</b>	<b>7.5%</b>	<b>4.78E+13</b>	<b>3.9%</b>	<b>4.78E+13</b>	<b>2.6%</b>
Capture	5.76E+14	89.7%	1.15E+15	93.2%	1.73E+15	94.4%
Compression	1.81E+13	2.8%	3.61E+13	2.9%	5.42E+13	3.0%
<b>Total:</b>	<b>6.42E+14</b>	<b>100%</b>	<b>1.24E+15</b>	<b>100%</b>	<b>1.83E+15</b>	<b>100%</b>

The energy invested in materials and drilling is relatively small compared to the energy needed for capture and compression, after 10 years of operation 7.5% was used for materials and drilling compared to the 92.5% for compression and capture. More than 89% of the total energy consumption is used for the capture process. Concluding: the invested energy in materials and drilling is minor compared to the energy intensive capture process.

## 8.7 Exergy production by geothermal well

In this section, the aim is to calculate the theoretical exergy production from the geothermal well. All the parameters used in the calculations can be found in Table 8.10.

Table 8.10: Parameters exergy calculations

Symbol	Value	Description
$c_p$	4184 J/(kg.K)	Water heat capacity at constant pressure
$\rho_w$	1000 kg/m <sup>3</sup>	Water density
$\rho_s$	8145 kg/m <sup>3</sup>	Steel density
$\rho_c$	1440 kg/m <sup>3</sup>	Cement density
$\mu_w$	0.001 Pa.s	Water viscosity
$T_0$	15 °C + 273.15 = 288.15 K	Ambient temperature
$T_1$	40 °C + 273.15 = 313.15 K	Injected water temperature
$T_2$	80 °C + 273.15 = 353.15 K	Produced water temperature
$D$	0.18 m (7")	Tubing inner diameter
$W$	2000 m	Reservoir width
$L_{t,p}$	3100 m	Tubing length production well
$L_{t,i}$	1800 m	Tubing length injection well
$L_w$	2000	Distance between production and injection well
$\delta$	32+18=50 m	Thickness of the production interval
$k_D$	495x10 <sup>-15</sup> m <sup>2</sup> (495 mD)	Absolute permeability of the Delft sandstone member
$f$	0.005	Friction factor
$\eta_{pump}$	0.80 (0.70 – 0.90)	Pump efficiency
$\eta_{driver}$	0.95	Pump Driver efficiency
$\eta_{elec}$	0.45	Electricity Production efficiency
$\eta$	0.34	Overall pump efficiency ( $\eta = \eta_{pump} \times \eta_{driver} \times \eta_{elec}$ )

Figure 8.5 shows a schematic overview how the heat is extracted from the geothermal reservoir. As can be seen from the figure a pump is required to get the water up to the surface. After the heat is extracted the “cold” water is send back to the geothermal reservoir (aquifer).

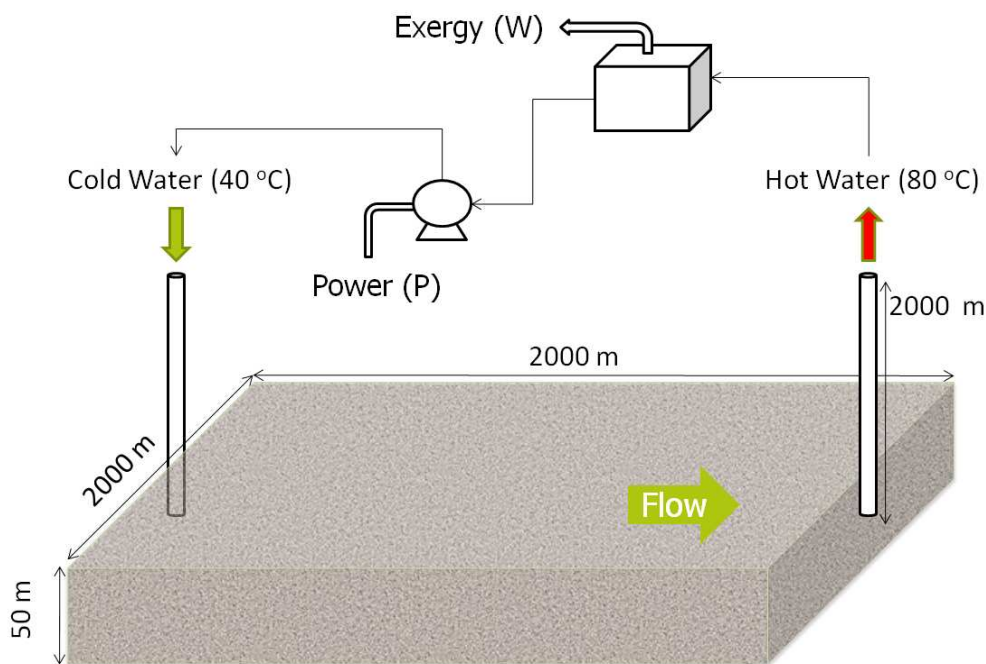


Figure 8.5: Schematic overview how to extract heat from the geothermal reservoir

The produced exergy is calculated at flow rate  $Q$ . It is assumed that the water produced from this geothermal reservoir enters the surface facilities at  $T_2$  (80 °C), and is reinjected into the reservoir at  $T_1$  (40 °C). The ambient temperature is assumed  $T_0$ . This is the same as the average surface temperature in the Netherlands (15 °C). Eq. 1 gives the total energy produced by the geothermal well, this does not consider the pressure effect on enthalpy and exergy, this will have only a minor effect.

$$\Delta Ex = Ex_2 - Ex_1 = c_p(T_2 - T_1) - c_p T_0 \ln\left(\frac{T_2}{T_1}\right) \quad , \quad (1)$$

where  $c_p$  is the water heat capacity at constant pressure. A fixed  $c_p$  is used so it does not change with different temperature. Note that temperatures in these equations are in Kelvin. The first and second term on the right side of Eq.(1) are the energy and anergy terms, respectively. The energy produced from this reservoir in terms of the production (flow) rate,  $Q$ , is:

$$\text{Exergy Power} = Q \times \rho_w \times (Ex_2 - Ex_1) \quad , \quad (2)$$

where  $\rho_w$  is the water density. There are two factors accounted to be power losses and both depending on the flow rate:

- dissipation due to friction along the wells,
- power loss in the reservoir.

So the available exergy power is calculated by subtracting the power loss in the well and the power loss in the reservoir from the produced exergy.

### 8.8 Power loss along the wells

Potential loss along the wells is a result of friction of the fluid to the tubing surface of both wells. To compensate the friction a pump is needed. Assuming that water is produced and injected along the tubing, the potential loss in terms of  $Q$  is calculated for each of the wells as follows:

$$\Delta\Phi_w = \frac{2\rho_w v^2 L_t f}{\eta D} ; v = Q / A_t ; A_t = \pi D^2 / 4 \rightarrow \Delta\Phi_w = \frac{32\rho_w L_t f}{\eta \pi^2 D^5} Q^2 \quad (3)$$

where  $v$  is the water velocity inside the production/injection tubing,  $L_t$  is the tubing length,  $D$  is the inner diameter of the tubing, and  $f$  is the friction factor. Also is considered a tubing roughness of 0.001.

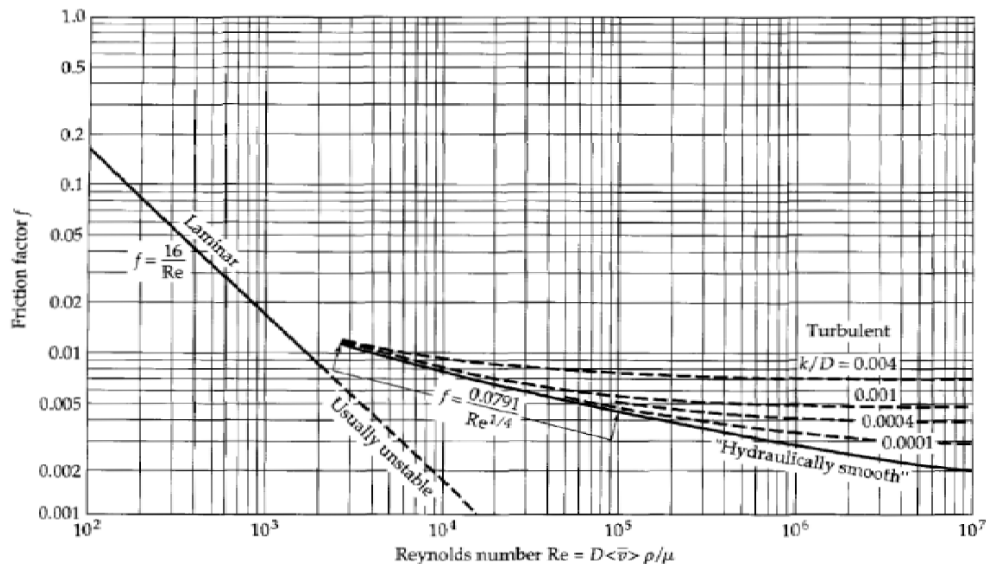


Figure 8.6: Friction factor - Reynolds number (Janssen and Warmoeskerken, 2001)

As can be seen from Figure 8.6, the friction factor  $f$  is approximately equal to 0.005 in the range of Reynolds numbers that were encountered in this study. The length of the production and injection well are 3100 and 1800 meters respectively. Because the diameter of the tubes depends on depth and dissipation increase by

decreasing diameter size, the smallest tubing diameter ( $\varnothing = 0.18$  m or 7") is used for a realistic outcome. Substituting these values in Eq.(3) gives:

$$\Delta\Phi_w = \frac{32\rho_w L_t f}{\eta \pi^2 D^5} Q^2 = 583.9 Q^2 \text{ MPa} \quad (4)$$

This is the potential loss along each well. For the dissipation along both wells, we write:

$$\text{Dissipation in the wells} = 2 \times \Delta\Phi_w \times Q = \frac{64\rho_w L_t f}{\eta \pi^2 D^5} Q^3 = 1167.8 Q^3 \text{ MW} \quad (5)$$

Dissipation in the wells is correlated with the well tubing diameter; a smaller diameter causes more friction with the walls and by that more pumping energy is required. Figure 8.7 shows the power loss along the wall of wells of 3 different diameters. This loss has to be compensated by the pump to get the water up to the surface.

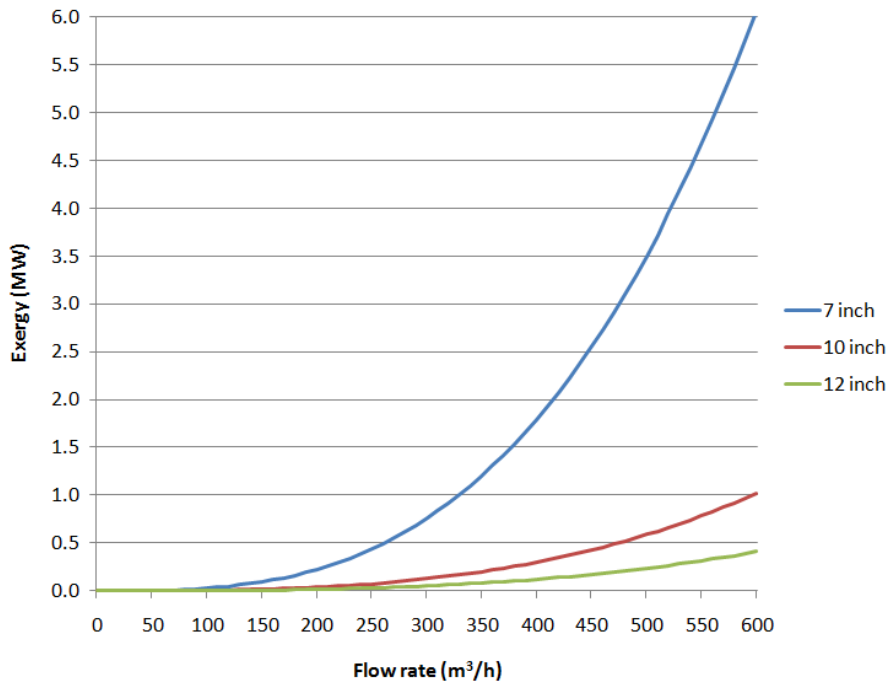


Figure 8.7: Effect of diameter on the power loss along the walls of the wells

## 8.9 Power loss in the reservoir

The potential loss in the reservoir depends on fluid viscosity, permeability and flow velocity, here calculated as follows:

$$\Delta\Phi_r = \mu_w u L_w / k; \quad u = Q / A_c; \quad A_c = \delta \cdot W \quad , \quad (6)$$

where  $\mu_w$  is the water viscosity,  $u$  is the Darcy velocity,  $L_w$  is the distance between the wells,  $k$  is the absolute permeability of the reservoir,  $A_c$  is the total cross section of the production zone,  $\delta$  is the thickness of the production zone, and  $W$  is the width of the reservoir.

$$\Delta\Phi_r = \frac{\mu_w L_w}{\delta \cdot W \cdot k} Q = 40.4 Q \text{ MPa} \quad (7)$$

To calculate the dissipation or the power loss in the reservoir, we also consider the pump efficiency ( $\eta$ ) equal to 36% into account:

$$\text{Dissipation in the reservoir} = \frac{\Delta\Phi_r \times Q}{\eta} = \frac{\mu_w L_w}{\delta \cdot W \cdot k \cdot \eta} Q^2 = 112.2 Q^2 \text{ MW} \quad (8)$$

Dissipation in the reservoir is affected its permeability, i.e.; a higher permeability results in a better injection or production flow. Consequently, the energy needed for pumping decreases with increasing permeability. Figure 8.8 shows the power loss in the reservoir at 3 different permeability's (0.5, 1.0 and 10 Darcy).

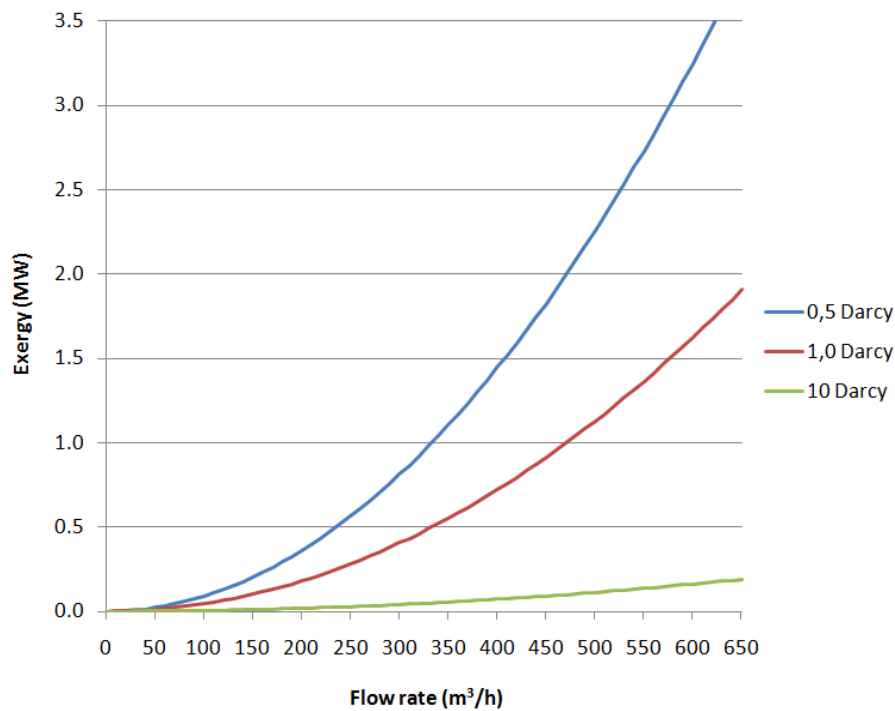


Figure 8.8: Effect of permeability on the power loss in the reservoir

DAP aims at a flow rate of 150 - 200 m<sup>3</sup>/h, so the losses are still minor. Note that the Figure 8.7 and Figure 8.8 show that the effect of both well diameter and permeability increase exponentially with the flow rate.

### 8.10 Determination of the optimal flow rate

The exergy produced by the reservoir is compensated with the losses by dissipation, providing the available net exergy. Figure 8.9 shows the available exergy (purple line) as a function of flow rate (Q). The maximum available power from this geothermal reservoir is 0.66 MW at a flow rate of 180 m<sup>3</sup>/hr. Note: the energy invested in materials and construction have not been taken into account in this figure.

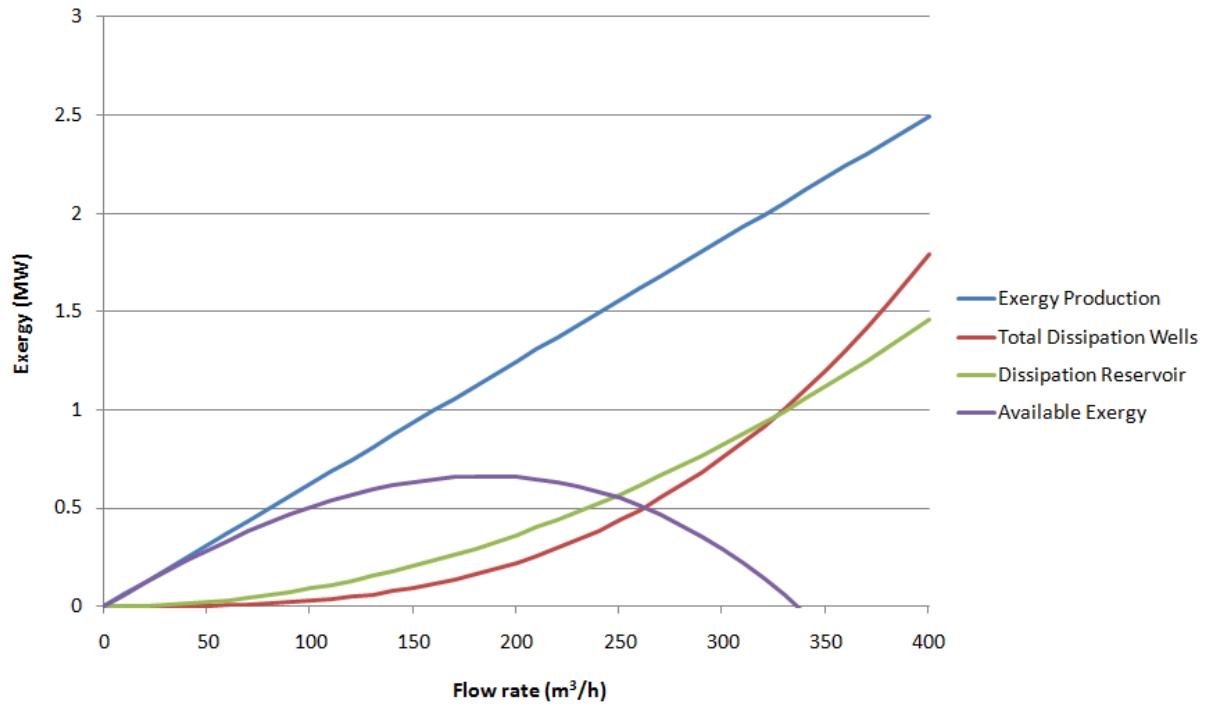


Figure 8.9: Available Exergy

Table 8.11 shows the values of Figure 8.9. This table is a summary of the whole table (step size 10 m<sup>3</sup>) which can be found in Appendix P. The dissipation loss in the well is very dependent on the diameter of the wells. Because the diameter of the tubes change depending on depth, the smallest tubing diameter (∅ = 0.18 m or 7") is used to get a realistic outcome.

Table 8.11: Available Exergy

Flow rate [m <sup>3</sup> ]	Exergy Production [MW]	Power loss in wells (Exergy) [MW]	Power loss in reservoir (Exergy) [MW]	Available Exergy [MW]
0	0.00	0.00	0.00	0.00
50	0.31	0.00	0.02	0.29
100	0.62	0.03	0.09	0.50
150	0.93	0.09	0.21	0.63
200	1.25	0.22	0.36	0.66
250	1.56	0.44	0.57	0.55
300	1.87	0.76	0.82	0.29
350	2.18	1.20	1.12	-0.14
400	2.49	1.79	1.46	-0.76

Currently the Delft University of Technology consumes 11 million cubic meters of natural gas to run the combined heat and power plant. Of this 11 million cubic meters, around 5 million cubic meters can be saved by using geothermal energy instead of natural gas to heat the university. Table 8.12 shows that at a flow rate of 200 m<sup>3</sup>/h of water the annual heat demand of Delft University of Technology in terms of thermal power, can be covered. Also the energy needed to run the pump is taken into account. However, for cold periods and peak demand higher flow rates and additional heating with (gas) boilers are applied for:

- During the winter months the thermal energy demand is much higher compared to the heat demand during autumn and spring.
- During the autumn and spring the system can fulfill 80 – 100% of the thermal energy demand.

The available heat will go down when the flow rate exceeds 200 m<sup>3</sup>/h because much more pumping power is required due to higher losses in the reservoir and along the walls of the wells. When the system produces more than the demand the excess heat could be used to heat for example a swimming pool or other public building in the vicinity of the plant. It is also possible to extract more heat from the water when another source can use the rest heat of the University. This rest heat, with a lower quality, can be used to heat for example a swimming pool which could use water within a temperature range of 30 °C till 40 °C (see Lindal Diagram, Figure 2.3). Consequently, the avoided CO<sub>2</sub> emission depends on the heat demand and the amount of extracted heat from the heat exchanger.

**Table 8.12:** Exergy and heat production (thermal MW) as a function of flow rate (without losses)

Flow rate [m <sup>3</sup> /h]:	Exergy [MW]	Heat Produced [MW <sub>th</sub> ]	Pumping Power [MW]	Pumping Power* [%]	Available Heat** [MW <sub>th</sub> ]	Heat demand*** [MW <sub>th</sub> ]	Available Heat**** [%]
100	0.62	4.65	0.12	0.19	3.76	5.02	75%
150	0.93	6.97	0.30	0.32	4.74	5.02	94%
200	1.25	9.30	0.59	0.47	4.91	5.02	98%
250	1.56	11.62	1.01	0.65	4.11	5.02	82%

\* Percentage of the exergy used to run the pump  
 \*\* Available heat after subtracting the exergy used to run the pump  
 \*\*\* Heat demand of Delft University, based on the annual natural gas consumption used for heating (5 million cubic meter)  
 \*\*\*\* Available heat after subtraction of the energy needed to run the pump

Pumps are required to compensate for the losses by dissipation in the wells and reservoir (Figure 8.7 and Figure 8.8). Table 8.12 and Figure 8.10 show the comparison between exergy and heat production. To get an objective comparison, the losses by pumping are mentioned separately.

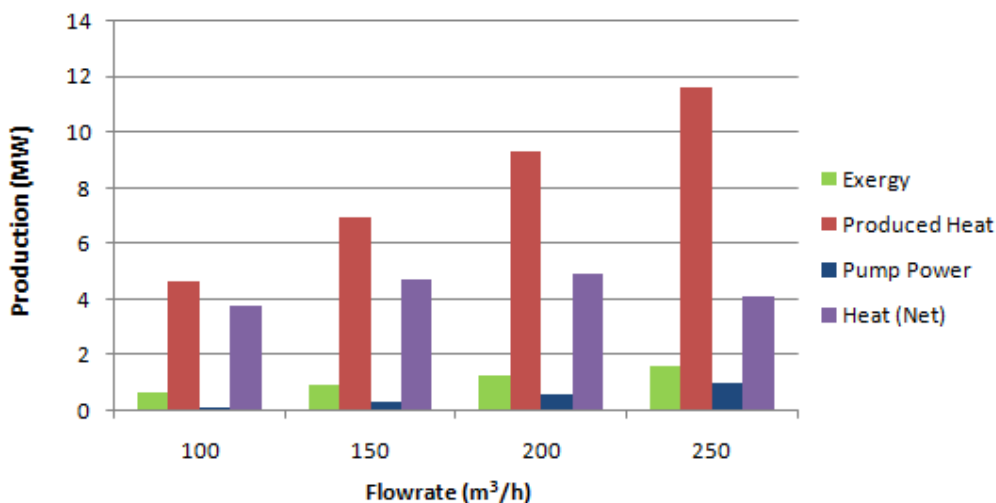


**Figure 8.10:** Annual heat production compared with exergy. The pumping power is needed to generate both exergy and heat.

### 8.11 Energy payback time

Figure 8.11 shows the net energy production for the entire process, over 30 years of operation. In this figure it is assumed that the university is heated for 60% by the central heating system which runs on natural gas and 40% on geothermal heat. Note that the CCS-activities and pumping pressure are included. Figure 8.11 and Figure 8.12 show a comparison of two systems; system 1 (blue line): 100% energy production by natural gas, system 2 (red line): 60% energy production by natural gas and 40% by geothermal energy. The energy pay-back time (compensation time) could not be determined in this figure, Figure 8.12 shows a close up of the first year.

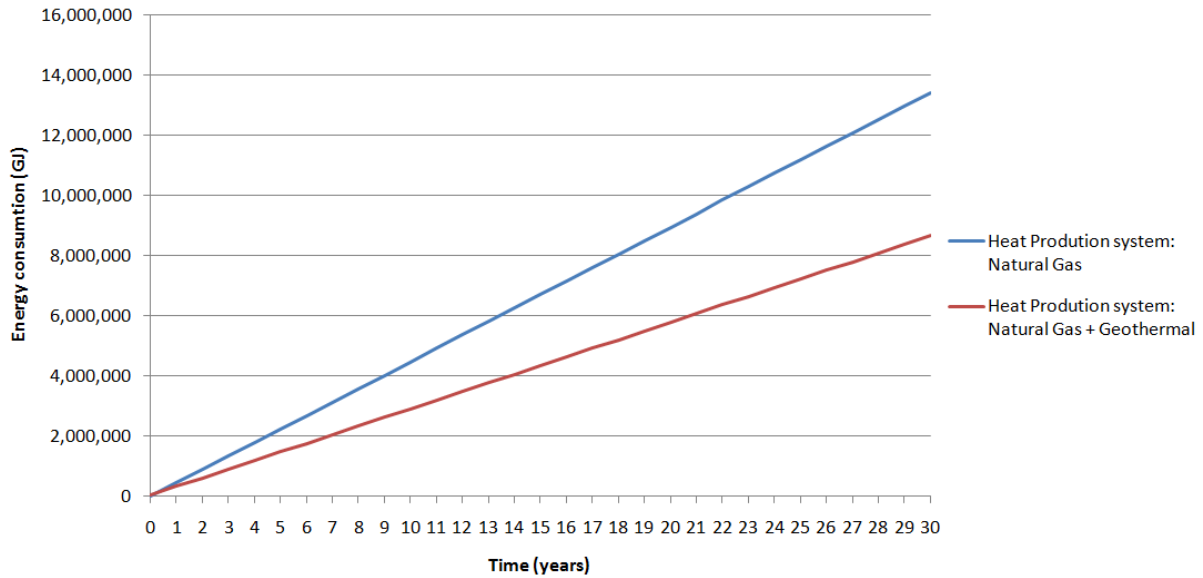


Figure 8.11: Energy Consumption (years)

In both figures the red line starts at **47,837 GJ** but this was not visible in Figure 8.11. This amount (47,837 GJ) represents the energy investments in drilling, production of steel and cement for both wells (production and injection). As can be seen from Figure 8.12 it takes less than 4 months before the energy investments are paid back by the energy (heat) production of the geothermal well.

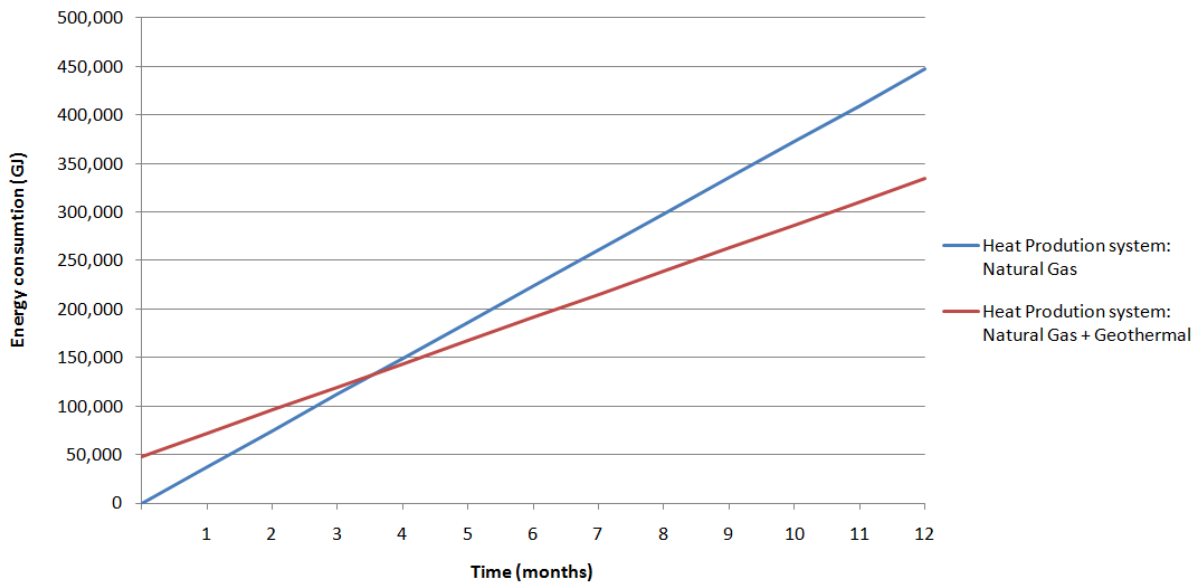


Figure 8.12: Energy Consumption (months)

## 9 CO<sub>2</sub> Emission

During the construction of the Carbon Capture and Storage facility a lot of CO<sub>2</sub> is being emitted into the atmosphere. Also when the plant is in operation it consumes energy, to run the pumps, absorber, compressor etc. In this chapter an analysis is made of all the CO<sub>2</sub> which is emitted during building of the whole facility and all the emissions during its use. With this kind of calculation a carbon footprint of the CCS process is made. According to the Centre of Sustainability Accounting (CenSa) the definition of carbon footprint is:

**“The Carbon footprint is a measure of exclusive amount of carbon dioxide emissions that is directly and indirectly caused by an activity” (Censa, 2002).**

In Appendix H the extended version of paragraphs 9.1 and 9.2 can be read.

### 9.1 CO<sub>2</sub> Emission during the production of steel pipes

As can be seen in the figure of Appendix H coal and coke are causing the largest emission of carbon dioxide during the production of iron and steel. Table 9.1 shows the energy consumption, CO<sub>2</sub> emissions and CO<sub>2</sub> intensity in 1986 and 1994. The big difference in CO<sub>2</sub> intensity is caused by the difference in process routes being used. Currently there exist two main process routes for the crude steel production (Gielen and Moriguchi, 2002):

- Basic oxygen furnace (BOF)
- Electric arc furnace (EAF)

**Table 9.1:** Energy consumption and CO<sub>2</sub> emissions in the steel industry in 1986 and 1994 (Kim et al, 2002)

	Energy consumption (PJ)		CO <sub>2</sub> Emissions (Mton C)		CO <sub>2</sub> intensity (t C/ton)	
	1986	1994	1986	1994	1986	1994
<b>Korea</b>	294.6	658.7	6.4	14.8	0.44	0.44
<b>Mexico</b>	186.7	244.4	3.6	4.5	0.50	0.44
<b>Brazil</b>	508.1	597.2	6.7	8.8	0.31	0.34
<b>China</b>	2034.7	3262.3	48.0	78.8	0.92	0.85
<b>India</b>	561.7	793.1	14.1	19.9	1.15	1.03
<b>US</b>	2202.5	2469.1	47.2	50.4	0.64	0.55

When comparing Table 9.1 with the paper of Sandberg (2001) and Table 9.2 (Chang-qing, 2006) it can be concluded that the BOF route consumes ~3.5 times more energy than the EAF route. In the paper of Kim et al. it was not clear which route was used, when comparing both tables it can be concluded that it was the EAF route.

**Table 9.2:** Total primary energy consumption and CO<sub>2</sub> emissions (global average) per ton of steel

	Total primary energy consumption (GJ)			Total CO <sub>2</sub> emissions (ton)		
	Average	Maximum	Minimum	Average	Maximum	Minimum
<b>BF-BOF: coil and plate</b>	25.5	31.7	21.45	1.97	2.60	1.61
<b>EAF: section</b>	11.2	15.3	8.6	0.54	0.77	0.31
<b>EAF: rebar-wire rod-eng</b>	11.8	16.4	5.0	0.59	1.08	0.15

Table 9.2 shows that the average emission during the production of steel is 1.97 ton CO<sub>2</sub>/ton steel coil. Bert Gols from Corus Research Development & Technology, confirmed during a telephone call this number. This results in the total emission, during the whole manufacturing process of steel pipes, of 641.1 ton x 1.97 = **1263 ton CO<sub>2</sub>**.

### 9.1.1 Total CO<sub>2</sub> emission for the production and placing of steel pipes

In this paragraph all the individual results of the previous paragraphs (see Appendix H, paragraph 9.2) are combined, Table 9.3 shows the total CO<sub>2</sub> emissions for laying 1 km of pipeline for different diameters.

Table 9.3: Total CO<sub>2</sub> emissions for laying a pipeline

Diameter (inch)	CO <sub>2</sub> emissions (ton/km pipe)					Total
	Steel production & pipe rolling	Transport (1000 km)	Equipment fuel usage	Coating & welding	Overhead	
16	133.7	9.9	49.2	6.9	40.7	240.4
20	206.4	16.0	53.4	8.6	40.7	325.1
24	258.6	22.3	84.0	10.4	40.7	415.9
36	543.0	48.8	119.7	15.8	40.7	768.0
48	973.7	85.6	138.6	21.5	40.7	1260.1

Figure 9.1 shows the same average total CO<sub>2</sub> emissions of a pipeline project for several diameters per kilometre. It also illustrates the carbon dioxide emissions of Nacap (pipeline contractor) in relation to the emissions of steel pipe suppliers. The calculated amount of emissions per kilometre of pipeline for a diameter of 48 inches is more than **1260 tons of CO<sub>2</sub>**.

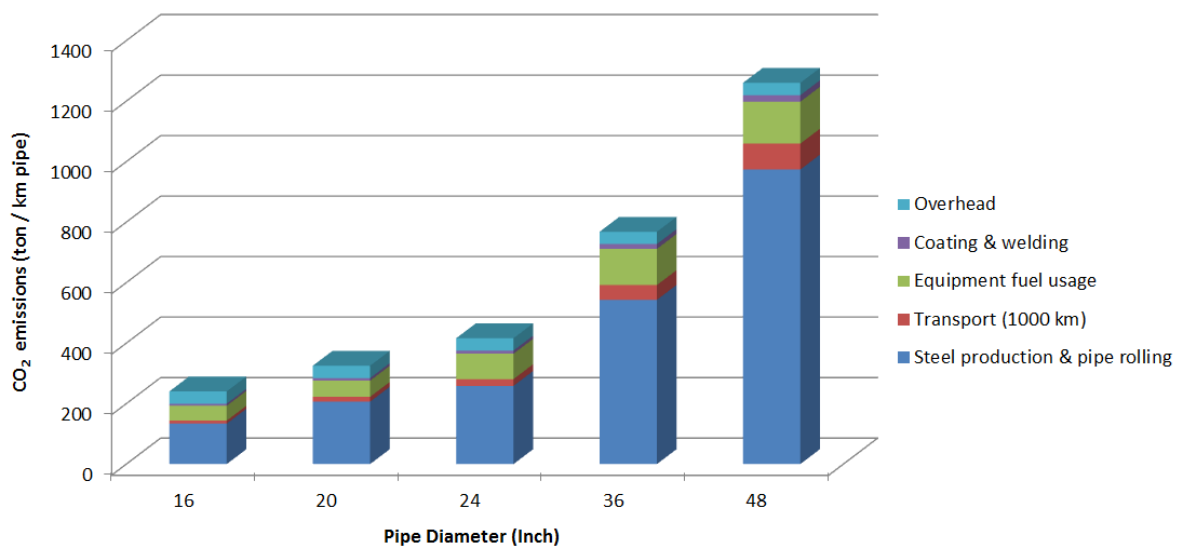


Figure 9.1: Total CO<sub>2</sub> emissions for laying a pipeline

The chart shows that the most important cause of CO<sub>2</sub> emissions is the pipe production. This can either be reduced by using stronger kinds of steel, which allows for a smaller pipe thickness. Another way is to examine whether it is possible to use steel from a different production process, for example by re-using scrap. Up to now it is not possible to create steel with the right quality for oil and gas pipelines.

## 9.2 CO<sub>2</sub> Emission during the production of cement

The CO<sub>2</sub> emitted during the production of Portland cement falls into 3 categories:

- CO<sub>2</sub> derived from decarbonation of limestone,
- CO<sub>2</sub> from fuel combustion in the kiln and
- CO<sub>2</sub> produced by vehicles in cement plants and distribution.

The production of 1 ton of cement produces about 0.55 tons of chemical CO<sub>2</sub> by carbonate dissociation (CaO +

CO<sub>2</sub>), at 1450 °C. Additionally, 0.4 tons of CO<sub>2</sub> is produced by the fuel and finally 0.05 ton is produced by vehicles in cement plants and distribution. resulting into a total emission of 1.0 tons of CO<sub>2</sub> per ton of cement (Davidovits, 2004). The total amount of cement used for the casing of the wells is 223,207 kg or 223.2 tons, which results in **223.2 tons of CO<sub>2</sub>**.

### 9.3 CO<sub>2</sub> Emission during drilling

According to the previous section on drilling, 8712 GJ is needed to construct the geothermal doublet. The emission factor of diesel for the Netherlands is 74.3 kg/GJ (see Appendix K), giving 8712 GJ x 74.3 kg/GJ = 647,302 kg CO<sub>2</sub>, or **647.3 ton CO<sub>2</sub>**.

### 9.4 CO<sub>2</sub> Emission during CO<sub>2</sub> capture

The energy consumption of a CO<sub>2</sub>-capture unit is approximately 1.5 kWh/kg CO<sub>2</sub> (5400 kJ/kg). The capture facility consumes 57,562 GJ/year to capture 90% of the emitted CO<sub>2</sub> by the central heating system. Heat is used to run the capture process, to produce this heat natural gas is used. The emission factor of natural gas is 56.7 kg/GJ. 42,639 GJ x 56.7 kg/GJ = 2,417,610 kg/year, or **3264 ton/year**.

### 9.5 CO<sub>2</sub> Emission during CO<sub>2</sub> compression

The compressor (with an efficiency of 80%) uses 1805 GJ/year of electricity to compress the CO<sub>2</sub> up to 40 bars. The emission factor of electricity in the Netherlands is 0.479 kg/kWh (US DOE, EIA-1605, 2007). The compressor emits 240,200 kg of CO<sub>2</sub>, or **240.2 ton CO<sub>2</sub>** annually.

### 9.6 CO<sub>2</sub> Emission avoided by geothermal energy

Currently the Delft University consumes 11 million cubic meters of natural gas annually, 40% of this is avoided due to use of geothermal energy. Using the heating value (HV) of natural gas (31.65 MJ/Nm<sup>3</sup>), gives an energy consumption of 348,150 GJ/year (=11.04 MW) for heating. Using the emission factor for natural gas (56.7 kg CO<sub>2</sub>/GJ), gives a cumulative CO<sub>2</sub> emission of 19.740 ton/year, or 54.08 ton/day at 100% natural gas use. In the DAP case 40% CO<sub>2</sub> is avoided which results in **7896 ton CO<sub>2</sub>** annually. This emission gain depends on the seasonal variations.

### 9.7 Total CO<sub>2</sub> emission over 30 years of operation

Figure 9.2 shows the total amount of CO<sub>2</sub> emitted during 30 years of operation. The net result (purple line) is positive. This means that more CO<sub>2</sub> is captured and saved, by using geothermal energy instead of natural gas, than is consumed during construction of the geothermal plant with co-injection and 30 years of operation (capture and compression). It is very difficult to determine the pay-back time using Figure 9.2, Figure 9.3 zooms in and only shows the first year of operation.

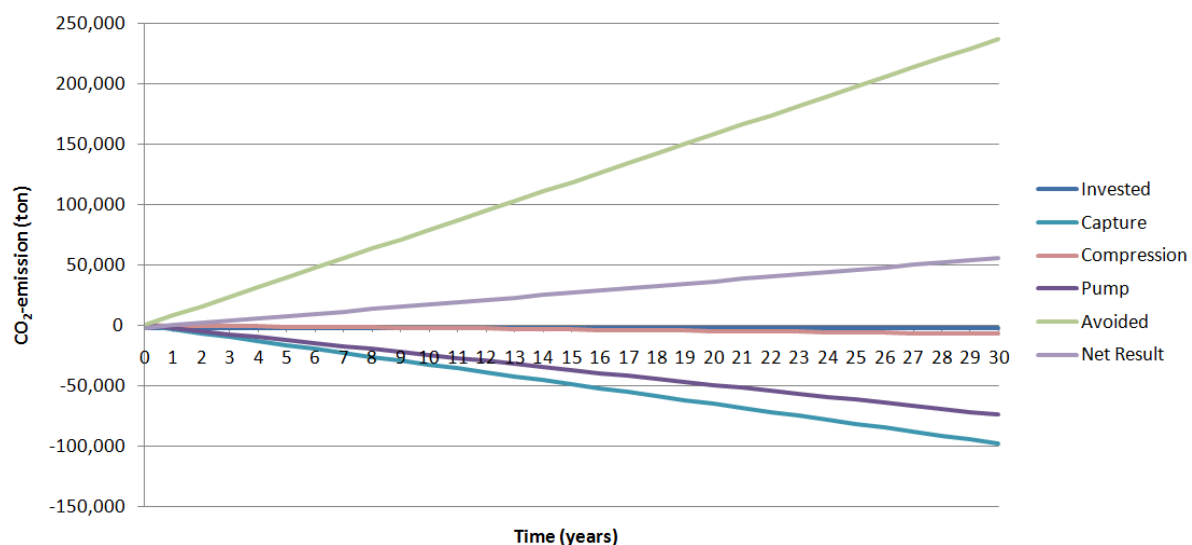


Figure 9.2: Total CO<sub>2</sub> emission over 30 years of operation

Figure 9.3 shows that the “pay-back” time is within the first year. The orange line shows the net result, when this line crosses the X-axis the invested CO<sub>2</sub> is pay-back. The line starts at -2133.5 tons of CO<sub>2</sub>, this is the invested CO<sub>2</sub> to produce the steel pipes, cement and the emission of the diesel engine which drives the drilling rig. The net result line crosses the X-axis after 1 year of operation.

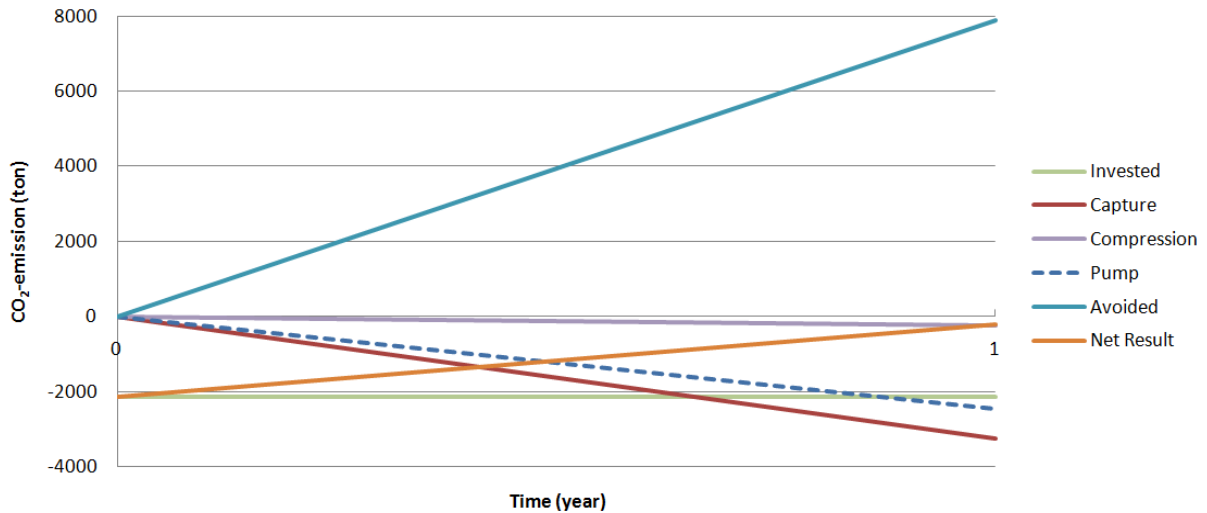


Figure 9.3: CO<sub>2</sub> emission within the first year of operation

Figure 9.4 makes it more clear, this figure only shows the invested CO<sub>2</sub> (green line) and the net result (orange line). The net result represent the avoided CO<sub>2</sub> minus the CO<sub>2</sub> emissions due to energy consumption during pumping of water and capture and compression of CO<sub>2</sub>. The net result has an up-ward slope which means that more CO<sub>2</sub> is avoided than emitted during the whole process. The net result line crosses the X-axis after 13 months of operation.

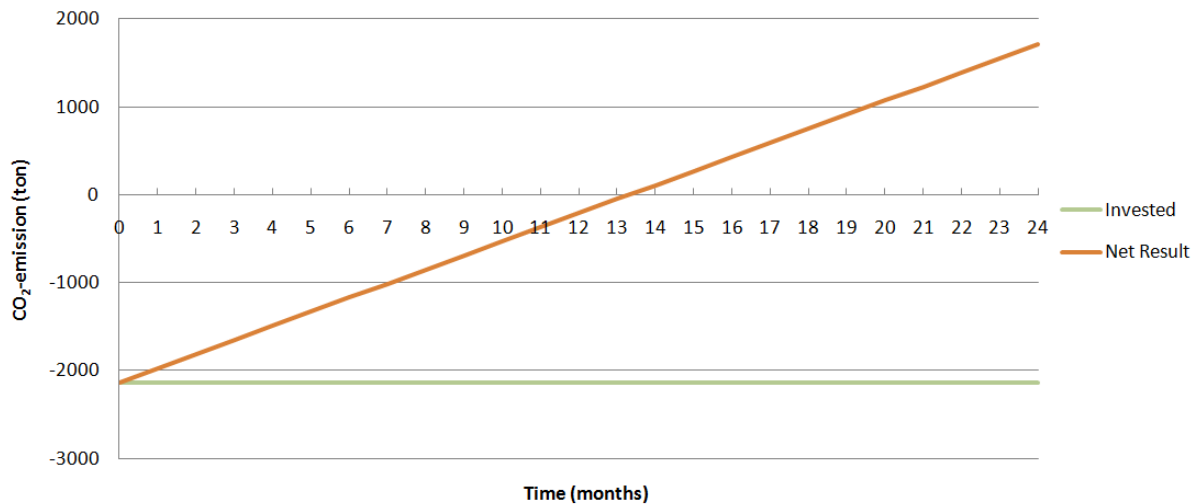


Figure 9.4: CO<sub>2</sub> emission within the first year of operation (basic)

## 10 Conclusion

- Currently the Delft University of Technology (DUT) consumes 11 million cubic meters of natural gas to fuel the combined heat and power plant. This causes an emission of 54 tons CO<sub>2</sub> every day, 19,740 ton/year. This emission can be lowered by using geothermal energy as a second energy source. Because the DUT uses a combined heat and power plant it is not convenient to produce 100% of the heat demand by the geothermal plant because the combined heat and power plant will also produce heat when it produces electricity. In this thesis 40% of the heat is produced by the geothermal doublet and 60% by the power plant. These values will fluctuate depending on the season.
- In the case of DAP, the potential amount of heat that can be delivered by the geothermal plant, can cover the annual heat demand for DUT. However, compensation for peak demand reduces the total supply; the remainder has to be produced by the conventional heating system using natural gas.
- By combining a geothermal doublet with a carbon capture and storage plant the total invested energy, CO<sub>2</sub> and also likely money will be lower than building both plants separately. When both plants are combined only once an investment in drilling energy and materials has to be done. So when a site is suitable for both technologies, always try to combine those.
- Right from the start the geothermal system produces more energy than the amount of energy needed for capture and compression. However, before energy is produced a lot of energy is already invested in the whole facility. In the case of geothermal energy a lot of energy is needed to drill the doublet and produce the required steel and cement. This investment in energy has to be earned back otherwise the investment is useless. In the case of DAP the invested energy and the energy needed to capture 90% of the emitted CO<sub>2</sub> by the combined heat and power plant (running at 60% capacity) is paid back within 4 months, this is of course under ideal conditions.
- The amount of energy invested in drilling and materials (steel and cement) is only a minor part of the total energy consumed over the whole life time of a geothermal system, including CO<sub>2</sub> co-injection. The largest energy consumption is caused by the capture process, which consumes around 93 % of the total energy input over a 30 year life time of the system.
- Not only energy is invested into the system, also CO<sub>2</sub>. During drilling and the production of the materials a large amount of CO<sub>2</sub> is emitted into the atmosphere. To produce 1 kg of steel 1.97 kg CO<sub>2</sub> is emitted. During the production of cement around 1 kg CO<sub>2</sub> is emitted for every kilogram cement produced, more than half of this emission is caused by carbonate dissociation. This investment is “paid back” (compensated) by avoiding more CO<sub>2</sub> than the amount of CO<sub>2</sub> which is emitted during capture and compression. By using geothermal heat instead of natural gas for heating purposes a lot of CO<sub>2</sub> can be avoided. In the case of DAP 40 % of the heat demand is produced by the geothermal well, which results in avoiding 7896 ton CO<sub>2</sub> annually. Under optimum conditions, the CO<sub>2</sub> pay-back time is within the first year, around 9 months.
- Even if the optimum conditions are not reached by far, the amount of CO<sub>2</sub> which is invested in the facility is always “paid back” within its lifetime of 30 years.
- Next to capturing and compression, losses in the production of geothermal energy can be seen as an energy investment. The two factors accounted to be power losses, i.e., dissipation due to friction along the wells (tubing), and reservoir permeability, both depend on the flow rate.
- Tubing diameter: Dissipation in the wells is correlated with the well tubing diameter; a smaller diameter causes more friction with the walls and by that an exponential increase of pumping energy is required.
- Reservoir permeability: Dissipation in the reservoir is affected by its permeability, i.e.; increasing permeability will result in decreasing energy consumption by the pump.

## 11 Recommendations and future work

- The result of this study depended on the availability and the quality of the data. To increase the accuracy of the excel model, more information has to be combined.
- For this thesis a model has been built to calculate the amount of energy and CO<sub>2</sub> which is consumed and avoided for an idealized case. Variations in input parameters, such as all temperatures, spacing, diameters, reservoir properties, etc. can be updated in the future when more site specific data is available.
- At the moment the model includes several parameters, to have a more accurate model more parameters have to be implemented in the future.
- Information with respect to heat exchanger and CCS infrastructure and associated energy investments for production and construction are minimal. This topic has to be included in the exergy analysis to make it complete. Note that the impact will be comparable to the input from the well configuration and probably will be minor.
- Transportation over land has not been included, since in the case of DAP the sites are next to each other. For other CCS-geothermal systems, transport could be an important contribution, so has to be included to make a good estimate and comparison between two potential sites.
- The model does not take into account that the cold re-injected water will be reheated slowly by the ground. To calculate the life-time of the geothermal well this is an important parameter to take into account.
- This work contributes to the modeling work for CO<sub>2</sub>-brine reservoir behavior as providing input parameters for the well configurations and (pre-defined) reservoir conditions.

## References

- Abanades, J.C., (2002): "Short communication The maximum capture efficiency of CO<sub>2</sub> using a carbonation/calcination cycle of CaO/CaCO<sub>3</sub>", Chemical Engineering Journal, 90, pp. 303–306
- Abu-Zahra, M.R.M., Niederer, J.P.M., Feron, P.H.M., Versteeg, G.F., (2007): "CO<sub>2</sub> capture from power plants - Part II. A parametric study of the economical performance based on mono-ethanolamine", International journal of greenhouse gas control 1 (2007) pp. 135 – 142
- Adam, D., (Article Guardian), (2008), "World carbon dioxide levels highest for 650,000 years, says US report", 13 May 2008.
- Anheden et al, (2005): "Denitrogenation (or Oxyfuel Concepts)", Oil & Gas Science and Technology – Rev. IFP, Vol. 60 (2005), No. 3, pp. 485-495
- Aspelund, A., Mølnvik, M.J. and De Koeijer, G., (2006): "Ship transport of CO<sub>2</sub> – technical solutions and analysis of costs, energy utilization, energy efficiency and CO<sub>2</sub> emissions", Chem. Eng. Res. Des. (Official journal of the European Federation of Chemical Engineering: Part A), pp. 847–855, 84–A9.
- Bailey, D.W. and Feron, P.H.M., (2005): "Post-combustion Decarbonisation Processes", Oil & Gas Science and Technology – Rev. IFP, Vol. 60 (2005), No. 3, pp. 461-474
- Barbier, E., (2002): "Geothermal energy technology and current status: an overview", Renewable and Sustainable Energy Reviews, 6, pp. 3–65.
- Beardsmore, G.R. & Cull, J.P., (2001): "Crustal Heat Flow – A guide to measurement and modelling". Cambridge University Press.
- Bentham, M. and Kirby, G., (2005): "CO<sub>2</sub> Storage in Saline Aquifers", Oil & Gas Science and Technology – Rev. IFP, Vol. 60, No. 3, pp. 559-567.
- Bertani, R. and Thain, I., (2002): "Geothermal power generating plant CO<sub>2</sub> emission survey", IGA News, 49, pp. 1-3, [www.geothermal-energy.org](http://www.geothermal-energy.org)
- Dewulf, J., H. V. Langenhove, et al. (2000): "Illustrations towards quantifying the sustainability of technology." Green Chemistry, Vol. 2, Issue 3, pp 108-114
- Bloomfield, K.K., Moore, J.N. and Neilson, R.N., (2003). "Geothermal energy reduces greenhouse gases", Geothermal Resources Council Bulletin, 32, pp. 77-79.
- BP, (2009): "BP Statistical Review of World Energy 2009", link: [www.bp.com/statisticalreview](http://www.bp.com/statisticalreview)
- BP, (2010): "BP Statistical Review of World Energy, June 2010", link: [www.bp.com/statisticalreview](http://www.bp.com/statisticalreview)
- Bryan Boggs, B. et al, (2005): "Extracting CO<sub>2</sub> from coal-fired plants using the benfield process", Submitted to: PPG Industries, Inc. at Natrium
- CATO Booklet, (2009): "Catching carbon to clear the skies: Experiences and highlights of the Dutch R&D programme on CCS", pp. 1-71
- CenSa, (Centre of Sustainability Accounting), (2002): UK research report, written by Thomas Wiedmann and Jan Minx.
- Chang-qing, H., Li-yun, C., Chun-xia, Z., Yuan-hong, Q. and Rui-yu, Y., (2006): "Emission Mitigation of CO<sub>2</sub> in Steel Industry: Current Status and Future Scenarios", Journal of Iron and Steel Research International, Volume 13, Issue 6, pp. 38-42

CO<sub>2</sub>NET, (2007): 5 Powerpoint Lectures on Carbon Capture and Storage, made by: Egmond, S., Damen, K., Hagedoorn, S., Lysen, E., (Utrecht Centre for Energy research)

Costa, M.M., Schaeffer, R. and Worrell, E., (2001): "*Exergy accounting of energy and materials flows in steel production systems*", Energy, 26, pp. 363–384

Damen, K., (2007): Book, Title: "*Reforming Fossil Fuel Use, The Mertis, Costs and Risks of Carbon Dioxide Capture and Storage*".

Damen, K., Faaij, A., Turkenburg, W., (2009): "*Pathways towards large-scale implementation of CO<sub>2</sub> capture and storage: A case study for the Netherlands*", International Journal of Greenhouse Gas Control, 3, pp. 217-236

Daniëls, B.W., Farla, J.C.M., (2006): "*Potentieelverkenning klimaatdoelstellingen en energiebesparing tot 2020. Analyses met het Optiedocument energie en emissies 2010/2020*", Energy research Centre of the Netherlands, National Institute for Public Health and the Environment, Petten.

DAP, (2008): "*Feasibility study*". Stichting Delft Aardwarmte Project & Delft Aardwarmte Project B.V.

Davidovits, J., (2004): "*Up to 80% reduction of CO<sub>2</sub> Greenhouse Gas Emissions during Cement Manufacture*", Geopolymer Institute, website: [www.geopolymer.org/library](http://www.geopolymer.org/library)

Davison, J., (2007): "*Performance and costs of power plants with capture and storage of CO<sub>2</sub>*", Energy, 32, pp. 1163 – 1176

Handbook of Delucchi: <http://www.its.ucdavis.edu/people/faculty/delucchi/index.php#AdvancedVehicles>, visited 08-07-2010

Dickson, M. H. and Fanelli, M., (2004): "*What is Geothermal Energy?*", Istituto di Geoscienze e Georisorse, CNR, Pisa, Italy, For: The International Geothermal Association, link: <http://www.geothermal-energy.org/>

De Jager, J. et al, (1996): "*Hydrocarbon habitat of the West Netherland Basin*". In: Rondeel, et al. (eds), Geology of gas and oil under the Netherlands, Kluwer Academic Publishers, pp.191-209.

De Jager, J., (2007): "*Geological Development*". In: Wong, Th. E., Batjes, D.A.J. & De Jager, J., Geology of the Netherlands, Royal Netherlands Academy of Arts and Sciences, pp. 5-26.

Den Boer, C., (August 2008): "*BSc thesis: Doublet spacing in the "Delft Aardwarmte Project"*". TU Delft.

Den Hartog Jager, D.G., (1996): "*Fluviomarine sequences in the Lower Cretaceous of the West Netherlands Basin: correlation and seismic expression*" In: Rondeel, et al. (eds), Geology of gas and oil under the Netherlands, Kluwer Academic Publishers, pp.229-241.

Drbal, L.F., (1996): "Black & Veatch power plant engineering. New York: Chapman & Hall, In: Zhang, Z.X., Wang, G.X., Massarotto, P., and Rudolph, V., (2006): "Optimization of pipeline transport for CO<sub>2</sub> sequestration", Energy Convers Manage 47, 6, pp. 702–715.

Duana, Z. and Sun, R, (2003): "*An improved model calculating CO<sub>2</sub> solubility in pure water and aqueous NaCl solutions from 273 to 533 K and from 0 to 2000 bar*", Chemical Geology, 193, pp. 257– 271

Duan, Z., Sun, R., Zhu, C. and Chou, I., (2006): "*An improved model for the calculation of CO<sub>2</sub> solubility in aqueous solutions containing Na<sup>+</sup>, K<sup>+</sup>, Ca<sup>2+</sup>, Mg<sup>2+</sup>, Cl<sup>-</sup>, and SO<sub>4</sub><sup>2-</sup>*", Marine Chemistry, 98, pp. 131–139

Ecofys (Vosbeek, M. (Ecofys) and Warmenhoven, H. (Spinconsult)), (2006): "*Making large-scale Carbon Capture and Storage CCS in the Netherlands Work, An agenda for 2007-2020 Policy, Technology and Organisation.*", This report has been written at the request of EnergieNed and the Dutch Ministries of the Environment and Economic Affairs.

- Ecofys, (2009): Energiesymposium 16 oktober 2009, title document: "Factsheet Diepe Geothermie", website: <http://geothermie.nl/actueel/nieuws/nieuws-single-display/article/factsheet-diepe-geothermie-geactualiseerd/>
- Eide L.I. and Bailey, D.W., (2005): "Precombustion Decarbonisation Processes", Oil & Gas Science and Technology – Rev. IFP, Vol. 60 (2005), No. 3, pp. 475-484
- European Industrial Gases Association (EIGA), (2008): "Carbon Dioxide Source Qualification Quality Standards and Verification", IGC Doc 70/08/E
- Frost, M., (2008): "Carbon Capture and Storage", website: <http://www.martinfrost.ws/>
- Gale, J. and Davison, J., (2004): "Transmission of CO<sub>2</sub>—safety and economic considerations", Energy, 29, pp. 1319 – 1328
- Gielen, D. and Moriguchi, Y., (2002): "CO<sub>2</sub> in the iron and steel industry: an analysis of Japanese emission reduction potentials", Energy Policy, 30, pp. 849 - 863
- Gilding, D.T., (2010): "Master Thesis: Heterogeneity determination of the Delft subsurface for heat flow modelling", TU Delft
- Gozalpour, F., Ren, S.R. and Tohidi, B., (2005): "CO<sub>2</sub> EOR and Storage in Oil Reservoirs", Oil & Gas Science and Technology – Rev. IFP, Vol. 60 (2005), No. 3, pp. 537-546
- Grobbelen, J., Van Driel, W.W., De Coo, J.C.M., 2009: "Aardwarmte Pijnacker", Geologisch onderzoek Ammerlaan Grond- & Hydrocultuur, Panterra Rapport G746 (2009).
- Gudmundsson, J.S., (1988): "The elements of direct uses", Geothermics, 17, pp. 119 – 136
- Gupta, H. and Fan, S., 2002: "Carbonation-Calcination Cycle Using High Reactivity Calcium Oxide for Carbon Dioxide Separation from Flue Gas", Ind. Eng. Chem. Res. 2002, 41, pp. 4035-4042
- Hamilton, M.R., Herzog, H.J. and Parsons, J.E., (2008): "Project financing of new coal power plants with carbon capture and sequestration", Proceedings of the 9th International Conference on Greenhouse Gas Control.
- Heggum, G., Weydahl, T., Mo, R., Møltnvik, M., and Austegard, A., (2005): "CO<sub>2</sub> conditioning and transportation", In: D.C. Thomas and S.M. Benson, Editors, *Carbon Dioxide Capture for Storage in Deep Geologic Formations* Vol. 2, Elsevier, Oxford, UK
- Hepbasli, A., (2008): "A key review on exergetic analysis and assessment of renewable energy resources for a sustainable future", Renewable and Sustainable Energy Reviews, 12, pp. 593–661
- Herzog, H. and Golomb, D., (2004): "Carbon capture and storage from fossil fuel use", *Encyclopedia of Energy*, Elsevier Science Inc., New York (2004), pp. 277–287.
- International Energy Agency Greenhouse Gas R&D Programme (IEA GHG), 2002: "Opportunity for early application of CO<sub>2</sub> sequestration technology", Report Number PH4/10 September 2002
- IEA Greenhouse Gas R&D Programme, (2009): "CO<sub>2</sub> capture and storage: What is CO<sub>2</sub> capture and storage", website: <http://www.co2captureandstorage.info/whatisccs.htm>, visited on 21-08-2009.
- IPCC, (2005): "IPCC Special Reports, title: Carbon Dioxide Capture and Storage", link: <http://www.ipcc.ch/>
- Janssen, L.P.B.M. and Warmoeskerken, M.M.C.G., (2001): "Transport Phenomena: Data Companion", Table: Friction factor for flow in tubes, page 84.

- Karakus, A.A., Boyar, S., Akdeniz, R.C. and Hepbasli, A., (2002): "An exergy analysis in a mixed feed industry: evaluation of an extruder pellet line", EE&AE'2002 – International Scientific Conference – 04-06.04.2002, Rousse, Bulgaria
- Kim, Y. and Worrel, E., (2002) : "*International comparison of CO<sub>2</sub> emission trends in the iron and steel industry*", Energy Policy, 30, pp. 827 - 838
- Klein Goldewijk, K., Olivier, J.G.J., Peters, J.A.H.W., Coenen, P.W.G.H., Vreuls, H.H.J., (2005): "*Greenhouse Gas Emissions in the Netherlands 1990–2003*", National Inventory Report 2005. National Institute for Public Health and the Environment. RIVM/MNP, Bilthoven
- Koornneef, J., Spruijt, M., Molagb, M., Ramirez, A., Faaija, A. and Turkenburg, W., (2009): "*Uncertainties in risk assessment of CO<sub>2</sub> pipelines*", Energy Procedia, 1, pp. 1587 - 1594
- Kvamsdala, H.M., Jordala, K., Bollandb, O., (2007): "*A quantitative comparison of gas turbine cycles with CO<sub>2</sub> capture*", Energy, 32, pp. 10–24
- Leijnse, S., (2008): BSc Thesis: "Drilling hazards for the DAP geothermal wells", July 2008
- Lenzen, M. And Dey, C.S., (2000): "*Truncation Error in Embodied Energy Analysis of Basic Iron and Steel Production*", Energy, 25, pp. 577 – 585
- Lindal, B., (1973): "*Industrial and other applications of geothermal energy*", In: Armstead, H.C.H., ed., Geothermal Energy, UNESCO, Paris, pp.135 – 148
- Lokhorst, A & Wong, Th. E., 2007: "*Geothermal Energy*". In: Wong, Th. E., Batjes, D.A.J. & De Jager, J., Geology of the Netherlands, Royal Netherlands Academy of Arts and Sciences, pp. 5-26.
- McCoy, S., and Rubin, E., (2008): "*An engineering–economic model of pipeline transport of CO<sub>2</sub> with application to carbon capture and storage*", International Journal of Greenhouse Gas Control 2, 2, pp. 219–229.
- MacKenzie, A., Granatstein, D.L., Anthony, E.J. and Abanades, J.C., (2007): "*Economics of CO<sub>2</sub> Capture Using the Calcium Cycle with a Pressurized Fluidized Bed Combustor*", Energy & Fuels, 21, pp. 920 - 926
- NACAP, writers: Nazary, S. and Griffioen, A., Title document: "*Carbon Footprint of pipeline projects: A cradle-to-gate research*"
- Oexmann, J., Kather, A., (2009): "*Post-combustion CO<sub>2</sub> capture in coal-fired power plants: comparison of integrated chemical absorption processes with piperazine promoted potassium carbonate and MEA*", Energy Procedia, 1, pp. 799 - 806
- Ogden, J., Yang, C., Johnson, N., Ni, J., Johnson, J., (2004): "*Conceptual Design of Optimized Fossil Energy Systems with Capture and Sequestration of Carbon Dioxide*", Report to the U.S. Department of Energy National Energy Technology Laboratory (September 30, 2004)
- Parker, N., (2004): "*Using Natural Gas Transmission Pipeline Costs to Estimate Hydrogen Pipeline Costs*", UCD-ITS-RR-04-35, Institute of Transportation Studies – University of California, Davis
- Pochodaj, D., (2005): "*Wall thickness and diameter of pipelines*", Norwegian University of Science and Technology, Department of Petroleum Engineering and Applied Geophysics
- Rao, A. and Rubin, E., (2002): "*Technical, Economic and Environmental Assessment of Amine-based CO<sub>2</sub> Capture Technology for Power Plant Greenhouse Gas Control*", Environ. Sci. Technol., 36, pp. 4467-4475
- REN21, (2007): "*Renewables 2007: Global Status Report*", A Pre-Publication Summary for the UNFCCC COP13 REN21 Renewable Energy Policy Network for the 21st Century, location: Bali, Indonesia - December 2007

- Romano, M., (2008): "*Coal-fired power plant with calcium oxide carbonation for post-combustion CO<sub>2</sub> capture*", Energy Procedia, 1, pp. 1099 - 1106
- Samuel G. R. and McColpin G., (2001): "*Wellbore Hydraulic Optimization with positive displacement motor and bit*", paper by SPE (Society of Petroleum Engineers), IADC/SPE 72320
- Sandberg, H., Lagneborg, R., Lindblad, B., Axelsson, H. and Bentell, L., (2001): "*CO<sub>2</sub> emissions of the Swedish steel industry*", Scandinavian Journal of Metallurgy, 30, pp. 420 – 425
- SenterNovem, (2009): "*The Netherlands: list of fuels and standard CO<sub>2</sub> emission factors*", research request of the Ministry of VROM (Spatial Planning, Housing and the Environment). Originally approved in 2004 by the Steering Committee Emission Registration, revised on 25 April 2006 and 21 April 2009
- Shi, J.Q. and Durucan, S., (2005): "*CO<sub>2</sub> Storage in Deep Unminable Coal Seams*", Oil & Gas Science and Technology – Rev. IFP, Vol. 60 (2005), No. 3, pp. 547-558
- Simmelink, H.J., Vandeweyer, V., Ramaekers, J., 2007: "*Geologisch locatiespecifiek onderzoek voor het Business Plan Geothermie Den Haag Zuid-West*". TNO-Rapport ([www.geothermie.nl](http://www.geothermie.nl)).
- Smits, P.F., 2008: "*MSc thesis paper: Construction of an integrated reservoir model using the Moerkapelle field for geothermal development of the Delft sandstone.*" TU Delft.
- Swaan Arons, de J. and Kooi, van der H., (2004): "*Efficiency and Sustainability in the Energy and Chemical Industries*", Book by Marcel Dekker Inc., ISBN: 0-8247-0845-8
- Szargut, J.T., (2003): "*Anthropogenic and natural exergy losses (exergy balance of the Earth's surface and atmosphere)*", Energy, 28, pp. 1047–1054
- TNO-NITG, (2006): "*Olie en gas in Nederland. Jaarverslag 2005 en prognose 2006–2015*", Netherlands Institute of Applied Geoscience TNO – National Geological Survey, Den Haag
- Undrum, H., Bolland, O., and Aarebrot, E., (2000): "*Economical assessment of natural gas fired combined cycle power plant with CO<sub>2</sub> capture and sequestration*", Proceedings of the 5th Greenhouse Gas Control Technologies Conference (GHGT5), 13 - 16 August, Cairns, Australia, CSIRO Publishing
- US Department of Energy, Energy Efficiency & Renewable Energy, 2006: "*Geothermal Technologies Program, 2006, Geothermal FAQs*", link: <http://www1.eere.energy.gov/geothermal/faqs.html>
- U.S. Department of Energy Energy Information Administration, (2007): "*Voluntary Reporting of Greenhouse Gases: Appendix F. Electricity Emission Factors*", Form EIA-1605, pp. 121 – 128
- Van Adrichem Boogaert, H.A. & Kouwe, W.F.P., 1993: "*Stratigraphic nomenclature of The Netherlands; revision and update by RGD and NOGEPA*". Mededelingen Rijks Geologische Dienst, nr 50.
- Vis, G.-J., Van Gessel, S.F., Mijnlief, H.F., Pluymaekers, M.P.D., Hettelaar, J.M.M., Stegers D.P.M. 2010: "*Lower Cretaceous Rijnland Group aquifers in the West Netherlands Basin: suitability for geothermal Energy*", TNO-034-UT-2009-02410
- Wall, G., (1987): "*Exergy Conversion in the Swedish Society*", report no. 80-1, Physical Resource Theory Group, Göteborg, *Resources and Energy*, vol. 9, pp. 55-73
- Wong, C.S., and Matear, R., (1993): "*The storage of anthropogenic carbon dioxide in the ocean*," Energy Conversion Management, volume 34, issues 9-11, pp. 873–880.
- Worldwatch Institute: "*World Population Prospects between 1950 – 2050*", Worldwatch Institute data from U.N. Population Division, World Population Prospects

Worrell, E., Price, L., Martin, N., (2001): "*Energy efficiency and carbon dioxide emissions reduction opportunities in the US iron and steel sector*", *Energy*, 26, pp. 513 – 536

Zeman, M., (2008): "Lecture Document: Chapter 1: Introduction to photovoltaic solar energy" Course: Solar Cells, TU Delft

Zeman, F. & Lackner, K. (2008), "*The Reduced Emission Oxygen Kiln: A White Paper Report for the Cement Sustainability Initiative of the World Business Council on Sustainable Development*", Lenfest Center for Sustainable Energy, Columbia University in New York, Report No. 2008.01

Zhang, Z.X., Wang, G.X., Massarotto, P., and Rudolph, V., (2006): "*Optimization of pipeline transport for CO<sub>2</sub> sequestration*", *Energy Convers Manage* 47, 6, pp. 702–715.

# Appendix

## List of Figures Appendix

Figure 3.1: <i>CO<sub>2</sub> capture and storage from power plants</i> .....	58
Figure 4.1: <i>Emissions of CO<sub>2</sub> from fossil fuel use (2010)</i> .....	61
Figure 4.2: <i>World map of CO<sub>2</sub> emitters (point sources)</i> .....	62
Figure 5.1: <i>Post-combustion process in power cycle (Damen, 2007)</i> .....	64
Figure 5.2: <i>Pre-combustion (Damen, 2007)</i> .....	65
Figure 5.3: <i>Oxy-fuel (Damen, 2007)</i> .....	65
Figure 5.4: <i>Technology options for CO<sub>2</sub> separation and capture (Rao, A. and Rubin, E., 2002)</i> .....	66
Figure 5.5: <i>Chemical and physical absorption (CO<sub>2</sub>Net, 2007)</i> .....	67
Figure 5.6: <i>Chemical and physical adsorption (CO<sub>2</sub>Net, 2007)</i> .....	67
Figure 5.7: <i>Natural gas fired combined cycle with post combustion CO<sub>2</sub> capture (Undrum et al., 2000)</i> .....	69
Figure 5.8: <i>Simplified flow sheet of CO<sub>2</sub> capture process by wet chemical absorption (MEA)</i> .....	70
Figure 5.9: <i>Schematic overview of the Benfield Process (Boggs et al, 2005)</i> .....	71
Figure 5.10: <i>Calcium sorbent cycle for carbon dioxide capture (MacKenzie, 2007)</i> .....	71
Figure 5.11: <i>CO<sub>2</sub> captured vs. CO<sub>2</sub> avoided (Herzog and Golomb, 2004)</i> .....	72
Figure 6.1: <i>Blueprint for a pipeline infrastructure (CATO, 2009)</i> .....	74
Figure 6.2: <i>Main processes in the transport system (Aspelund et al., 2006)</i> .....	75
Figure 6.3: <i>Optimal transport pressure (Aspelund et al., 2006)</i> .....	76
Figure 6.4: <i>Typical arrangements for a CO<sub>2</sub> ship (Aspelund et al., 2006)</i> .....	76
Figure 7.1: <i>Different types of storage options (Frost, 2008)</i> .....	78
Figure 7.2: <i>Conceptual diagrams of storage in unconfined and confined aquifers (Bentham, 2005)</i> .....	80
Figure 7.3: <i>Simplified diagram of the Sleipner CO<sub>2</sub> storage project</i> .....	80
Figure 7.4: <i>A schematic of coal structure</i> .....	81
Figure 7.5: <i>Enhanced oil recovery</i> .....	81
Figure 7.6: <i>Storage availability in time (Damen et al., 2009)</i> .....	82
Figure 7.7: <i>The locations and sizes of potential storage sites in the Netherlands (CATO, 2009)</i> .....	83
Figure 9.1: <i>Crude steel production (Kim et al, 2002)</i> .....	88
Figure 9.2: <i>CO<sub>2</sub> emissions for the iron and steel industry (Kim et al, 2002)</i> .....	89
Figure 9.3: <i>CO<sub>2</sub> intensities for the iron and steel industry (Kim et al, 2002)</i> .....	89
Figure 9.4: <i>Final energy use for US iron and steel production (Worrel et al, 2001)</i> .....	90
Figure 9.5: <i>Carbon dioxide emissions from the energy consumption in the US iron and steel industry</i> .....	90
Figure 9.6: <i>Steel pipe production process (Nacap)</i> .....	92
Figure 9.7: <i>CO<sub>2</sub> emissions in steel pipe production</i> .....	93
Figure 9.8: <i>CO<sub>2</sub> emissions for the transport of pipes and equipment</i> .....	94
Figure 9.9: <i>CO<sub>2</sub> emissions of equipment</i> .....	95
Figure 9.10: <i>CO<sub>2</sub> emissions from other items</i> .....	95
Figure 9.11: <i>Total CO<sub>2</sub> emissions for laying a pipeline</i> .....	96
Figure 9.12: <i>Intersection of cylinder (Pochodaj, 2005)</i> .....	103

## List of Tables Appendix

Table 3.1: <i>Current maturity of CCS system components (IPCC report 2005, page 8)</i> .....	59
Table 4.1: <i>Purity of CO<sub>2</sub> sources (CO<sub>2</sub>NET, 2009)</i> .....	61
Table 5.1: <i>Commercially available chemical solvent processes (Website NETL)</i> .....	64
Table 5.2: <i>Integration of CO<sub>2</sub> capture technologies in power cycles</i> .....	66
Table 5.3: <i>CO<sub>2</sub> capture matrix</i> .....	69
Table 5.4: <i>Performance summary (Undrum, 2000)</i> .....	70
Table 6.1: <i>Properties of gaseous supercritical and liquid CO<sub>2</sub> (Zhang et al, 2006)</i> .....	74
Table 6.2: <i>CO<sub>2</sub> transport analysis (Aspelund et al., 2006)</i> .....	76
Table 7.1: <i>Properties of CO<sub>2</sub> storage site (IPCC, 2005)</i> .....	78
Table 7.2: <i>The worldwide capacity of potential CO<sub>2</sub> storage reservoirs (Herzog, 2004)</i> .....	79
Table 7.3: <i>Technical CO<sub>2</sub> storage potential in the Netherlands (Damen et al., 2009)</i> .....	82
Table 9.1: <i>Energy consumption and CO<sub>2</sub> emissions in 1986 and 1994 (Kim et al, 2002)</i> .....	91
Table 9.2: <i>Total primary energy consumption and CO<sub>2</sub> emissions (global average) per ton of steel</i> .....	91
Table 9.3: <i>CO<sub>2</sub> emissions in steel pipe production</i> .....	92
Table 9.4: <i>CO<sub>2</sub> emissions for the transport of pipes and equipment</i> .....	93
Table 9.5: <i>CO<sub>2</sub> emissions of different type of equipment</i> .....	94
Table 9.6: <i>CO<sub>2</sub> emissions from other items</i> .....	95
Table 9.7: <i>Total CO<sub>2</sub> emissions for laying a pipeline</i> .....	96

## Appendix A: Article Guardian

### World carbon dioxide levels highest for 650,000 years, says US report

- *Rise in chief greenhouse gas worse than feared*
- *Earth may be losing ability to absorb CO<sub>2</sub>, say scientists*

**David Adam, environment correspondent**

**The Guardian, Tuesday 13 May 2008**

The concentration of carbon dioxide in the atmosphere has reached a record high, according to the latest figures, renewing fears that climate change could begin to slide out of control.

Scientists at the Mauna Loa observatory in Hawaii say that CO<sub>2</sub> levels in the atmosphere now stand at 387 parts per million (ppm), up almost 40% since the industrial revolution and the highest for at least the last 650,000 years.

The figures, published by the US National Oceanic and Atmospheric Administration on its website, also confirm that carbon dioxide, the chief greenhouse gas, is accumulating in the atmosphere faster than expected. The annual mean growth rate for 2007 was 2.14ppm - the fourth year in the last six to see an annual rise greater than 2ppm. From 1970 to 2000, the concentration rose by about 1.5ppm each year, but since 2000 the annual rise has leapt to an average 2.1ppm.

Scientists say the shift could indicate that the Earth is losing its natural ability to soak up billions of tonnes of CO<sub>2</sub> each year. Climate models assume that about half our future emissions will be reabsorbed by forests and oceans, but the new figures confirm this may be too optimistic. If more of our carbon pollution stays in the atmosphere, it means emissions will have to be cut by more than is currently projected to prevent dangerous levels of global warming.

Martin Parry, co-chair of the Intergovernmental Panel on Climate Change's working group on impacts, said: "Despite all the talk, the situation is getting worse. Levels of greenhouse gases continue to rise in the atmosphere and the rate of that rise is accelerating. We are already seeing the impacts of climate change and the scale of those impacts will also accelerate, until we decide to do something about it."

Perched some 11,000ft up a volcano, the Mauna Loa observatory has been measuring carbon dioxide in the atmosphere since 1958. It is regarded as producing among the most reliable data sets because of its remote location, far from any possible source of the gas that could confuse the sensors.

Over the decades, the Mauna Loa readings, made famous in Al Gore's documentary *An Inconvenient Truth*, show the CO<sub>2</sub> level rising and falling each year as foliage across the northern hemisphere blooms in spring and recedes in autumn. But they also show an upward trend as human emissions pour into the atmosphere, and each spring, the total CO<sub>2</sub> level creeps above the previous year's high to set a new record.

Robin Oakley, head of Greenpeace's climate change campaign, said: "We're now witnessing a key moment in the climate change story, and it's not good news. The last time the atmosphere was this choked with CO<sub>2</sub> humans were yet to evolve as a species. To even consider building new runways and coal-fired power stations at this juncture in history is an unpardonable folly, but Gordon Brown seems determined to stumble forward regardless with his ill-conceived plans in the face of the science and widespread public opposition."

A study last year suggested that the recent surge in atmospheric CO<sub>2</sub> levels was down to three processes: growth in the world economy, heavy use of coal in China, and a weakening of natural "sinks", forests, seas and soils that absorb carbon. The scientists said the increase was 35% larger than they expected.

They said about half of the carbon surge was down to the Chinese reliance on coal, which has forced up the carbon intensity of the overall world economy since 2000, reversing a trend of increasing energy efficiency since the 1970s.

---

## Appendix B: Chapter 3: Carbon Capture and Storage (CCS)

### 3 Carbon Capture and Storage (CCS)

This chapter describes carbon capture and storage (CCS). The chapter is divided into four paragraphs. The first paragraph describes what CCS is. After this the following paragraphs describe the environmental effects, risks and maturity of CCS.

#### 3.1 What is CCS?

Carbon capture and storage is a set of technologies aimed at capturing carbon dioxide emitted from industrial and energy-related processes before it enters the atmosphere, compressing the CO<sub>2</sub>, and storing it for long-term (indefinitely) in formations such as depleted natural gas fields, deep saline aquifers and unmineable coal seams. CCS is not a new technology. CO<sub>2</sub> has been captured for nearly 100 years for industrial purposes or to increase oil or gas production. CCS technology can reduce carbon dioxide emissions from large industrial sources and coal-fired power stations by approximately 85 - 90% depending on the type of capture technology used (Undrum et al, 2000). CCS has the potential to be an essential technology to significantly reduce greenhouse gas emissions and allow the continued use of fossil fuels for energy security, without further damaging climate security. According to Koornneef (2009) carbon capture and storage is often considered in literature as one of the temporary technological solutions to control CO<sub>2</sub> emissions from large point sources.

#### 3.2 Environmental effects

The merit of CCS systems is the reduction of CO<sub>2</sub> emissions by up to 85 – 90%, depending on plant type. Generally, environmental effects from use of CCS arise during power production, CO<sub>2</sub> capture, transport and storage. Additional energy is required for CO<sub>2</sub> capture, and this means that substantially more fuel has to be used, depending on the plant type. For new supercritical pulverized coal (PC) plants using current technology, the extra energy requirements range from 24-40%, while for natural gas combined cycle (NGCC) plants the range is 11-22% and for coal-based gasification combined cycle (IGCC) systems it is 14-25% (IPCC, 2005). Obviously, fuel use and environmental problems arising from mining and extraction of coal or gas increase accordingly. Plants equipped with flue gas desulfurization (FGD) systems for SO<sub>2</sub> control require proportionally greater amounts of limestone, and systems equipped with selective catalytic reduction (SCR) systems for NO<sub>x</sub> require proportionally greater amounts of ammonia.

IPCC has provided estimates of air emissions from various CCS plant designs. While CO<sub>2</sub> is drastically reduced (though never completely captured), emissions of air pollutants increase significantly, generally due to the energy penalty of capture. Hence, the use of CCS entails a reduction in air quality.

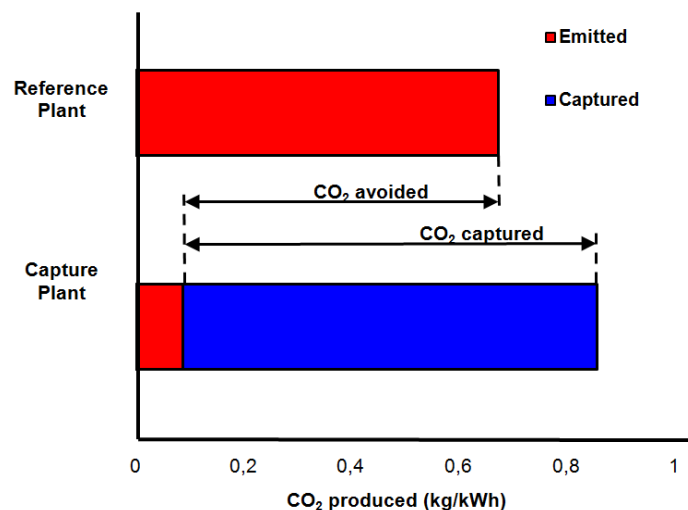


Figure 3.1: CO<sub>2</sub> capture and storage from power plants

Figure 3.1 shows the CO<sub>2</sub> emission of a power plant with and without capture plant. The capture plant causes a loss in overall efficiency for the power plant. Additional energy is required for capture, transport and storage and any leakage from transport. This results in a larger amount of “CO<sub>2</sub> produced per unit of product” (lower bar) relative to the reference plant (upper bar) without capture (IPCC, 2005).

### 3.3 Risk of CCS

A major concern with CCS is whether leakage of stored CO<sub>2</sub> will compromise CCS as a climate change mitigation option. For well-selected geological storage sites, IPCC (Intergovernmental Panel on Climate Change) estimates that risks are comparable to those associated with current hydrocarbon activity. CO<sub>2</sub> could be trapped for millions of years, and well selected stores are likely to retain over 99% of the injected CO<sub>2</sub> over 1000 years. For ocean storage, the retention of CO<sub>2</sub> would depend on the depth; IPCC estimates 30–85% would be retained after 500 years for depths 1000 – 3000 m. Mineral storage is not regarded as having any risks of leakage. The IPCC recommends that limits be set to the amount of leakage that can take place. The IPCC is a scientific intergovernmental body tasked with reviewing and assessing the most recent scientific, technical and socio-economic information produced worldwide relevant to the understanding of climate change.

It should also be noted that at the conditions of the deeper oceans, (about 400 bar or 40 MPa, 280 K) water–CO<sub>2</sub>(l) mixing is very low (where carbonate formation/acidification is the rate limiting step), but the formation of water–CO<sub>2</sub> hydrates is favourable (a kind of solid water cage that surrounds the CO<sub>2</sub>).

To further investigate the safety of CO<sub>2</sub> sequestration, we can look into Norway's Sleipner gas field, as it is the oldest plant that stores CO<sub>2</sub> on an industrial scale. According to an environmental assessment of the gas field which was conducted after ten years of operation, the author affirmed that geosequestration of CO<sub>2</sub> was the most definite way to store CO<sub>2</sub> permanently.

"Available geological information shows absence of major tectonic events after the deposition of the Utsira formation [saline reservoir]. This implies that the geological environment is tectonically stable and a site suitable for carbon dioxide storage. The solubility trapping is the most permanent and secure form of geological storage."

### 3.4 Maturity of CCS

In Table 3.1 the X's indicate the highest level of maturity for each component. For most components, less mature technologies also exist (IPCC report, 2005, page 8).

**Table 3.1:** Current maturity of CCS system components (IPCC report 2005, page 8)

CCS Component	CCS technology	Research phase	Demonstration phase	Economically feasible under specific conditions	Mature market
<b>Capture</b>	Post-combustion			X	
	Pre-combustion			X	
	Oxyfuel combustion		X		
	Industrial separation (natural gas processing, ammonia production)				X
<b>Transportation</b>	Pipeline				X
	Shipping			X	
<b>Geological storage</b>	Enhanced Oil Recovery (EOR)				X
	Gas or oil fields			X	
	Saline formations			X	
	Enhanced Coal Bed Methane recovery (ECBM)		X		
<b>Ocean storage</b>	Direct injection (dissolution type)	X			
	Direct injection (lake type)	X			
<b>Mineral carbonation</b>	Natural silicate minerals	X			
	Waste materials		X		
<b>Industrial uses CO<sub>2</sub></b>					X

---

## Appendix C: Chapter 4: CO<sub>2</sub> sources

## 4 CO<sub>2</sub> sources

The main sources of CO<sub>2</sub> emission are power generation, industrial processes, transportation and residential and commercial buildings. Figure 4.1 shows a pie chart of the CO<sub>2</sub> emissions per sector in 2001. The total world emission of CO<sub>2</sub> in 2001 was 23,684 Mt/year (Davison, 2007). According to CO<sub>2</sub>Net (2007) the total CO<sub>2</sub> emissions are much higher because Davison does not include the emission caused by land use (deforestation). The emission caused by land use are 1.6 Gt C/year (6 Gt CO<sub>2</sub>/year), the emission caused by fossil fuels consumption are 6 Gt C/year (23.625 Gt CO<sub>2</sub>/year). Hence the total emission of anthropogenic CO<sub>2</sub> will be around 30 Gt CO<sub>2</sub>/year of which 80% is caused by the use of fossil fuels and 20% caused by the use of land.

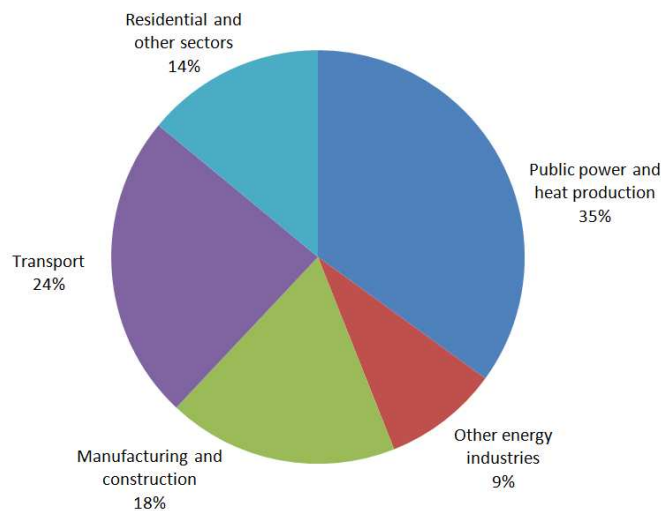


Figure 4.1: Emissions of CO<sub>2</sub> from fossil fuel use (2010)

The annual Dutch CO<sub>2</sub> emission is nearly 180 Mt CO<sub>2</sub> at present, of which approximately 100 Mt CO<sub>2</sub>/year emitted by the energy and manufacturing industry (Klein Goldewijk et al., 2005). Table 4.1 shows a list of CO<sub>2</sub> producers and the purity of their CO<sub>2</sub> stream.

Table 4.1: Purity of CO<sub>2</sub> sources (CO<sub>2</sub>NET, 2009)

Sources	Purity
Ammonia	100%
Ethylene oxide	100%
Gas processing	100%
Hydrogen	10 – 100%
Cement	15 – 30%
Iron and steel	15%
Ethylene	10 – 15%
Power	3 – 15%
Refineries	3 – 13%

The purity of the CO<sub>2</sub> exit stream is very important, high purity emitters are preferable because the CO<sub>2</sub> can be captured at relatively low costs (EIGA, 2008 and IEA GHG, 2002). Obviously, high purity plants deserve preference for CO<sub>2</sub> capture. Especially ammonia plants, some hydrogen plants, ethylene oxide plants and gas processing plants emit almost pure CO<sub>2</sub>. As can be seen in Table 4.1 there is a big difference in CO<sub>2</sub> purity of the exhaust emitted by hydrogen plants, this is caused by the plants configuration. At older hydrogen plants, CO<sub>2</sub> is removed by a scrubbing process, thereby generating an almost pure CO<sub>2</sub> stream. At more modern hydrogen plants, a pressure swing absorption (PSA) unit is used to produce H<sub>2</sub>, thereby generating a gas stream containing CO<sub>2</sub> (about 50 %), un-recovered H<sub>2</sub>, CO, CH<sub>4</sub> and nitrogen. This stream is recycled to the reformer as fuel to reduce the natural gas input for steam reforming. The CO<sub>2</sub> concentration in the exhaust gas is low, around 10 % (CO<sub>2</sub>Net, 2009). Natural gas ensuing from wells often contains a significant fraction of CO<sub>2</sub>. Before the gas is transported to end-users the CO<sub>2</sub> is separated. Currently the separated CO<sub>2</sub> is vented, but can easily be captured. Other industrial processes that lend themselves for carbon capture facilities are large point

sources like the power generation sector and large energy-consuming industries like oil and gas processing, iron and steel, cement and chemicals production (Davison, 2007). By far the largest potential sources of CO<sub>2</sub> today are fossil fuelled power production plants. Power plants emit more than one-third of the CO<sub>2</sub> worldwide. Power plants are usually built in large centralized units, typically delivering 500–1000 MW of electrical power. A 1000 MW pulverized coal-fired power plant emits between 6 and 8 Mt/yr of CO<sub>2</sub>, an oil-fired single-cycle power plant emits about two thirds of that, and a natural gas combined-cycle power plant emits about half compared to the pulverized coal power plant. A good opportunities to use CO<sub>2</sub> capture will be during decarbonisation of carbon rich fuels, i.e., producing hydrogen fuels from carbon-rich feed stocks, such as natural gas, coal, and biomass. The CO<sub>2</sub> by-product will be relatively pure and the incremental costs of carbon capture will be relatively low. The hydrogen can be used in fuel cells and other hydrogen fuel-based technologies, but there are major costs involved in developing a mass market and infrastructure for these new fuels (Herzog and Golomb, 2004). Figure 4.2 shows the distribution of CO<sub>2</sub> sources all over the world. The black dots represent pure CO<sub>2</sub> sources (IEA GHG, 2002).

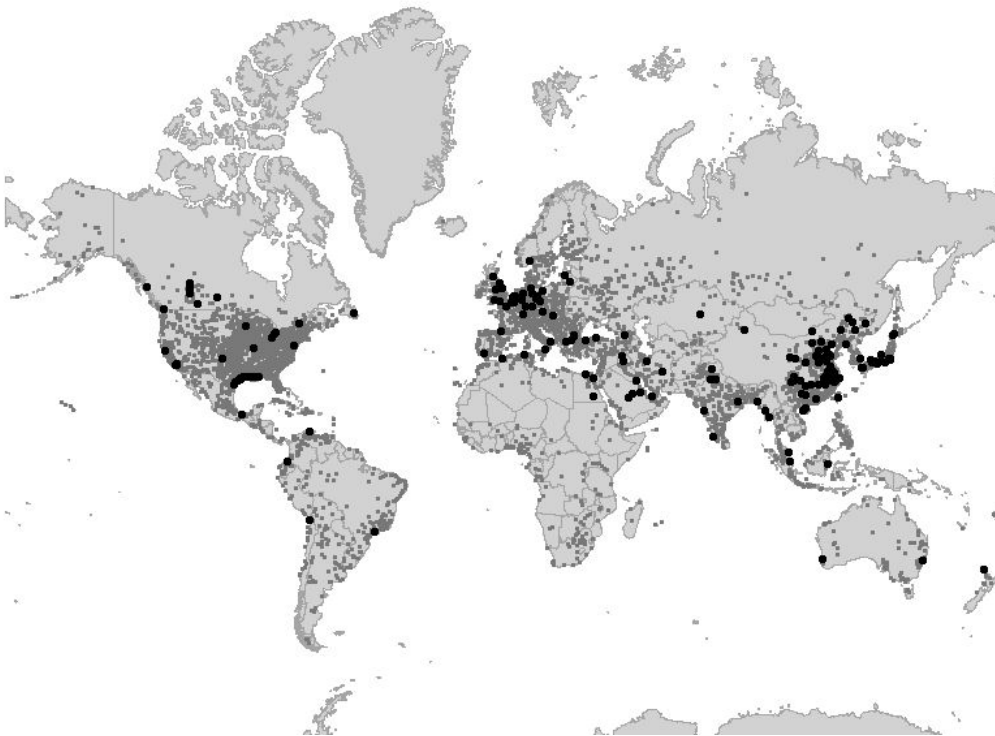


Figure 4.2: World map of CO<sub>2</sub> emitters (point sources)

---

## Appendix D: Chapter 5: CO<sub>2</sub> capture

## 5 CO<sub>2</sub> capture

Currently the best opportunity to optimize the capturing process of CO<sub>2</sub> can be applied to large point sources, such as large fossil fuel or biomass energy facilities, industries with major CO<sub>2</sub> emissions, natural gas processing, synthetic fuel plants and fossil fuel-based hydrogen production plants (Herzog and Golomb, 2004).

### 5.1 CO<sub>2</sub> capture systems

At the moment there are three different types of CO<sub>2</sub> capture systems: post-combustion, pre-combustion and oxyfuel combustion. Important factors of selecting these different types of capture systems are the concentration of CO<sub>2</sub> in the gas stream, the pressure of the gas stream and the fuel type (solid or gas). In the following paragraphs each of these capture systems is being discussed.

#### 5.1.1 Post-combustion

The principle of post-combustion capture is to remove CO<sub>2</sub> from flue gas produced by the combustion of fossil fuels or biomass. Figure 5.1 shows a schematic representation of the post-combustion process. The process can be applied to newly built plants or existing plants (retrofit), so the traditional energy conversion process remains intact. As can be seen from the figure a CO<sub>2</sub> capture process is added to the traditional system, this is shown in grey. The white components represent traditional components, grey represent new or adapted components. Concluding: darker components mean more rigorous adaptations (Damen, 2007). This paragraph is based on the article of Bailey and Feron, 2005.

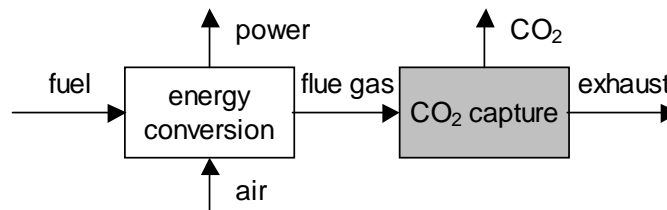


Figure 5.1: Post-combustion process in power cycle (Damen, 2007)

The leading technology in post-combustion capture is chemical absorption, using a monoethanolamine solvent. This technology is already use for years for the purification of gases. This technology is also used to produce high-purity CO<sub>2</sub> for urea production. In the future post-combustion capture can be applied at large power plants such as pulverized coal plants (PC), natural gas fired combined cycles (NGCC), boilers, furnaces and at stationary fuel cells such as solid oxide fuel cells (SOFC).

Table 5.1 shows examples of commonly used chemical solvents. These solvents are primarily used for acid gas (CO<sub>2</sub>, H<sub>2</sub>S, COS) removal from natural gas and synthesis gas and to a limited extent also for CO<sub>2</sub>-removal from flue gases. For the selection of good chemical solvents to remove CO<sub>2</sub> from the fuel gas it is important that the solvent has specific characteristics, like good CO<sub>2</sub>-loading capacity. This will result in low absorption liquid flow rates which will dominate the operating costs. The size of the equipment and the heat requirement for regeneration depends on the reaction rate. *“The loading capacity for chemical solvents is primarily dependent on the concentration of the active components and the achievable loading according to the thermodynamic equilibrium. For the range of alkanolamines the primary amines (MEA, DGA) will be more favourable in terms of reaction rates compared to secondary (DEA, DIPA), tertiary (MDEA) amines. However, achievable loadings and heat requirement for regeneration will be higher for primary amines”.*

Table 5.1: Commercially available chemical solvent processes (Website NETL)

Type of solvent	Example
Primary amines	Monoethanolamine (MEA) Diglycolamine (DGA)
Secondary amines	Diethanolamine (DEA) Diisopropanolamine (DIPA)
Tertiary amines	Methyldiethanolamine (MDEA) Triethanolamine (TEA)
Alkaline salt solutions	Potassium carbonate

### 5.1.2 Pre-combustion

The principle of pre-combustion capture is to remove CO<sub>2</sub> during the production of hydrogen. Figure 5.2 shows a pre-combustion capture scheme. Also for this figure holds that white components represent unadapted components and grey components represent new (dark-grey) or adapted (light-grey) components (Damen, 2007). This paragraph is based on the article of Eide and Bailey, 2005.

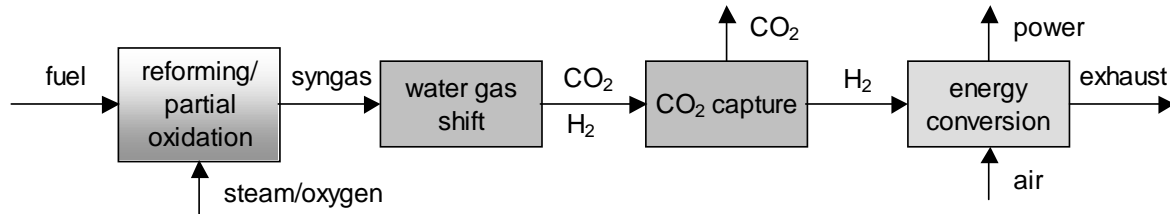
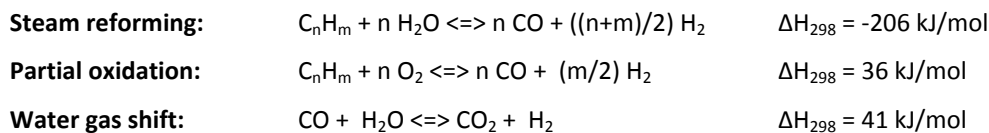


Figure 5.2: Pre-combustion (Damen, 2007)

In pre-combustion schemes, syngas, a mixture consisting mainly of CO and H<sub>2</sub>, is produced by reforming or partial oxidation of natural gas or by gasification of coal, oil residues or biomass at high pressure (between 20-80 bar, depending on the conversion technology). CO is further reacted with steam to produce CO<sub>2</sub> and more H<sub>2</sub> in the water-gas shift reactor, after which CO<sub>2</sub> is separated from H<sub>2</sub>. Steam reforming and partial oxidation are endothermic reactions, they consume heat. The water gas shift reaction is exothermic, it produces heat. The overall reaction (production of syngas) will be endothermic. All three reactions are shown below (CO<sub>2</sub>NET, 2009).



Although the complete integration of syngas production, shift, CO<sub>2</sub> capture and combustion of H<sub>2</sub> rich gasses is not implemented yet, syngas production and CO<sub>2</sub> capture from shifted syngas is a common practice in the chemical industry. In the future pre-combustion schemes can be applied at integrated coal gasification combined cycle (IGCC) or NGCC.

### 5.1.3 Oxyfuel combustion

The principle of oxy-fuel capture is to remove CO<sub>2</sub> from flue gas produced during combustion. Figure 5.3 shows an oxyfuel combustion scheme. In oxyfuel processes, fuel is combusted in an atmosphere of oxygen, which is produced by an air separation unit. A variety of technologies have been developed to separate nitrogen out of air. The three main technologies are: cryogenic distillation, pressure swing adsorption and vacuum swing adsorption. Instead of separating CO<sub>2</sub> from nitrogen as in post-combustion capture, oxygen is separated from nitrogen first, avoiding that the fuel is contacted with nitrogen. The flue gas consists mainly of CO<sub>2</sub> and steam, which can be separated easily by condensation. A part of the flue gas needs to be recycled to the combustion chamber to control the flame temperature, since current materials applied in power industry cannot handle such high temperatures. Oxy-fuel firing has been used for some time within the metal and glass manufacturing industries to achieve high temperatures, minimize energy losses and reduce emissions. Till now oxy-fuel firing has not been applied to full scale conventional steam boilers. In this case all the major components are available, in principle, and boilers and furnaces could be retrofitted for oxyfuel combustion, although this scheme is still in the demonstration phase. In the longer term, oxyfuel combustion could also be deployed in Brayton cycles, but this requires the development of new turbines. This paragraph is based on Anheden et al, 2005).

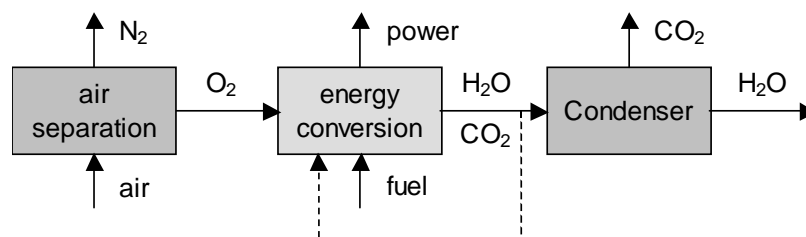


Figure 5.3: Oxy-fuel (Damen, 2007)

### 5.1.4 Integration of CO<sub>2</sub> capture technologies in power cycles

Table 5.2 shows the integration of CO<sub>2</sub> capture technologies in power cycles.

**Table 5.2:** Integration of CO<sub>2</sub> capture technologies in power cycles

Technology	CO <sub>2</sub> capture route	
PC + Chemical absorption	Post-combustion	State-of-the-art
NGCC + Chemical absorption	Post-combustion	
IGCC + Physical absorption	Pre-combustion	
NGCC + Chem./Phys. absorption	Pre-combustion	Advanced
Membrane reforming	Pre-combustion	
Sorption enhanced reforming	Pre-combustion	
AZEP	Oxyfuel	
Chemical looping combustion	Oxyfuel	
SOFC-GT	Oxyfuel	

## 5.2 CO<sub>2</sub> Capture Technologies

In this paragraph several different carbon capture technologies which are available at the moment are being treated. Figure 5.4 shows that a wide range of different technology options for CO<sub>2</sub> separation and capture from gas streams exist. The choice of a suitable technology depends on the characteristics of the flue gas stream, which depends on the power plant technology (Rao, A. and Rubin, E., 2002).

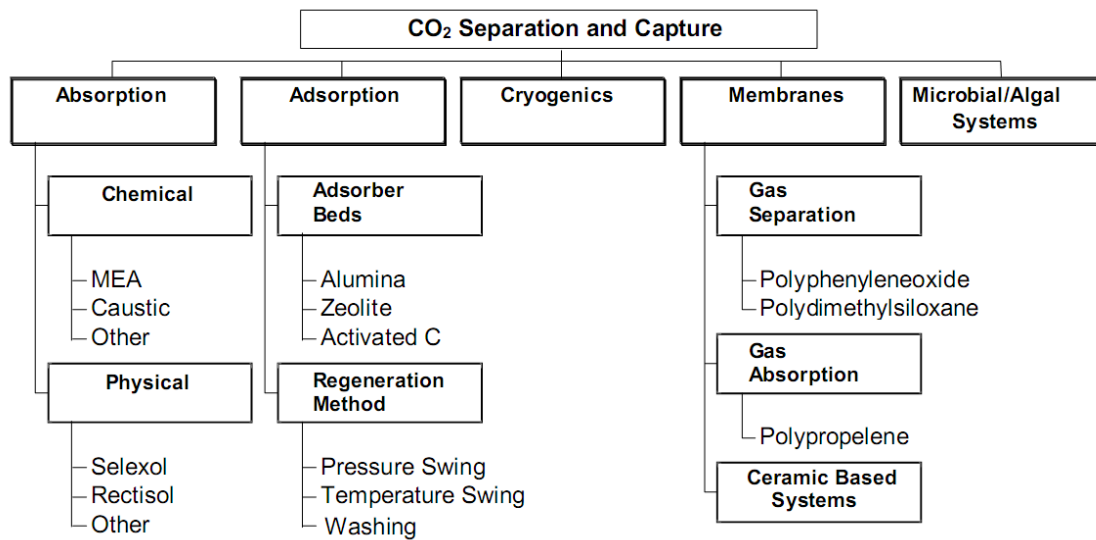


**Figure 5.4:** Technology options for CO<sub>2</sub> separation and capture (Rao, A. and Rubin, E., 2002)

CO<sub>2</sub> can be separated from other components on the basis of difference in physical and chemical features such as molecular weight, boiling point, solubility and reactivity. The most used separation technologies are:

- Absorption: Dissolution/permeation into matrix
- Adsorption: Attachment to surface
- Cryogenic: Separation based on the difference in boiling points
- Membranes: Separation based on the difference in physical/chemical interaction with membrane

Each of the four separation technologies mentioned above are treated more in depth in the following paragraphs.

### 5.2.1 Absorption

Figure 5.5 shows the difference between chemical and physical adsorption, each adsorption technique is explained more in depth in paragraph 5.2.1.1 and 5.2.1.2.

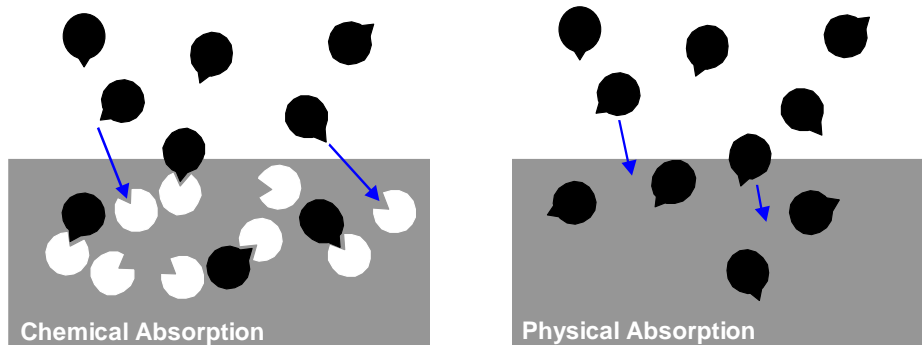


Figure 5.5: Chemical and physical absorption (CO<sub>2</sub>Net, 2007)

#### 5.2.1.1 Physical Absorption

Physical absorption is based on Van der Waals forces. Physical absorption is governed by Henry’s law, which states that the concentration of a gaseous substance in a solution is directly proportional to the partial pressure of that gas above the solution. Physical absorption is suited for processes with high partial pressure (>5 bar). Absorption occurs at high pressure and low temperature. Desorption occurs by pressure decrease.

#### 5.2.1.2 Chemical Absorption

In chemical absorption, CO<sub>2</sub> reacts chemically with an absorbent, which is generally an acid-base reaction (exothermic). Because of the limited amount of sorbent, the saturation effect limits the loading capacity of chemical solvent, which makes them less attractive for high CO<sub>2</sub>-levels. That why chemical absorption is more suited for post-combustion processes. Chemical absorption is more selective compared to physical absorption. Most common absorbents are alkanolamines. Regeneration occurs at increased temperature.

### 5.2.2 Adsorption

Figure 5.6 shows the difference between chemical and physical adsorption, each adsorption technique is explained more in depth in paragraph 5.2.2.1 and 5.2.2.2.

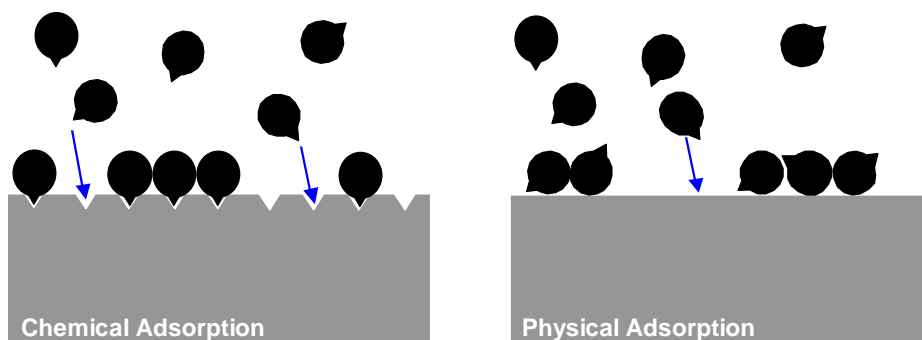


Figure 5.6: Chemical and physical adsorption (CO<sub>2</sub>Net, 2007)

### 5.2.2.1 Physical adsorption

Most of the adsorptive techniques rely upon physical adsorption, in which gas molecules are attached to the solid surface via relatively weak Van der Waals forces. Physical adsorption can be performed at high temperature. Adsorption processes can be classified by material or regeneration method. Adsorbents which can be used are zeolites, activated carbon and alumina. Zeolites, minerals that have a porous structure, are interesting adsorbents due to the large surface area. There are different regeneration (cyclic process) methods:

- Pressure Swing Adsorption (PSA)
- Temperature Swing Adsorption (TSA)
- Electrical Swing Adsorption (ESA)
- Hybrids (PTSA)

In PSA, desorption of adsorbed component is achieved by decreasing pressure. In TSA, the adsorbate is released by heating and in ESA by means of an electric current passing through the adsorbent. PSA is commercially applied in hydrogen production plants to separate hydrogen from contaminants such as CO, CO<sub>2</sub> and H<sub>2</sub>O.

### 5.2.2.2 Chemical adsorption

Chemical adsorption processes uses covalent bonds to capture CO<sub>2</sub>, like the carbonation-calcination loop. Materials which rely on chemical adsorption are metal oxides and hydrotalcites. Carbonation is the reaction between CaO and CO<sub>2</sub>. In principle, this loop can be applied to separate CO<sub>2</sub> in both post-combustion and pre-combustion systems. The disadvantage of this option that relatively large amounts of sorbents are required due to a decay in sorption activity, generating a new waste stream. Regeneration processes that can be used are Pressure Swing Adsorption (PSA) and Temperature Swing Adsorption (TSA).

## 5.2.3 Cryogenic

Cryogenic separation is applied to separate CO<sub>2</sub> from natural gas or separate air into oxygen (O<sub>2</sub>) and nitrogen (N<sub>2</sub>). CO<sub>2</sub> can be physically separated from other gases by condensing it into a liquid at low temperature. This liquid CO<sub>2</sub> can be transported by pipeline to the storage site. Cryogenic CO<sub>2</sub> separation is mainly feasible for gas streams with high CO<sub>2</sub> concentration such as certain natural gas streams and possibly also for syngas. It can also be deployed for purification of oxyfuel combustion flue gas, which contains mainly CO<sub>2</sub> and H<sub>2</sub>O, to separate CO<sub>2</sub> from N<sub>2</sub>, Argon (due to air leakage in boiler), excess O<sub>2</sub> and contaminants such as SO<sub>2</sub> and NO<sub>x</sub>. After water is removed, CO<sub>2</sub> is compressed to 30-40 bar and cooled to a temperature close to the triple point. Non-condensable gasses (Ar, O<sub>2</sub> and N<sub>2</sub>) will remain in gaseous conditions and can easily be separated. CO<sub>2</sub> can be further purified by distillation which separates CO<sub>2</sub> from SO<sub>2</sub> and NO<sub>2</sub>, which have higher boiling points. Theoretically, cryogenic distillation can also be applied for bulk removal of CO<sub>2</sub> from flue gas from conventional PC/NGCC/boilers, but this is a very energy intensive process due to the low CO<sub>2</sub> concentration, which requires high pressures in order to achieve a reasonable CO<sub>2</sub> recovery rate.

## 5.2.4 Membranes

Many types of membranes are available or are being developed. They can be classified on the basis of material, porosity, application, structure etc. Most important membrane features are permeability, selectivity and durability/stability. Selectivity (ratio of permeabilities) determines the purity of the end-product. At low selectivity, recycle or multi-stage plants may offer a solution. Permeability and selectivity are negatively correlated. Hence it is important to find an optimum. Also stability is an important issue. The less stable solution can be supported on a stable layer like glass, ceramic or metal to increase its stability.

### 5.2.5 CO<sub>2</sub> capture matrix

Table 5.3 integrates capture methods (row 1), principles of separation (column 1) and technologies (in cells). The table illustrates which capture technologies can be applied in which capture routes. The applicability of each capture technology depends on the conditions of the gas that contain the CO<sub>2</sub> (composition, temperature and pressure) and the degree of required CO<sub>2</sub> removal.

Table 5.3: CO<sub>2</sub> capture matrix

Capture method	Post-combustion decarbonisation	Pre-combustion decarbonisation	Denitrogenated conversion
<b>Principle of separation</b>			
<b>Adsorption</b>	<ul style="list-style-type: none"> <li>• Lime carbonation / calcinations</li> <li>• Carbon based sorbents</li> </ul>	<ul style="list-style-type: none"> <li>• Dolomite, hydrotalcites and other carbonates</li> <li>• Zirconates</li> </ul>	<ul style="list-style-type: none"> <li>• Adsorbents for O<sub>2</sub>/N<sub>2</sub> separation, perovskites</li> <li>• Chemical looping</li> </ul>
<b>Absorption</b>	<ul style="list-style-type: none"> <li>• Improved absorption liquids</li> <li>• Novel contacting equipment</li> <li>• Improved design of processes</li> </ul>	<ul style="list-style-type: none"> <li>• Improved absorption liquids</li> <li>• Improved design of processes</li> </ul>	<ul style="list-style-type: none"> <li>• Adsorbents for O<sub>2</sub>/N<sub>2</sub> separation</li> </ul>
<b>Cryogenic</b>	<ul style="list-style-type: none"> <li>• Improved liquefaction</li> </ul>	<ul style="list-style-type: none"> <li>• CO<sub>2</sub>/H<sub>2</sub> separations</li> </ul>	<ul style="list-style-type: none"> <li>• Improved distillation for air separation</li> </ul>
<b>Membranes</b>	<ul style="list-style-type: none"> <li>• Membrane gas absorption</li> <li>• Polymeric membranes</li> <li>• Ceramic membranes</li> <li>• Facilitated transport membranes</li> <li>• Carbon molecular sieve membranes</li> </ul>	CO <sub>2</sub> /H <sub>2</sub> separation based on: <ul style="list-style-type: none"> <li>• Ceramic membranes</li> <li>• Polymeric membranes</li> <li>• Palladium membranes</li> <li>• Membrane gas absorption</li> </ul>	<ul style="list-style-type: none"> <li>• O<sub>2</sub>-conducting membranes</li> <li>• Facilitated transport membranes</li> <li>• Solid oxide fuel cells</li> </ul>

### 5.2.6 MEA process

MEA (mono-ethanolamine) is being used for more than 60 years as capture solvent to remove H<sub>2</sub>S and CO<sub>2</sub> from natural gas streams. The CO<sub>2</sub> is captured from the exhaust gas using chemical absorption by an amine solution. Typically, about 75% - 90% of the CO<sub>2</sub> is captured using this technology, producing a nearly pure (>99%) CO<sub>2</sub> product stream (Rao, A. and Rubin, E., 2002). Figure 5.7 shows a typical configuration of a power plant with CO<sub>2</sub> capture facility.

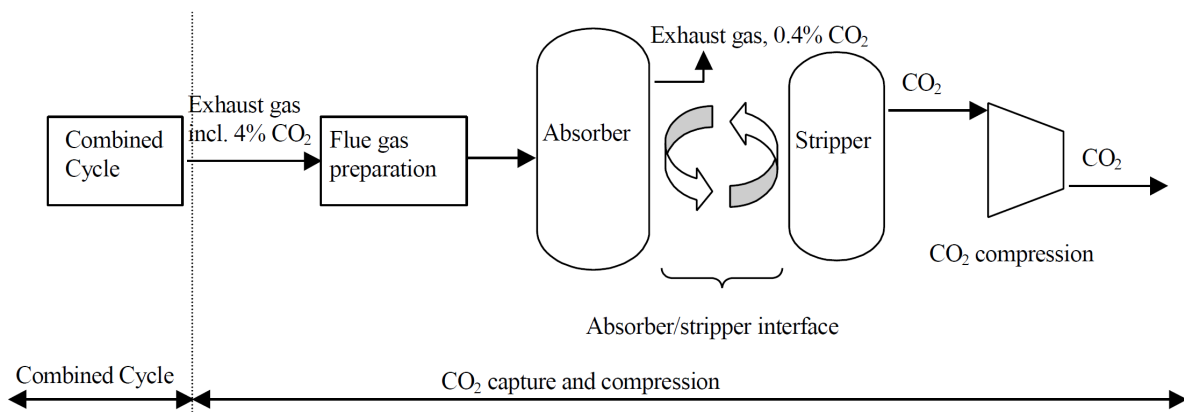


Figure 5.7: Natural gas fired combined cycle with post combustion CO<sub>2</sub> capture (Undrum et al., 2000)

In this concept CO<sub>2</sub> is separated from the exhaust gas by absorption using 30 wt% of MEA. The exhaust gas containing ~4% CO<sub>2</sub> in addition to mainly N<sub>2</sub>, O<sub>2</sub> and H<sub>2</sub>O, is cooled and fed to the absorption tower. Around 90% of the CO<sub>2</sub> is captured. The CO<sub>2</sub> rich amine is fed to the amine stripper in which the amine is regenerated and fed back to the amine absorption tower. The released

CO<sub>2</sub> and steam are cooled for water removal and the CO<sub>2</sub> is compressed for transportation and storage (Kvamsdal et al., 2007). Figure 5.8 shows a simplified flow sheet of a CO<sub>2</sub> capture process by wet chemical absorption (Oexmann and Kather, 2009).

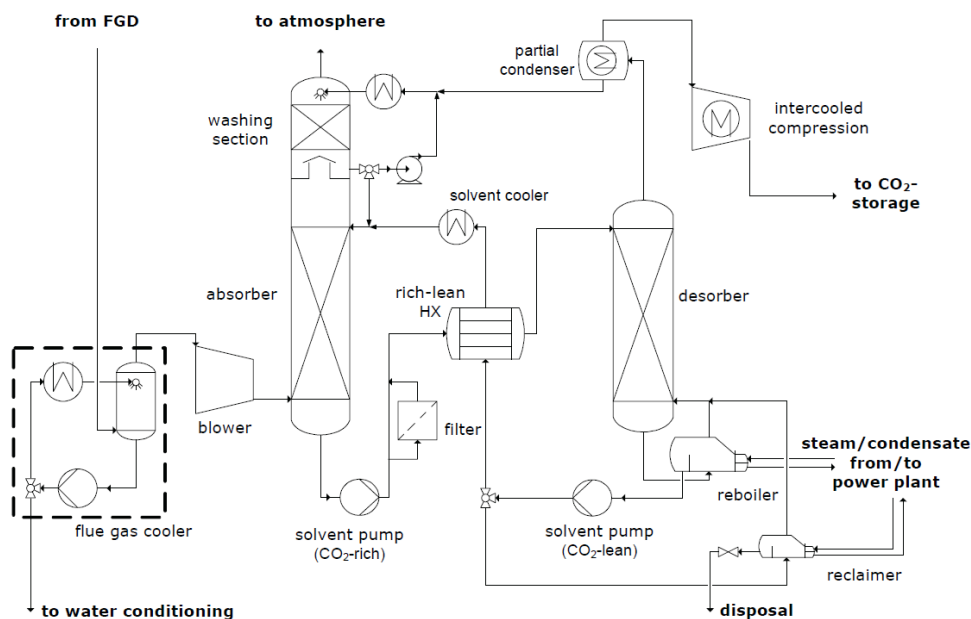


Figure 5.8: Simplified flow sheet of CO<sub>2</sub> capture process by wet chemical absorption (MEA)

To compare the different capture processes it is very important to know the amount of energy, which is consumed during the capturing process. According to study made by the Norwegian University of Science and Technology and Statoil, the energy consumption in the CO<sub>2</sub>-capture unit is approximately 1.3-1.7 kWh/kg CO<sub>2</sub>; 10 % is mechanical work for blowers and fans, the remainder is heat at about 130°C. An additional 0.1 kWh/kg CO<sub>2</sub> is required for compression to 150 bar. The efficiency penalty caused by capture and compression of CO<sub>2</sub> will be about 7 – 9 % points compared to conventional CC. Based on best available technology for CC and CO<sub>2</sub> capture, the total efficiency for this concept will be in the range 49-51 %. Table 5.4 shows a performance summary of an imaginary power plant. CC stands for combined cycle (Undrum, 2000).

Table 5.4: Performance summary (Undrum, 2000)

	Power Plant without capture	Power Plant with capture
CC power output (MW)	400	400
CC power output incl. CO <sub>2</sub> capture (MW)	-	338
Net Efficiency (%)	58	49
CO <sub>2</sub> emission (g/kWh)	363	60

First it is important to know the amount of input energy which is needed to produce an output energy of 400 MW. The efficiency of the whole process is 58 % (power plant without capture) so the required amount of energy is 400 MW / 0.58 = 690 MW. To have a good comparison between a power plant with or without capture facility, the power plants must have the same amount of energy input. The power plant with CO<sub>2</sub> capture facility has an output of 338 MW and the overall efficiency is 49 %.

The carbon dioxide emission of power plant without capture is 363 g/kWh = 363 kg/MWh

The carbon dioxide emission of power plant with capture is 60 g/kWh = 60 kg/MWh

The total CO<sub>2</sub> output of a 400 MW power plant without CO<sub>2</sub> capture is 400 MW \* (363 kg/MWh - 60 kg/MWh) = 121,200 kg CO<sub>2</sub>. This amount of CO<sub>2</sub> is being emitted during the combustion of 690 MWh of fuel equivalent.

When the power plant captures the emitted CO<sub>2</sub> the power output decreases from 400 to 338 MW, a decrease of 62 MW. Concluding: the capture facility “consumes” 62 MW, not all of this is really consumed some part is lost due to changing efficiency. For a good comparison between different capture facilities it is important to know the amount of energy required to capture 1 kg of CO<sub>2</sub>.

So for the precious case the amount of energy needed to capture 1 kg of CO<sub>2</sub> is:

121,200 kg CO<sub>2</sub> / 62,000 kWh (=62 MWh) = 1.95 kg CO<sub>2</sub>/kWh. This is 0.51 kWh/kg CO<sub>2</sub> = 1850 kJ/kg CO<sub>2</sub>.

The net efficiency of the process is 49% so 1850 kJ/kg CO<sub>2</sub>/49% = 3770 kJ/kg CO<sub>2</sub>.

### 5.2.7 Benfield process

The Benfield process was introduced over 30 years ago. The Benfield process is based on a thermally regenerated cyclical solvent that uses an activated, inhibited hot potassium carbonate solution to remove CO<sub>2</sub>, H<sub>2</sub>S and other acid gas components. The flue gas from the combustor is directed through the gas turbine and heat exchangers, before passing through a series of carbonators at a temperature of 650-700°C. CO<sub>2</sub> in the flue gas will readily react with CaO in the carbonator to form calcium carbonate (CaCO<sub>3</sub>) in an exothermic reaction. The resulting CaCO<sub>3</sub> is then directed to a series of calciners, where a high-carbon fuel such as petroleum coke or anthracite coal is burned in an oxygen atmosphere. This provides the heat needed to reverse the carbonation reaction and release the CO<sub>2</sub> captured earlier. The calciner exhaust gases will be highly concentrated CO<sub>2</sub> suitable for storage, use, or further treatment. The oxygen required in the calciners is only 1/3 that required for an oxyfuel process, reducing Air Separation Unit (ASU) capital and operating costs accordingly. Heat released during the carbonation process and generated in the calciners can be directed to the steam cycle to improve overall plant efficiency. It is estimated that a realistic CO<sub>2</sub> capture rate of up to 78% is possible in the carbonator using CaO as a sorbent, as well as 100% of the CO<sub>2</sub> generated in the calciner, resulting in an overall capture/removal of approximately 85% of the total CO<sub>2</sub> produced (Boggs et al, 2005).

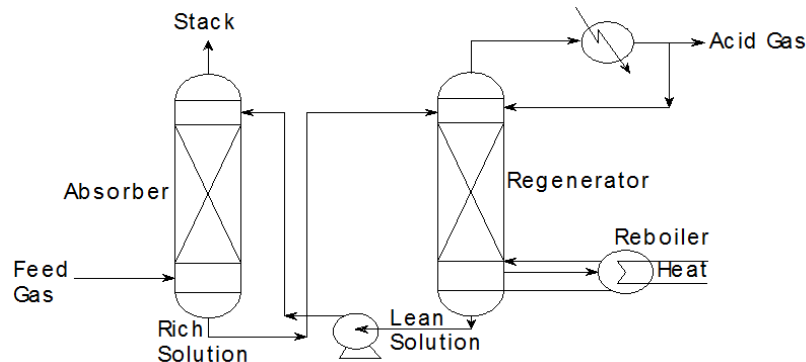


Figure 5.9: Schematic overview of the Benfield Process (Boggs et al, 2005)

### 5.2.8 CaO/CaCO<sub>3</sub> process

Figure 5.10 shows the calcium sorbent cycle for carbon dioxide capture. This capturing process uses the same principle as the Benfield process.

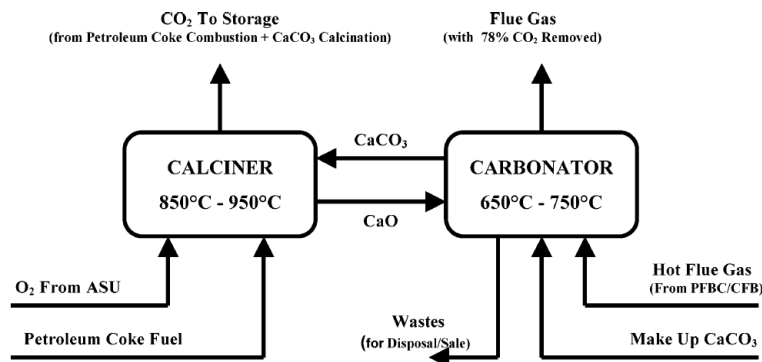


Figure 5.10: Calcium sorbent cycle for carbon dioxide capture (MacKenzie, 2007)

### 5.3 Energy Penalty / Emission factor

To do a good exergy analysis it is very important to keep in mind that for the whole carbon capture and storage process also energy is needed. For every m<sup>3</sup> of natural gas or oil and every kg of coal used for the CCS process CO<sub>2</sub> is being emitted. Also keep in mind all the electric power consumed by the whole process. This electrical energy is produced somewhere else where probably the CO<sub>2</sub> is being emitted into the atmosphere. Hence it is very important to calculate the capture efficiency of the process. The formula below can be used to calculate the capture efficiency.

$$\text{Capture efficiency} = \frac{CO_2 \text{ avoided}}{CO_2 \text{ captured}} = \frac{CO_2 \text{ captured} - CO_2 \text{ released CCS}}{CO_2 \text{ captured}}$$

Appendix K shows which kinds of fuel is being used in the Netherlands and the standard CO<sub>2</sub> emission factors of those fuels. Figure 5.11 compares two energy plants one with CO<sub>2</sub> capture facility and one without.

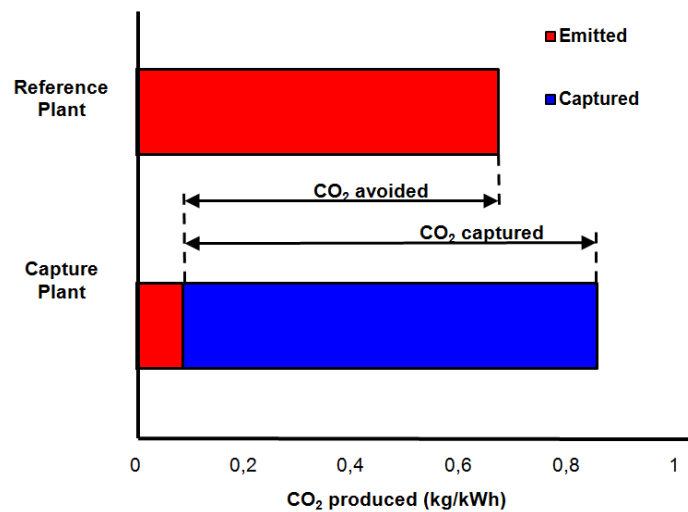


Figure 5.11: CO<sub>2</sub> captured vs. CO<sub>2</sub> avoided (Herzog and Golomb, 2004)

CO<sub>2</sub> mitigation costs is a measure, which enables comparison of various CCS technologies among each other and also with other CO<sub>2</sub> mitigation technologies (such as renewable energy and energy saving measures). The amount of CO<sub>2</sub> avoided is the difference in emission between the reference plant without capture and the remaining emission of the capture plant. The amount of CO<sub>2</sub> captured is larger than the amount of CO<sub>2</sub> avoided due to the additional energy requirements (and hence CO<sub>2</sub> production) caused by capturing CO<sub>2</sub> (Herzog and Golomb, 2004).

---

## Appendix E: Chapter 6: CO<sub>2</sub> transport

## 6 CO<sub>2</sub> transport

After the CO<sub>2</sub> has been captured at a large point source it has to be transported to a place where it can be stored. Between the capture and storage, the CO<sub>2</sub> has to be transported by one or a combination of several transport media like truck, train, ship or pipeline with possible intermediate storage (Koornneef et al, 2009). In this chapter transportation by pipeline and ship are being highlighted.

### 6.1 Pipeline

CO<sub>2</sub> can be transported through pipelines in three ways: in the form of a gas, a supercritical fluid or in the subcooled liquid state (Zang et al, 2006). Only two methods can be used to transport CO<sub>2</sub> over long distances: a supercritical fluid or a subcooled liquid (McCoy and Rubin, 2008). Transportation in the gas phase is disadvantaged because of the low density and consequently the large pipe diameter and high pressure drop. Most CO<sub>2</sub> pipelines are used for enhanced oil recovery, the CO<sub>2</sub> is transported as a supercritical fluid (Zang et al, 2006).

**Table 6.1:** Properties of gaseous supercritical and liquid CO<sub>2</sub> (Zhang et al, 2006)

Properties	Gas	Supercritical	Liquid
Density (g/cm <sup>3</sup> )	~0.001	0.2 – 1.0	0.6 – 1.6
Diffusivity (cm <sup>2</sup> /s)	0.1	0.001	0.00001
Viscosity (g/cm s)	0.0001	0.001	0.01

CO<sub>2</sub> critical parameters: T<sub>c</sub> = 31.1 °C; P<sub>c</sub> = 7.38 MPa; ρ<sub>c</sub> = 0.47 g/cm<sup>3</sup>.

According to Black & Veatch power plant engineering (1996) it is well established, for the quantities and distances required for CO<sub>2</sub> sequestration, that pipeline transport is the most economical. Pipelines are used all over the world for transportation in the energy sector, e.g. for natural gas, refined products, coal slurry and also CO<sub>2</sub> (Zang et al, 2006). Carrying CO<sub>2</sub> in pipelines onshore is not a new concept (Gale, 2004). Currently there is over 6000 km of CO<sub>2</sub> pipelines in operation in the USA, mainly for enhanced oil recovery (EOR). These pipelines are mainly situated in remote areas with low population densities. When CCS in the future will be implemented on a large scale, a large network of CO<sub>2</sub> pipelines will be needed. Part of this infrastructure will be located near densely populated areas, so safety issues are much more complex (Koornneef, 2009).

Figure 6.1 shows a blueprint of a pipeline infrastructure transporting just over 60 million tonnes of CO<sub>2</sub> in 2050 within the Netherlands.

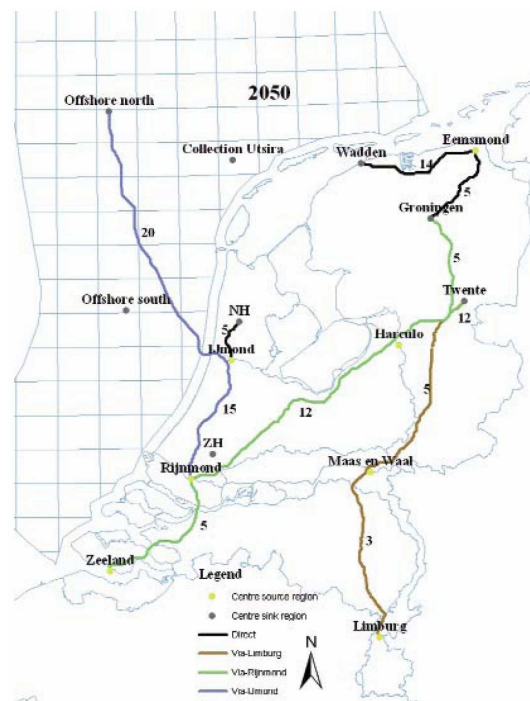


**Figure 6.1:** Blueprint for a pipeline infrastructure (CATO, 2009)

In the Netherlands an existing pipeline of 85 km is being used to transport CO<sub>2</sub> – at low pressure – from the Shell refinery in Pernis to greenhouses in the Westland area. However, large-scale CCS will require a new transportation infrastructure to link sources and sinks. In densely populated countries such as the Netherlands this can become a considerable challenge (booklet Cato2).

## 6.2 Ship

After the CO<sub>2</sub> has been captured, it has to be transported to a storage site. In chapter 7 we describe different ways of storing CO<sub>2</sub>. Due to the scattered CO<sub>2</sub> sources and the uncertainty in the growth of the CO<sub>2</sub> market, a cost effective and flexible transport system is required. In this paragraph transportation by ship is being discussed. Transport by ship is not a new concept because transportation of LNG and ethylene already exist. The use of ships for transporting CO<sub>2</sub> across the sea is today in an embryonic stage. Worldwide there are only four small ships used for this purpose (IPCC, 2005). The transported CO<sub>2</sub> can be used for EOR, which is done at several places onshore in the United States (Heggum et al., 2005). Although the potential for increased oil recovery is likely, CO<sub>2</sub> is currently not used for EOR in any offshore oilfield. The main source for this paragraph (paragraph 6.2) is Aspelund et al., 2006.

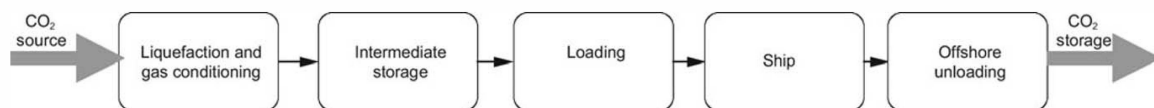


Figure 6.2: Main processes in the transport system (Aspelund et al., 2006)

Figure 6.2 shows the transport chain which comprises five main processes:

- Liquefaction and gas conditioning
- Intermediate storage
- Loading
- Ship
- Offshore unloading

The CO<sub>2</sub> mixture must contain sufficient amounts of CO<sub>2</sub> to be able to liquefy. CO<sub>2</sub> sources that fulfil such requirements are:

- CO<sub>2</sub> released during natural gas sweetening
- Ammonia production
- Hydrogen production (steam reforming and water-gas-shift reaction)
- CO<sub>2</sub> capturing at power plants

Both investments and operational costs for the liquefaction process are affected by the composition and purity of these CO<sub>2</sub> sources. It is assumed that the sources have to deliver CO<sub>2</sub> at 1.1 bar and 15 °C (298 K). The gas stream is saturated with water and contains 0.2 mol percent heavy hydrocarbons and 0.3 mol percent volatile gases. These impurities will influence the properties of CO<sub>2</sub> such as boiling point, dew point, density, and thereby the energy requirement of the transport system.

Figure 6.3 on the next page shows the optimal transport conditions for CO<sub>2</sub>. In order to transport CO<sub>2</sub> in large amounts, the gas must be transformed into a form with higher density. CO<sub>2</sub> can be transported in different phases: liquid, solid or supercritical. The cargo in LPG and LNG ships is kept as a liquid at atmospheric pressure through refrigeration. This way of transportation is not possible for CO<sub>2</sub> due to its triple point (TP) at 5.2 bar and -56.6°C. At lower pressures or temperatures CO<sub>2</sub> will exist either as vapour or in solid state as dry ice. At atmospheric pressure the sublimation point of CO<sub>2</sub> is -78°C. In theory the density of solid CO<sub>2</sub> is approximately 1500 kg/m<sup>3</sup>. Transportation of this solid CO<sub>2</sub> is not economically feasible due to complex (un)loading procedures. It is likely that transportation of CO<sub>2</sub> by ship will be at a pressure near the triple point, so in the liquid phase. CO<sub>2</sub> exists in liquid form at pressures between 5.2 bar, triple point and 73 bar, critical point (CP). The density of saturated liquid will range from 1200 kg/m<sup>3</sup> at the triple point, to 600 kg/m<sup>3</sup> at the critical point.

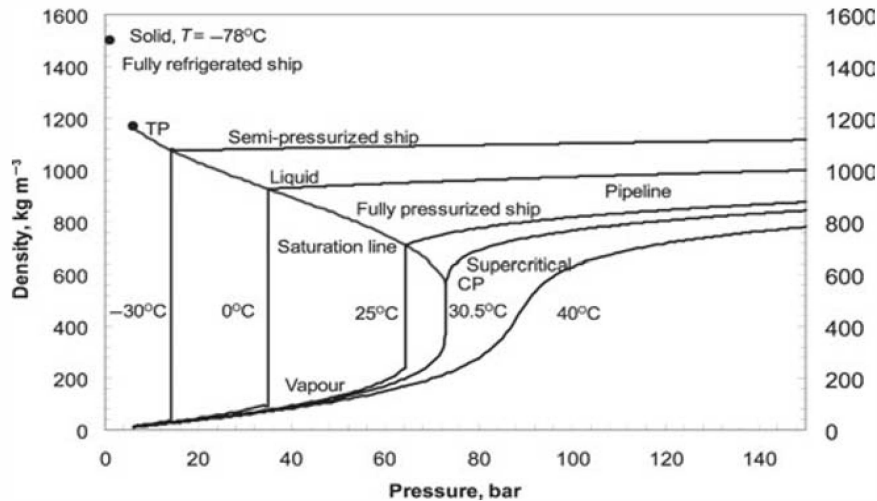


Figure 6.3: Optimal transport pressure (Aspelund et al., 2006)

Figure 6.4 shows typical arrangements for a CO<sub>2</sub> ship. There are three types of tank structures for liquid gas transport ships: pressure type, low temperature type and semi-refrigerated (IPCC, 2005). A ship for ethylene transport can carry up to 20,000 m<sup>3</sup>. These ships are semi-pressurized and are usually designed for a working pressure of 5 – 7 bar and operate at low temperatures (-48°C for LPG and -104°C for ethylene). Such vessels normally have two to six storage tanks of around 4500 m<sup>3</sup> each. It may be possible to convert a LPG or ethylene ship into a carrier which can transport CO<sub>2</sub>. However, since CO<sub>2</sub> is transported at slightly higher pressures, higher densities and lower temperatures than LPG, some difficulties may arise. Only a few of the existing LPG ships can withstand the CO<sub>2</sub> design requirements.

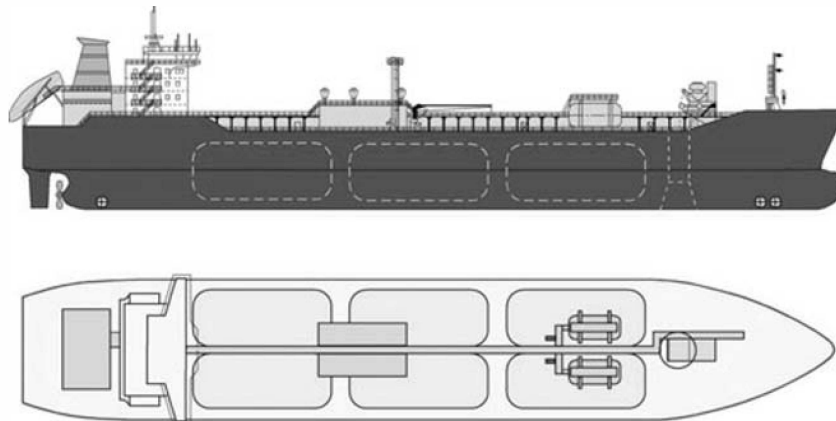


Figure 6.4: Typical arrangements for a CO<sub>2</sub> ship (Aspelund et al., 2006)

In Table 6.2 an analysis is made of transportation of CO<sub>2</sub> by ship. From this table can be seen that the liquefaction of the carbon dioxide will cost the most energy and exergy compared to the other energy consuming steps in whole process.

Table 6.2: CO<sub>2</sub> transport analysis (Aspelund et al., 2006)

	Liquefaction	Storage	Loading	Ship	Unloading	Total Chain
CO <sub>2</sub> inlet phase	V	L	L	L	D	
Inlet P (bar)	1.1	6.5	6.5	6.5	200	
Inlet T (°C)	15	-52	-52	-52	15	
Specific energy requirements (kWh/tonne)	110	0	0.2	25 (oil)	6.5	<b>142</b>
Specific exergy requirements (kWh/tonne)	60	0	0	0	0.1	<b>60</b>
Rational efficiency (%)	55	0	0	0	1.5	<b>42</b>
Relative CO <sub>2</sub> emissions (%)	0.3	0	0	0.65	0.45	<b>1.4</b>
Specific costs (2003 USD)	10.5	2.2	0.8	7.5	4	<b>25</b>

---

## Appendix F: Chapter 7: CO<sub>2</sub> storage

## 7 CO<sub>2</sub> storage

After the CO<sub>2</sub> has been captured it needs to be stored so that it will not be emitted into the atmosphere. The captured CO<sub>2</sub> can be transported to different sites where it will be stored. This permanent storage of CO<sub>2</sub> can be done in various forms. There are two potential storage options, which are (IEA, 2009):

- Storage in the oceans
- Storage in geological formations

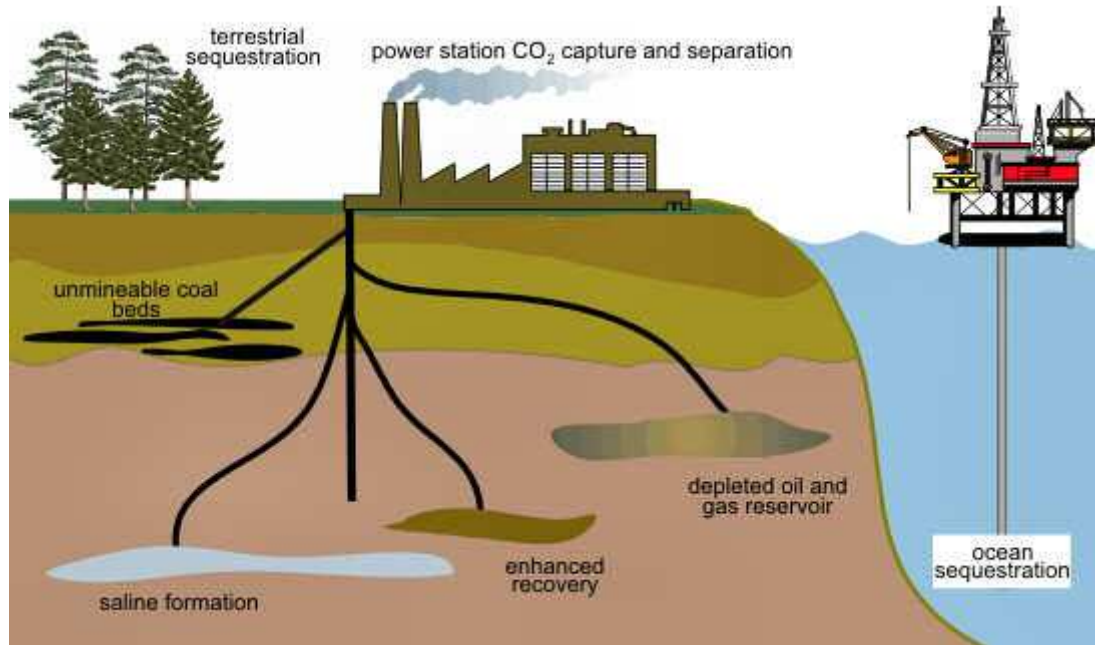


Figure 7.1: Different types of storage options (Frost, 2008)

Paragraphs 7.1 and 7.2 explain the storage in oceans and geological formations more thoroughly. Several key criteria must be applied to the storage method (Herzog, 2004):

- The storage period should be prolonged (>100 – 1000 years).
- Cost of storage, including the cost of transportation from the source to the storage site, should be minimized.
- Risk of accidents should be eliminated.
- The Environmental impact should be minimal.
- The storage method should not violate any national or international laws and regulations.

A storage site has to fulfill several properties to be a good CO<sub>2</sub> storage site. Table 7.1 shows some site selection criteria (IPCC, 2005).

Table 7.1: Properties of CO<sub>2</sub> storage site (IPCC, 2005)

High storage capacity:	High porosity
	Large reservoir
Efficient injectivity:	High permeability
Safe and secure storage:	Low geothermal gradient & high pressure
	Adequate sealing
	Geological & hydrodynamic stability
Low costs:	Good accessibility, infrastructure
	Source close to storage reservoir

## 7.1 Storage in oceans

The ocean represents the largest potential sink for anthropogenic CO<sub>2</sub>. At the moment the ocean already contains an estimated 40,000 GtC (gigatons or billion tons of carbon) of dissolved inorganic carbon as free CO<sub>2</sub> molecules and ions of bicarbonate (HCO<sub>3</sub><sup>-</sup>) and carbonate (CO<sub>3</sub><sup>2-</sup>), and another 2,000 -3,000 GtC of organic carbon in the water column (Wong, 1993). This is only a small amount compared to 750 GtC in the atmosphere and 2200 GtC in the terrestrial biosphere (Herzog, 2004).

There are two main concepts of CO<sub>2</sub> storage in oceans, dissolution and “lake” type deposits. During dissolution type deposits CO<sub>2</sub> is injected by a ship or pipeline into the water column at depths of 1000 meter or more. During lake type deposits CO<sub>2</sub> injected directly onto the sea floor at depths greater than 3000 meter. At these depths CO<sub>2</sub> is denser than water and is expected to form a “lake” that would delay dissolution of CO<sub>2</sub> into the environment (Frost, 2008). The following chemical reactions will happen to neutralize the anthropogenic CO<sub>2</sub>:

In the water column,



and on the seafloor, or with calcareous particles in the water column,



Another concept is to convert the injected CO<sub>2</sub> to bicarbonates using limestone or hydrates.

The ocean is taking up anthropogenic CO<sub>2</sub> at a rate of 2.2 0.7 GtC/year, this is about 40% of the total CO<sub>2</sub> emissions from fossil fuels and biomass (Wong, 1993).

Injection of CO<sub>2</sub> into the ocean for storage in generally has negative environmental effects because large CO<sub>2</sub> concentrations influences the acidity (pH) of the ocean water. The CO<sub>2</sub> reacts with water to form carbonic acid (H<sub>2</sub>CO<sub>3</sub>) (Frost, 2008).

## 7.2 Storage in geological formations

Geological storage also known as geo-sequestration involves injection of carbon dioxide, generally in supercritical form, directly into underground geological formations. Underground storage of CO<sub>2</sub> in geological formations is not a new technique; it has taken place for many years as a consequence of injecting CO<sub>2</sub> into oil fields to enhance recovery. There are a number of potential geological formations that can be used to store captured CO<sub>2</sub>. These include (Herzog, 2004):

- Depleted gas and oil fields
- Deep saline aquifers
- Deep unminable coal seams
- Formations for enhanced oil recovery

Together, these formations can hold for hundreds to thousands of gigatons of carbon. Table 7.2 shows the worldwide capacity of potential CO<sub>2</sub> storage reservoirs.

**Table 7.2:** *The worldwide capacity of potential CO<sub>2</sub> storage reservoirs (Herzog, 2004)*

Sequestration option	Worldwide capacity (Gt C)
Ocean	1000 – 10,000
Deep saline formations	100 – 10,000
Depleted oil and gas reservoirs	100 – 1000
Coal seams	10 – 1000
Terrestrial	10 – 100
Utilization	Currently < 0.1 Gt C/year

### 7.2.1 Deep saline aquifers

Saline aquifers are defined as porous and permeable reservoir rocks that contain saline fluid in the pore spaces between the rock grains (Bentham, 2005). These aquifers generally occur at depths greater than aquifers that contain potable water. Because of the high saline proportion and the depth, the water of these aquifers cannot be used for surface usage (Bentham, 2005). Deep saline formations (subterranean and subseabed) both may have the greatest CO<sub>2</sub> storage potential. Currently a lot of research is underway in trying to understand what percentage of these deep saline formations is suitable as a storage site (Herzog, 2004).

Storage of CO<sub>2</sub> in saline aquifers can be in both “confined” and “unconfined” aquifers (see Figure 7.2). The right side of the figure shows a confined aquifer, which relies on trapping the buoyant CO<sub>2</sub> by structural and/or stratigraphic features. *“In these simple structural traps, volumes and migration pathways of the injected CO<sub>2</sub> can be predicted and reservoir models constructed with a higher degree of certainty than in an unconfined aquifer, where the lateral boundaries are not well known.”* The left side of the figure shows a unconfined aquifer (Bentham, 2005).

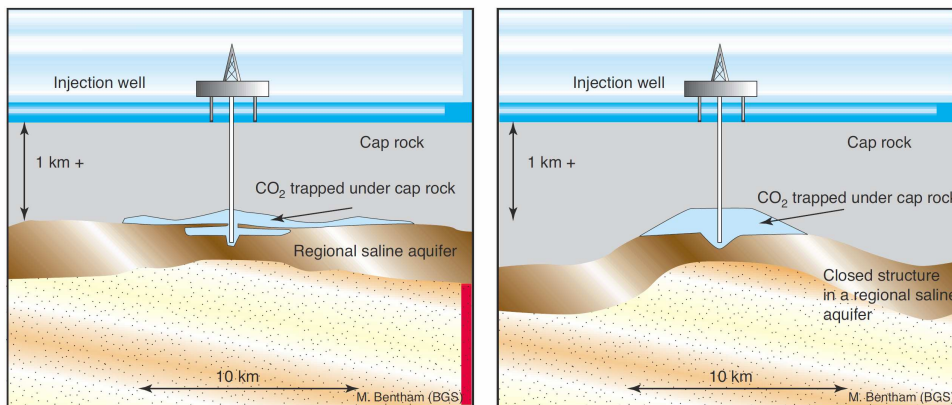


Figure 7.2: Conceptual diagrams of storage in unconfined and confined aquifers (Bentham, 2005).

The first and only commercial-scale project using deep saline formations for CO<sub>2</sub> storage is the Sleipner West gas field, operated by Statoil, located in the North Sea. Figure 7.3 show a simplified diagram of the Sleipner CO<sub>2</sub> storage project. The Sleipner CO<sub>2</sub> project is operational since 1996. The natural gas produced at the field has a CO<sub>2</sub> content of about 9%. In order to meet commercial specifications, the CO<sub>2</sub> content must be reduced to 2,5%. The CO<sub>2</sub> is stored in a (shallower) saline aquifer called the Utsira Sandstone Formation. The aquifer consists of unconsolidated sandstone and thin (horizontal) shale layers that spreads CO<sub>2</sub> laterally. The seal consists of an extensive and thick shale layer. Annually around 1Mt CO<sub>2</sub> is removed from gas plant. It is estimated that over the entire lifetime 20 Mt of CO<sub>2</sub> will be stored (Herzog, 2004).

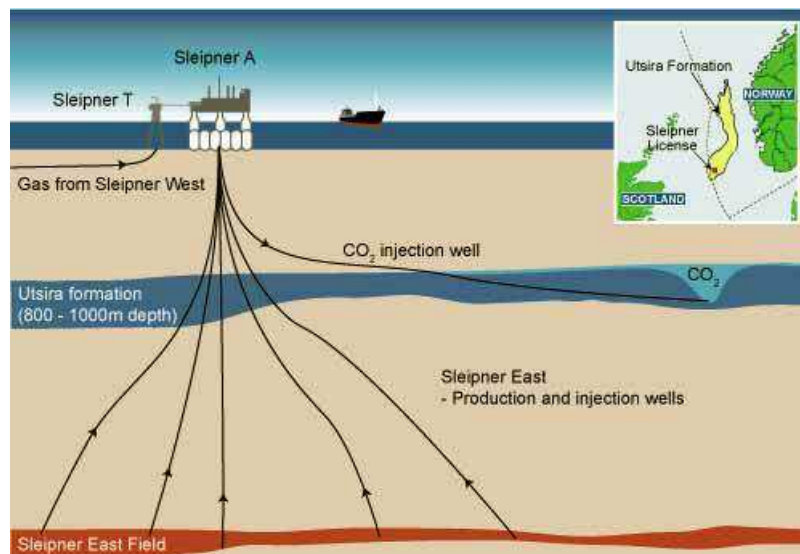


Figure 7.3: Simplified diagram of the Sleipner CO<sub>2</sub> storage project

### 7.2.2 Deep unminable coal seams

Storage of CO<sub>2</sub> in unminable coal seams is distinctively different from that in oil and gas reservoirs and aquifers because the storage in coal seams is based on adsorption. Over the last two decades coalbed methane (CBM) has become an important source of (unconventional) natural gas supply in the United States. Carbon dioxide enhanced coalbed methane recovery (CO<sub>2</sub>-ECBM) is an emerging technology, which has the potential to store large volumes of anthropogenic CO<sub>2</sub> in deep unminable coal formations (coalbeds), while improving the efficiency and potential profitability of coalbed methane recovery (Shi, 2005).

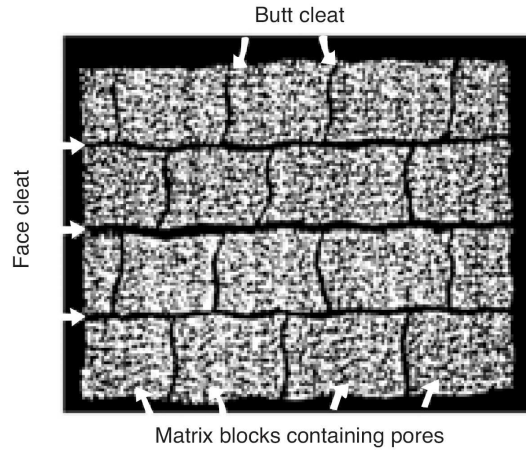


Figure 7.4: A schematic of coal structure

### 7.2.3 Formations for enhanced oil recovery

Oil reservoirs are good storage sites for CO<sub>2</sub> because they retained liquid and gas hydrocarbons for over millions of years. Enhanced Oil Recovery (abbreviated EOR) is a technique which is being used for increasing the amount of crude oil that can be extracted from an oil field (Gozalpour, 2005). Figure 7.5 shows the working of enhanced oil recovery.

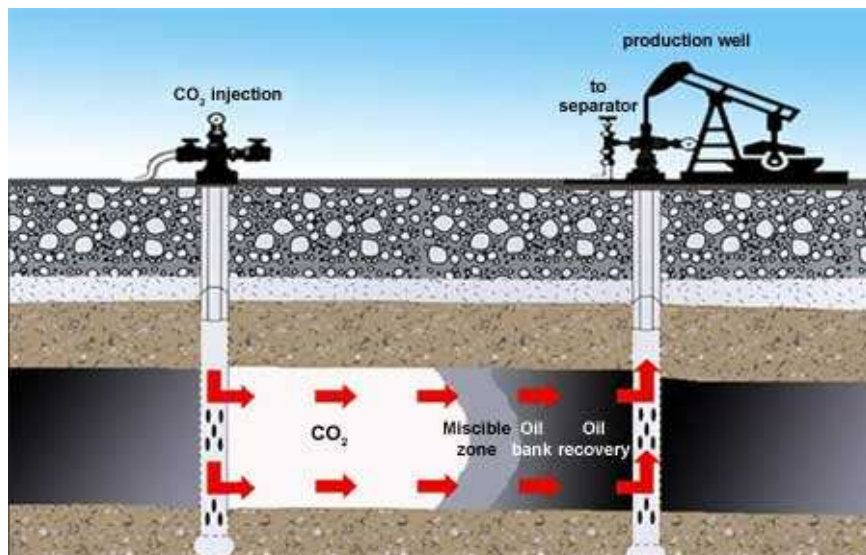


Figure 7.5: Enhanced oil recovery

Enhanced oil recovery has the potential to increase domestic oil recovery efficiency from about one-third to over 60%. The EOR technique that is attracting the most new market interest is carbon dioxide (CO<sub>2</sub>)-EOR. First tried in 1972 in Scurry County, Texas and has been successful on many locations since then. Most CO<sub>2</sub> used for EOR is coming from naturally-occurring sources. But new technologies are being developed to produce CO<sub>2</sub> from industrial applications such as natural gas processing, fertilizer, ethanol, and hydrogen plants in locations where naturally occurring reservoirs are not available (Gozalpour, 2005 and DOE).

### 7.3 Potential storage sites within the Netherlands

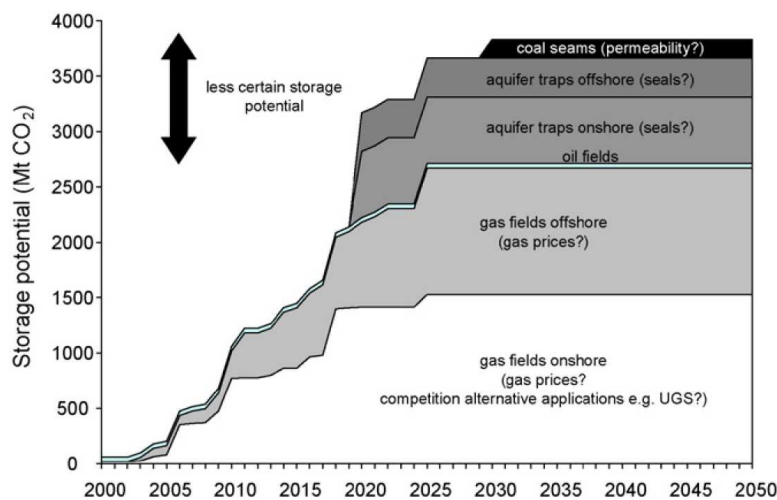
The annual Dutch CO<sub>2</sub> emission is nearly 180 Mt CO<sub>2</sub> at present, of which approximately 100 Mt CO<sub>2</sub>/year emitted by the energy and manufacturing industry (Klein Goldewijk et al., 2005). Around 15 Mt CO<sub>2</sub> can be avoided every year by 2020, when some of the larger gas fields, that become available in the coming decade, are used for storage of CO<sub>2</sub> (Daniëls and Farla, 2006). In the year 2050, the mitigation potential of CCS in the power sector, industry and transport fuel production is estimated at maximally 80–110 Mt CO<sub>2</sub>/year. But avoiding 30 – 60 Mt CO<sub>2</sub>/year is considered much more realistic given the storage potential represented by the Dutch gas fields. Storing larger amounts of CO<sub>2</sub>, due to aggressive climate policy, would only be possible if the Groningen gas field or large reservoirs in the British or Norwegian part of the North Sea becomes available (Damen et al., 2009).

Table 7.3 shows the technical capacity for CO<sub>2</sub> storage in the Netherlands and the continental shelf. Gas fields represent the major storage potential. The Dutch oil fields represent a relatively low storage potential. Aquifers and coal seams are not that well studied, which causes a relatively large uncertainty in storage capacity (Damen et al., 2009).

**Table 7.3:** Technical CO<sub>2</sub> storage potential in the Netherlands (Damen et al., 2009)

Reservoir	Storage capacity (Mt CO <sub>2</sub> )
Gas fields	
Groningen gas field	7350
Other gas field (onshore)	1600
Other gas field (offshore)	1150
Oil fields	40
Coal seams	170 (40 – 600)
Aquifer trap prospects	
Onshore	400
Offshore	350 (90 – 1100)

Figure 7.6 shows the storage capacity in the Netherlands is gradually increasing in the coming two decades, this is caused by the lifetime of the gas fields. Possibly, the lifetime of gas fields may be extended a few years with rising gas prices. According to TNO-NITG (2006) the Groningen gas field is not expected to become available before 2040, and possibly far beyond 2050. Every time when a gas field becomes available, a ‘window of opportunity’ for CO<sub>2</sub> storage is created. “Ideally, CO<sub>2</sub> injection into gas reservoirs starts immediately after the production of gas has ceased, in order to subdue changes in reservoir features, minimise water influx and allow for possible reuse of infrastructure (wells, pipelines, and platforms) and knowledge of the reservoir” (Damen et al., 2009).



**Figure 7.6:** Storage availability in time (Damen et al., 2009)

Figure 7.7 shows the potential storage sites in the Netherlands. “The majority of the gas fields are located in the northern part of the country and the continental shelf, whereas most large CO<sub>2</sub> sources are located in the western part of the country. The coal seams are predominantly located in the southern and eastern part of the country, whereas the aquifers are distributed more homogeneously” (Damen, 2009). So currently we can speak of a spatial mismatch between CO<sub>2</sub> sources and sinks.

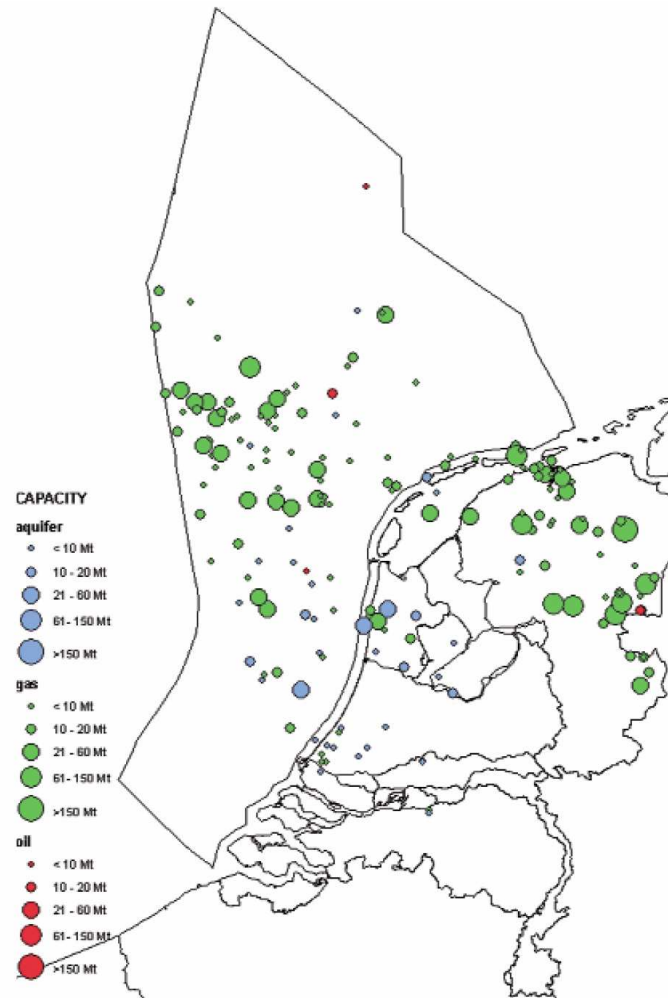


Figure 7.7: The locations and sizes of potential storage sites in the Netherlands (CATO, 2009).

## Appendix G: Exergy production (all steps)

In this section the complete calculation of the exergy production is described. The aim is to find the formula to calculate the exergy production in terms of the flow rate ( $Q$ ). Assumed that the water produced from this geothermal reservoir enters the surface facilities at  $T_2$ , and is reinjected into the reservoir at  $T_1$ . The ambient temperature is assumed  $T_0$ . All calculations are based on the book of Swaan Arons and van der Kooi (2004).

The useful work extracted from this reservoir is calculated by using the following equations. According to the first law of thermodynamics energy cannot be created or destroyed. The change in internal energy of the system is equal to the heat ( $Q$ ) added to the system minus the work ( $W$ ) done by the system, see Eq. 1.

$$\Delta U = Q + W \quad (1)$$

Rewriting Eq. (1) and ignoring macroscopic changes in the kinetic and/or potential energy of the flow in this process, Eq. (1) becomes

$$\dot{W}_{in} = \dot{m}\Delta H + \dot{Q}_{out} \quad (2)$$

The second law of thermodynamics for this process states

$$\dot{S}_{gen} = \dot{m}\Delta S + \dot{S}_0 \quad (3)$$

$$\Delta H = H_{P,T} - H_{P_0,T_0} \text{ and } \Delta S = S_{P,T} - S_{P_0,T_0} \quad (4)$$

Rewriting Eq. 1 gives

$$\dot{W}_{in}^{\min} = \dot{m}\Delta H + \dot{Q}_0^{\min} \quad (5)$$

The second part of the Second Law states that the entropy change of a system undergoing a reversible processes is given by:

$$\Delta S = \frac{Q}{T} \quad (6)$$

Rewrite Eq. 6 into

$$\dot{Q}_0^{\min} = T_0 \dot{S}_0 \quad (7)$$

Next combine Eqs. (X) and (X), and replace  $\dot{Q}_0^{\min}$  by Eq. 6, and find

$$\dot{W}_{in}^{\min} = \dot{m}(\Delta H - T_0 \Delta S) + T_0 \dot{S}_{gen} \quad (8)$$

There is no driving force in the process so

$$\dot{S}_{gen} = 0 \quad (9)$$

This causes that Eq. 7 becomes

$$\dot{W}_{in}^{\min} = \dot{m}(\Delta H - T_0 \Delta S) \quad (10)$$

Exergy can be defined according to

$$EX = \frac{W_{in}^{\min}}{m\dot{c}} \quad (11)$$

Eq. 12 shows the formula which is used to calculate the exergy content at a certain condition (condition i) as the amount of useful work confined in a unit of mass of the flow at conditions P and T with respect to the conditions of the environment.

$$EX_i = \left[ (H_{P,T} - H_{P_0,T_0}) - T_0(S_{P,T} - S_{P_0,T_0}) \right] \quad (12)$$

$$H_{P,T} = H_i \quad \text{and} \quad H_{P_0,T_0} = H_0 \quad (13)$$

$$S_{P,T} = S_i \quad \text{and} \quad S_{P_0,T_0} = S_0$$

Rewrite Eq. 12 by using Eq. 13 to obtain

$$EX_i = \left[ (H_i - H_0) - T_0(S_i - S_0) \right] \quad (14)$$

$$S_i - S_0 = c_p \ln \left( \frac{T_i}{T_0} \right) \quad C_p = \text{constant, not good for flows} \quad (15)$$

The entropy term of Eq. 14 can be rewritten, when assuming that the pressure under these conditions can be neglected, by using Eq. 15, we obtain:

$$EX_i = \left[ (H_i - H_0) - c_p T_0 \ln \left( \frac{T_i}{T_0} \right) \right] \quad (16)$$

Assuming that the specific heat of liquid water is constant and neglecting enthalpy changes due to the constant pressure, we can write:

$$H_i - H_0 = c_p (T_i - T_0) \quad C_p = \text{constant, not good for flows} \quad (17)$$

The enthalpy term of Eq. 16 can be rewritten, when assuming that the pressure under these conditions can be neglected, by using Eq. 17, we obtain:

$$EX_i = c_p (T_i - T_0) - c_p T_0 \ln \left( \frac{T_i}{T_0} \right) \quad (18)$$

Eq. 19 calculates the exergy content of the water which is being reinjected into the geothermal well after extracting the heat.

$$EX_1 = c_p (T_1 - T_0) - c_p T_0 \ln \left( \frac{T_1}{T_0} \right) \quad (19)$$

Eq. 20 calculates the exergy of the water coming out of the production well (condition 2):

$$EX_2 = c_p (T_2 - T_0) - c_p T_0 \ln \left( \frac{T_2}{T_0} \right) \quad (20)$$

Subtracting of Eq. 20 by Eq. 19 gives the total exergy produced by the geothermal well

$$\Delta Ex = Ex_2 - Ex_1 = c_p(T_2 - T_1) - c_p T_0 \ln\left(\frac{T_2}{T_1}\right) \quad (21)$$

where  $c_p$  is the water heat capacity at constant pressure. Note that temperatures in Eq.(21) must be in the Kelvin unit. The first and second terms on the right side of Eq.(21) are the energy and anergy terms, respectively.

The exergy power produced from this reservoir in terms of the production rate,  $Q$ , is:

$$\text{Exergy Power} = Q \times \rho_w \times (Ex_2 - Ex_1) \quad (22)$$

where  $\rho_w$  is the water density. However, there are several factors accounted as power losses that must be taken into account in the exergy analysis. In this study, two losses which are dependent on the flow rate (production speed) are: dissipation due to friction along the wells and power loss in the reservoir.

---

## Appendix H: Paragraph 9.1 and 9.2

## 9 CO<sub>2</sub> Emissions

During the production of the Carbon Capture and Storage facility a lot of CO<sub>2</sub> is being emitted into the atmosphere. Also when the plant is in operation it consumes energy, to run the pumps, absorber, compressor etc. In this chapter an analysis is made of all the CO<sub>2</sub> which is emitted during building of the whole facility and all the emissions during its use. With this kind of calculation a carbon footprint of the CCS process is made. According to the Centre of Sustainability Accounting (CenSa) the definition of carbon footprint is:

**“The Carbon footprint is a measure of exclusive amount of carbon dioxide emissions that is directly and indirectly caused by an activity” (Censa, 2002)**

In this appendix the extended version of paragraphs 9.1 and 9.2 can be read.

### 9.1 CO<sub>2</sub> emissions during steel production

In this paragraph the emission of carbon dioxide from energy use in the iron and steel industry is being treated. The iron and steel industry is one of the most energy-intensive sectors, accounting for about 7% of the total anthropogenic CO<sub>2</sub> emissions. To make a good estimation of the carbon dioxide emission during the production of steel, a comparison is made between 6 major steel producing countries: Republic of Korea (South Korea), Mexico, Brazil, China, India, and the United States of America (US). Almost all of these countries, excluding Mexico, have always been among the top 10 of steel producing countries in the 1990s (Kim et al, 2002).

Figure 9.1 shows the crude steel production, from the year 1995 China is the largest crude steel producer of the world.

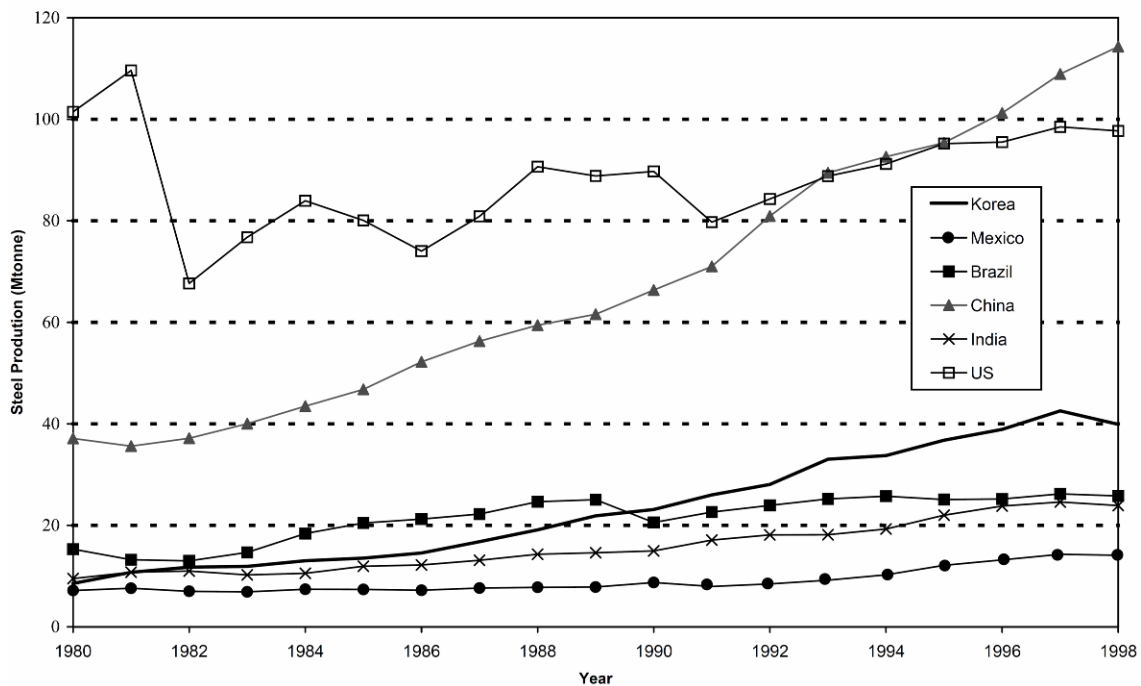


Figure 9.1: Crude steel production (Kim et al, 2002)

Figure 9.2 shows the CO<sub>2</sub> emissions for the iron and steel industry. Within this figure India is the third largest country with regard to CO<sub>2</sub> emissions, while it is the fifth in total steel production.

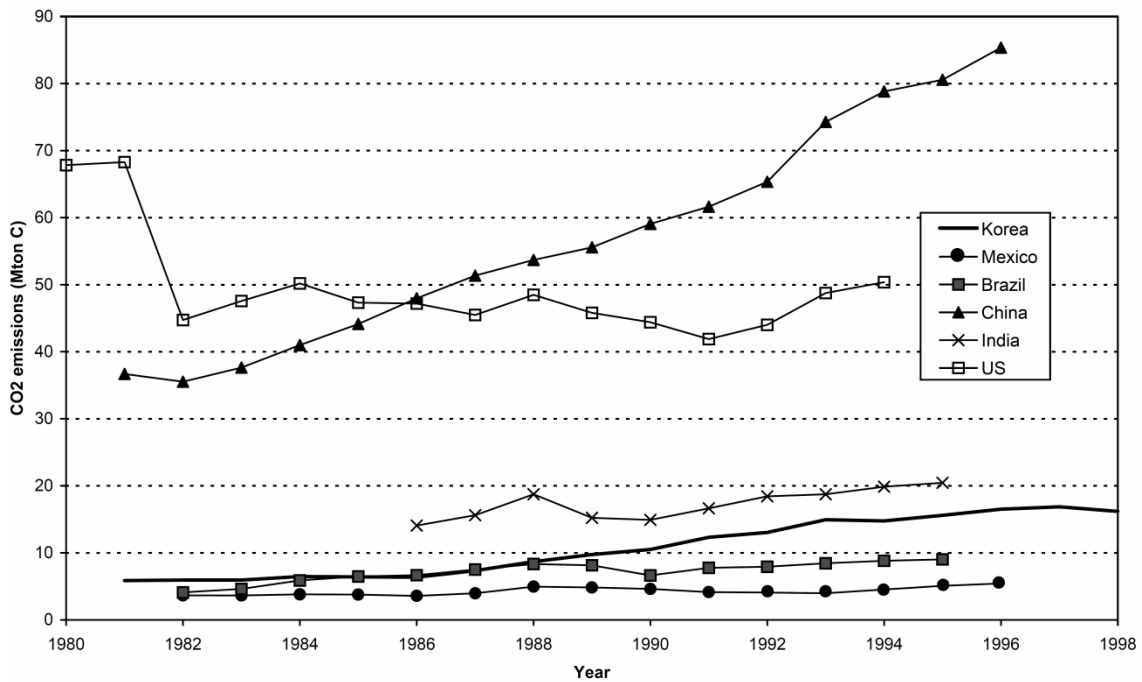


Figure 9.2: CO<sub>2</sub> emissions for the iron and steel industry (Kim et al, 2002)

When the total CO<sub>2</sub> emissions (Figure 9.2) are divided by the total steel production (Figure 9.1) we get the carbon dioxide emission per ton of steel per country (Figure 9.3). From Figure 9.3 can be seen that the carbon dioxide emission per ton of steel is decreasing over the years (-1,4% – -1,9% per year, except Brazil + 1,0%) but that there is still a very big difference among countries. The CO<sub>2</sub> intensities in India and China are much higher compared to other countries. The numbers from Figure 9.3 can be found in Table 9.1.

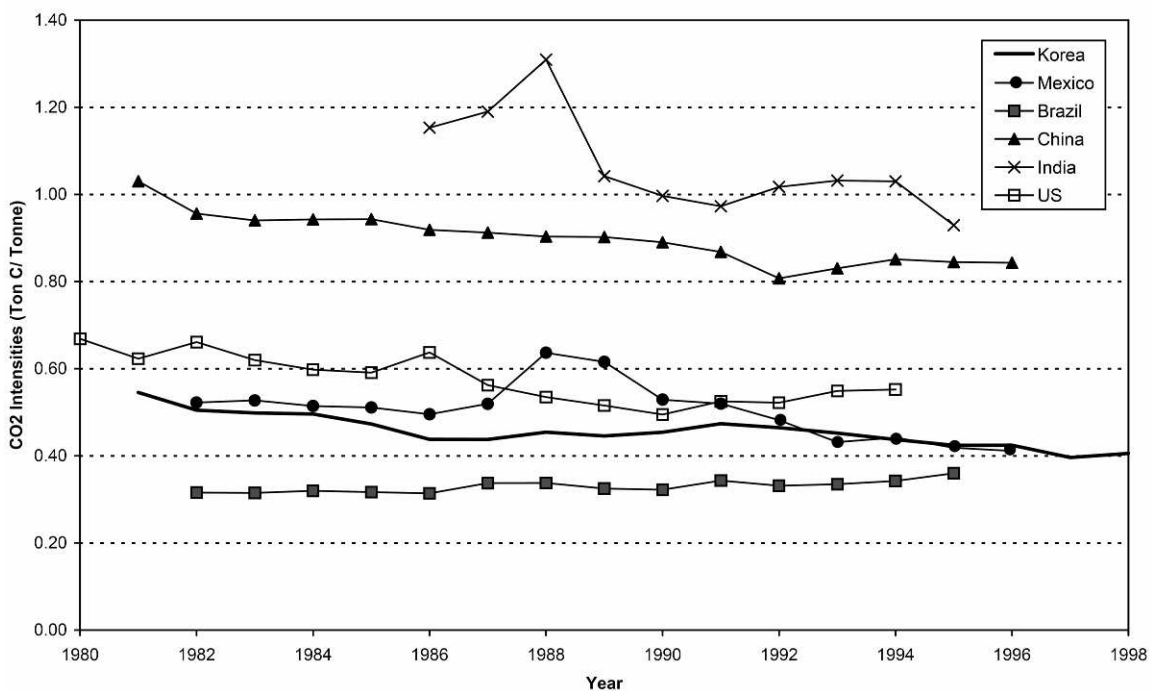


Figure 9.3: CO<sub>2</sub> intensities for the iron and steel industry (Kim et al, 2002)

Figure 9.4 show the final energy use for US iron and steel production, expressed in PJ (petajoule,  $10^{15}$  J). The figure excludes the transportation losses for purchased electricity. The figure shows the amount of different types of energy used during the whole process. Coal and coke are the biggest energy supplier of the process, followed by gas. Electricity and oil contribute for a very small part.

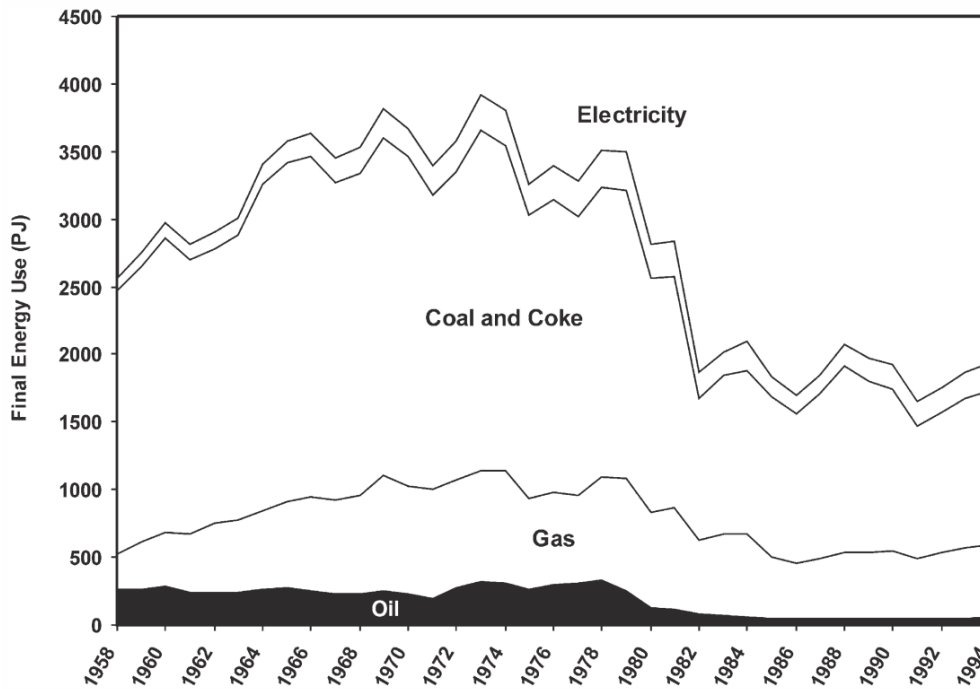


Figure 9.4: Final energy use for US iron and steel production (Worrel et al, 2001)

Figure 9.5 shows the carbon dioxide emissions from the energy consumption in the US iron and steel industry, expressed in MtC (Mega ton Carbon). The emissions exclude the emissions from electricity production of the purchased electricity.

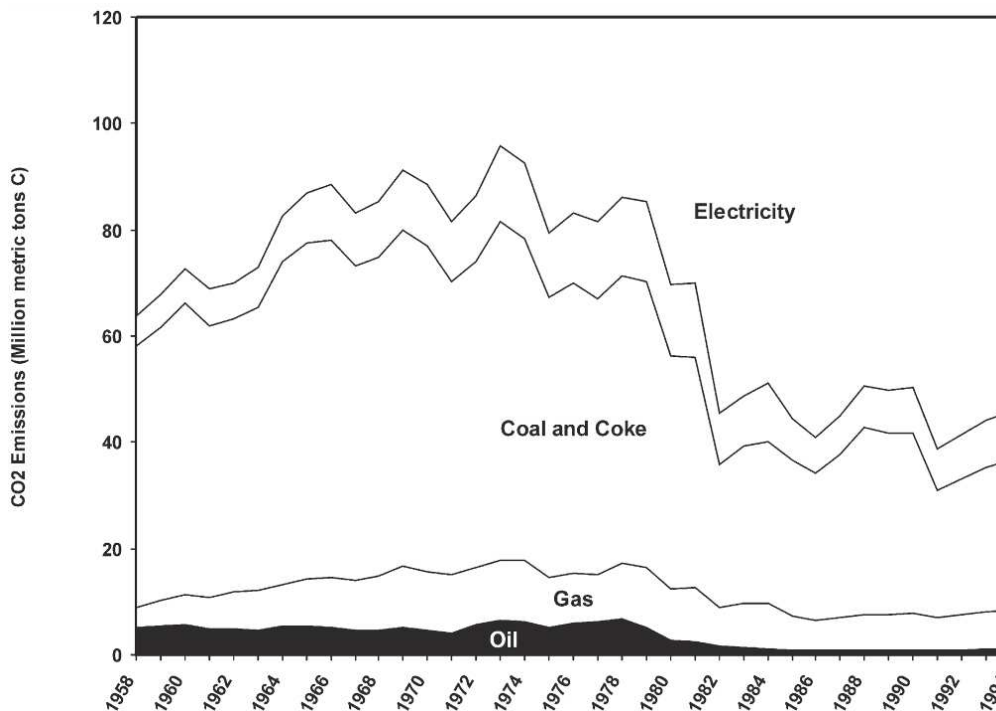


Figure 9.5: Carbon dioxide emissions from the energy consumption in the US iron and steel industry

As can be seen from Figure 9.5 coal and coke are causing the largest emission of carbon dioxide during the production of iron and steel. Table 9.1 shows the energy consumption, CO<sub>2</sub> emissions and CO<sub>2</sub> intensity in 1986 and 1994. The big difference in CO<sub>2</sub> intensity is caused by the difference in process routes being used. Currently there exist two main process routes for the crude steel production (Gielen and Moriguchi, 2002):

- Basic oxygen furnace (BOF)
- Electric arc furnace (EAF)

**Table 9.1:** Energy consumption and CO<sub>2</sub> emissions in 1986 and 1994 (Kim et al, 2002)

	Energy consumption (PJ)		CO <sub>2</sub> Emissions (Mton C)		CO <sub>2</sub> intensity (t C/ton)	
	1986	1994	1986	1994	1986	1994
<b>Korea</b>	294.6	658.7	6.4	14.8	0.44	0.44
<b>Mexico</b>	186.7	244.4	3.6	4.5	0.50	0.44
<b>Brazil</b>	508.1	597.2	6.7	8.8	0.31	0.34
<b>China</b>	2034.7	3262.3	48.0	78.8	0.92	0.85
<b>India</b>	561.7	793.1	14.1	19.9	1.15	1.03
<b>US</b>	2202.5	2469.1	47.2	50.4	0.64	0.55

When comparing Table 9.1 with the paper of Sandberg (2001) and Table 9.2 (Chang-qing, 2006) it can be concluded that the BOF route consumes ~3.5 times more energy than the EAF route. In the paper of Kim et al. it was not clear which route was used, when comparing both tables it can be concluded that it was the EAF route.

**Table 9.2:** Total primary energy consumption and CO<sub>2</sub> emissions (global average) per ton of steel

	Total primary energy consumption (GJ)			Total CO <sub>2</sub> emissions (ton)		
	Average	Maximum	Minimum	Average	Maximum	Minimum
<b>BF-BOF: coil and plate</b>	25.5	31.7	21.45	1.97	2.60	1.61
<b>EAF: section</b>	11.2	15.3	8.6	0.54	0.77	0.31
<b>EAF: rebar-wire rod-eng</b>	11.8	16.4	5.0	0.59	1.08	0.15

The average emission during the production of steel is 1.97 ton CO<sub>2</sub> /ton steel coil, so the total emission for manufacturing the steel pipes is 252.4 ton \* 1.97 = **497.3 ton CO<sub>2</sub>**.

## 9.2 CO<sub>2</sub> emissions during the production of steel pipes

This chapter describes the production of the steel pipes and their CO<sub>2</sub> emissions. The production process of the pipes is by far the largest emitter of carbon dioxide in the carbon footprint of pipeline projects. It requires significant energy to convert raw material into steel pipes. The main source of this paragraph is a report made by two Nacap employees, Syamak Nazary and Alfred Griffioen, the title of the document is: “Carbon Footprint of pipeline projects: A cradle-to-gate research”.

### 9.2.1 Steel production & pipe rolling

Figure 9.6 shows the production route of steel pipes, this route consists of three main steps. The first step is the reduction of iron ore in the blast furnace, the second step is the continuous casting and the final step is roll bending process.

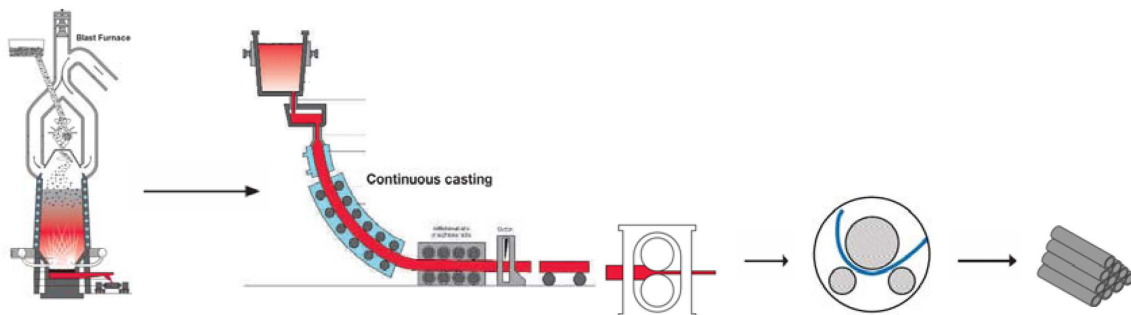


Figure 9.6: Steel pipe production process (Nacap)

The steel used contains between 1 to 1.8% manganese in order to increase depth and improve strength and hardness. The first step in the production process is melting of iron in the blast furnace. The iron in the blast furnace contains between 4 and 4.5 % carbon and is therefore brittle and unsuitable for forging or rolling into other products, although it is used for castings, where its rigidity and machinability are important. Most iron, however, is produced for processing into steel.

The reduction of Iron ore to hot metal in blast furnace and other reduction processes is almost entirely based on coal products; therefore the steel industry emits large amounts of carbon dioxide. The global average of CO<sub>2</sub> emissions resulting from the production of 1 ton of steel is 1.6 tons CO<sub>2</sub>. In Europe the average is around 1.5 tons/per ton steel and 1.8 tons/per ton steel in China. In these paragraphs an average of 1.55 is used.

The emissions can hardly be avoided as there is no other method to produce steel pipes. There are still other routes (such as electric arc furnace) for creating steel; however the other routes either emit more CO<sub>2</sub> and other green house gases compared to the blast furnace route, or the quality of steel produced by the other routes is not sufficient enough for pipelines. It is not yet known whether new processes can contribute to fewer emissions in the steel industry.

After the blast furnace the hot metal goes to the continuous casting process where the molten metal is poured directly into a casting machine to produce billets, blooms or slabs. After the billets are being produced the final step in the production of pipes is going to take place: the roll bending process. Table 9.3 shows the emissions of each step of the production of a pipe at different diameters.

Table 9.3: CO<sub>2</sub> emissions in steel pipe production

Diameter (inch)	Thickness (mm)	Weight (ton/km pipe)	CO <sub>2</sub> emissions (ton/km pipe)			
			Blast furnace	Continuous casting	Rolling & pipe production	Total
16	7.95	77.9	120.7	1.1	11.9	133.7
20	9.82	120.3	186.4	1.7	18.4	206.4
24	10.25	150.6	233.5	2.1	23	258.6
36	14.35	316.3	490.3	4.4	48.3	543
48	19.3	567.2	879.2	7.9	86.7	973.7

Figure 9.7 is a diagram made from Table 9.3 and shows the emissions of each step of the production of a pipe at different diameters.

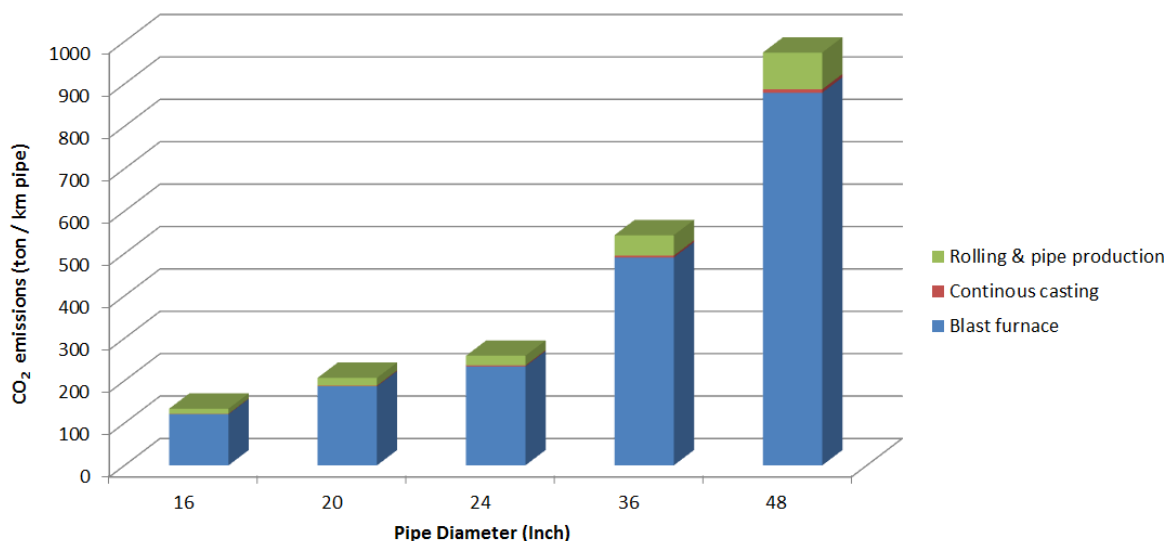


Figure 9.7: CO<sub>2</sub> emissions in steel pipe production

### 9.2.2 Transport emissions

Table 9.4: illustrates the emissions given in kilograms CO<sub>2</sub> caused by the transport activities required to transport a certain diameter of pipeline project over 1,000 kilometres. These 1,000 km's are taken as an average. This component only concentrates on the heavy transportation of pipeline projects. The transportation of personnel and business flights are included in the overhead.

The transportation activity is divided into two different parts; the equipment and the pipes. The equipment weight per km of pipe is calculated by dividing the average tonnage of equipment used in a pipeline project for a specific diameter by the average length of such a project.

Table 9.4: CO<sub>2</sub> emissions for the transport of pipes and equipment

Diameter (inch)	Weight (ton/km pipe)		CO <sub>2</sub> emissions (ton/km pipe)		
	Pipes	Equipment	Pipe transport	Equipment	Total
16	77.9	16.8	7.79	2.07	9.85
20	120.3	32.0	12.03	3.94	15.96
24	150.6	58.7	15.06	7.22	22.28
36	316.3	139.2	31.63	17.12	48.75
48	567.2	234.7	56.72	28.86	85.59

The table shows the difference between the transportation of equipment and pipes. The reason is that the equipment is in most cases comparable in weight than a truckload full of pipes, but is used over a much longer stretch. The emissions are based on an average of 0.1 kg of CO<sub>2</sub> per tonne.km of transportation by ship, rail and road, since all three mentioned transportation methods are used by pipe contractors, due to the diversity of locations for pipeline projects.

The table shows an almost linear growth of the transportation activities. The larger the diameter the more equipment is required to place a pipeline. The weight of the pipelines with similar thickness is also more or less linear in their emissions.

Figure 9.8 is a diagram made from Table 9.4: and shows the emissions of each step of the production of a pipe at different diameters.

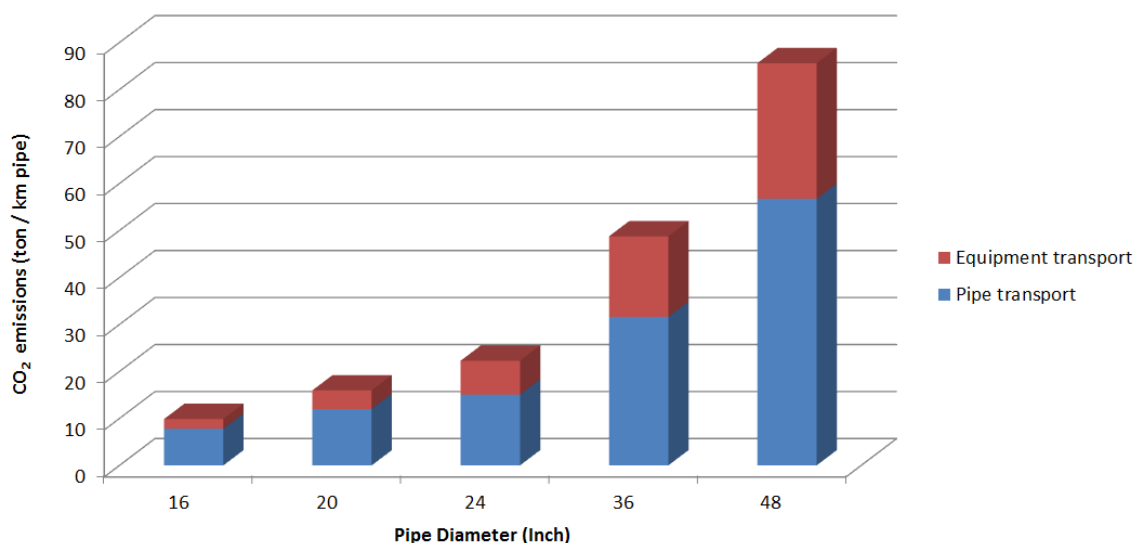


Figure 9.8: CO<sub>2</sub> emissions for the transport of pipes and equipment

### 9.2.3 Equipment fuel usage emissions

The equipment used during pipeline construction is an important contributor of the total emissions during a pipeline set up. The equipment is grouped into five separate equipment sections: the earth moving equipment, heavy lifting equipment, typical pipeline equipment, transport equipment and others (compressors, pumps etc.).

Table 9.5 illustrates the emissions of the equipment. Various projects were used to calculate the emissions per km of pipeline accurately. The emissions are calculated by multiplying the equipment fuel usage by the CO<sub>2</sub> conversion factor for diesel.

Table 9.5: CO<sub>2</sub> emissions of different type of equipment

Diameter (inch)	CO <sub>2</sub> emissions (ton/km pipe)					Total
	Earth moving equipment	Heavy lifting equipment	Pipeline equipment	Transport equipment	Other equipment	
16	27.80	1.30	3.40	15.90	3.30	49.20
20	24.20	10.50	11.20	3.40	4.30	53.40
24	37.30	5.50	7.40	6.50	27.30	84.00
36	54.10	25.50	14.60	18.00	7.60	119.70
48	68.60	25.80	10.80	24.90	8.50	138.60

Figure 9.9 highlights the difference in emissions between a 24 inch and a 36 inch pipeline being higher than emissions between 36 inch and 48 inch, while their difference in diameter is similar (12 inches). The explanation is the usage of heavy lifting material during the projects. For instance, projects under the diameter of 30 inches use less side-booms in terms of hours and fuel usage. However the largest emitter group within the equipment section is the earth moving equipment due to the high fuel consumption required to move large amounts of soil to place the pipes.

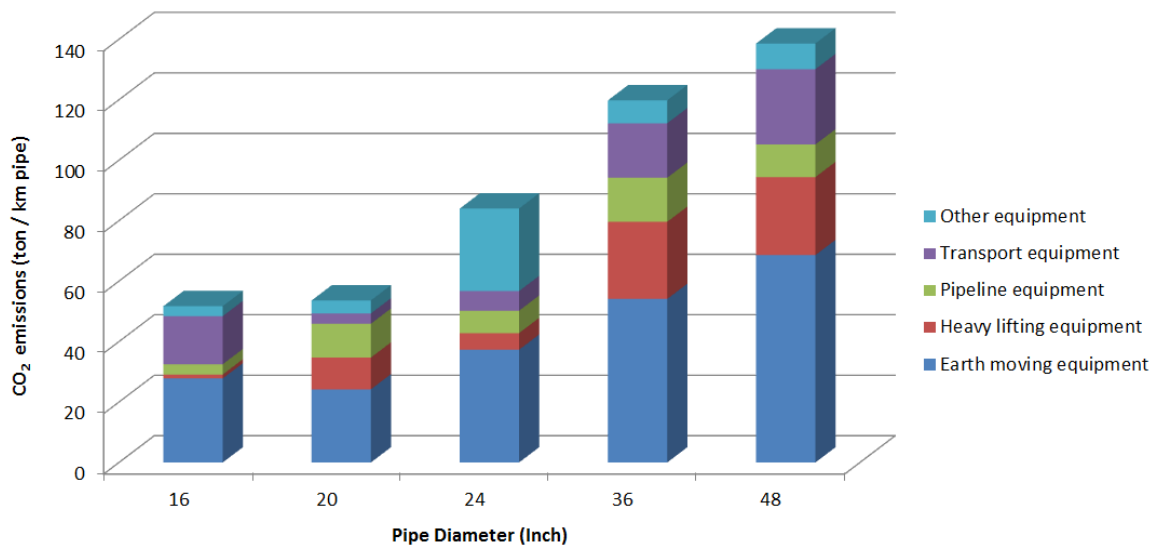


Figure 9.9: CO<sub>2</sub> emissions of equipment

### 9.2.4 Others

Others are materials or equipment which is consumed, destroyed, wasted, dissipated and or spent during the production/execution period of a pipeline project. In this research we have focussed on the coating material used during the welding process and on the welding electrodes. Table 4 and Figure 9.10 illustrate the calculated emissions of these items for pipeline projects.

Table 9.6: CO<sub>2</sub> emissions from other items

Diameter (inch)	Weight (ton/km pipe)		CO <sub>2</sub> emissions (ton/km pipe)		
	Coating	Electrodes	Coating	Electrodes	Total
16	4.0	0.04	6.8	0.06	6.9
20	5.0	0.07	8.5	0.12	8.6
24	6.0	0.09	10.2	0.16	10.4
36	9.0	0.27	15.3	0.47	15.8
48	12.0	0.66	20.4	1.13	21.5

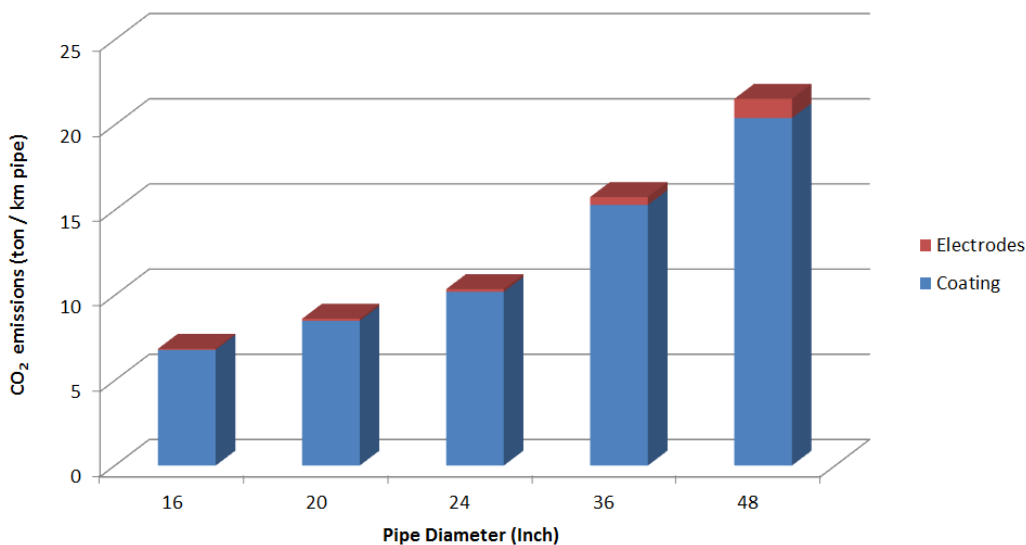


Figure 9.10: CO<sub>2</sub> emissions from other items

### 9.2.5 Overhead

The overhead emissions calculated consist out of business flights, transportation of personnel working in 8 different regional offices and on site, and finally the emissions caused by the facilities used. The carbon dioxide emissions are all based on the activities of Nacap in 2008. The overhead component is not divided in diameters due to the fact that these activities will still be executed regardless of any diameter pipeline project.

### 9.2.6 Total

In this paragraph all the individual results of the previous paragraphs are combined, Table 9.7 shows the total CO<sub>2</sub> emissions for laying 1 km of pipeline for different diameters.

Table 9.7: Total CO<sub>2</sub> emissions for laying a pipeline

Diameter (inch)	CO <sub>2</sub> emissions (ton/km pipe)					Total
	Steel production & pipe rolling	Transport (1000 km)	Equipment fuel usage	Coating & welding	Overhead	
16	133.7	9.9	49.2	6.9	40.7	240.4
20	206.4	16.0	53.4	8.6	40.7	325.1
24	258.6	22.3	84.0	10.4	40.7	415.9
36	543.0	48.8	119.7	15.8	40.7	768.0
48	973.7	85.6	138.6	21.5	40.7	1260.1

Figure 9.11 shows the same average total CO<sub>2</sub> emissions of a pipeline project for several diameters per kilometer. It also illustrates the carbon dioxide emissions of Nacap (pipeline contractor) in relation to the emissions of steel pipe suppliers. The calculated amount of emissions per kilometer of pipeline for a diameter of 48 inches is more than **1,260 tons of CO<sub>2</sub>**.

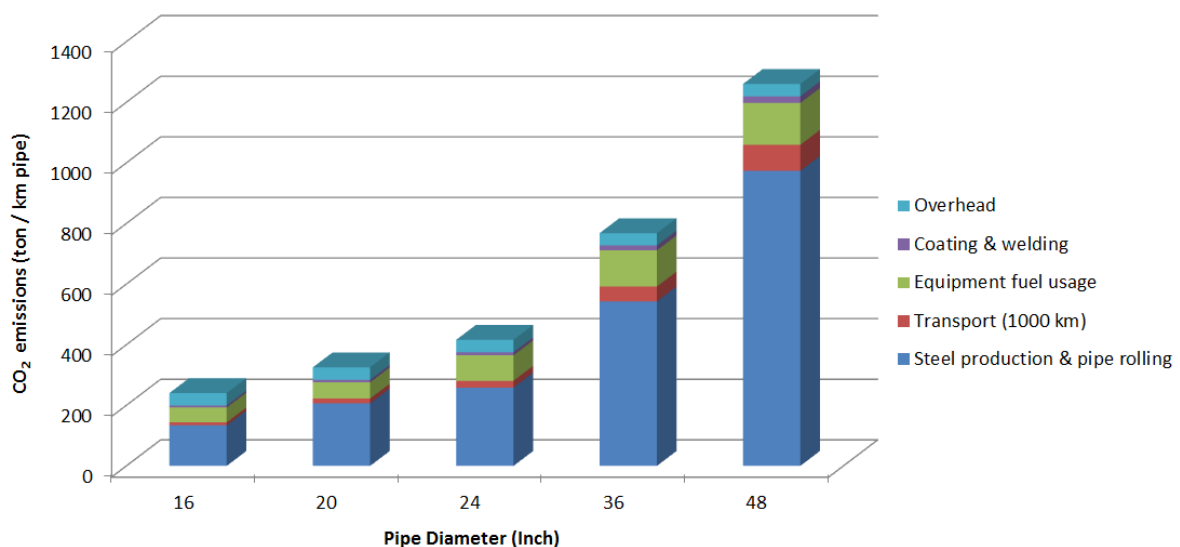


Figure 9.11: Total CO<sub>2</sub> emissions for laying a pipeline

The chart shows that the most important cause of CO<sub>2</sub> emissions is the pipe production. This can either be reduced by using stronger kinds of steel, which allows for a smaller pipe thickness. Another way is to examine whether it is possible to use steel from a different production process, for example by re-using scrap. Up to now it is not possible to create steel with the right quality for oil and gas pipelines.

## Appendix I: Conversion Factors

Source: website Berkeley University, link: [http://astro.berkeley.edu/~wright/fuel\\_energy.html](http://astro.berkeley.edu/~wright/fuel_energy.html)

1 Therm = 100,000 Btu

1 Btu = 1055.6 Joules (J)

1 MJ =  $10^6$  J

1 GJ =  $10^9$  J

1 TJ =  $10^{12}$  J

1 PJ =  $10^{15}$  J

29.0 PJ = 1 million tonnes of coal equivalent

41.868 PJ = 1 million tonnes of oil equivalent

3.60 MJ = 1 kilowatt-hour (kWh)

1 barrel condensate = 0.935 barrels of oil equivalent

1 PJ of Natural Gas = 172,000 barrels of oil equivalent

1 tonne LPG = 8.46 barrels of oil equivalent

1 cubic meter ( $m^3$ ) = 35.315 cubic feet

1 tonne = 1000 Kg

1 kilolitre = 6.2898 barrels

## Appendix J: Energy Density

Source: website Berkeley University, link: [http://astro.berkeley.edu/~wright/fuel\\_energy.html](http://astro.berkeley.edu/~wright/fuel_energy.html)

NB: Actual calorific values vary depending on fuel composition.

Solid Fuel		GJ/tonne		
Black Coal	Export coking coal	29.0		
	Export steaming coal	27.0		
	Local coal (electricity)	24.0		
Brown Coal		9.5		
Coke		27.0		
Wood	Dry	16.2		
Bagasse		9.6		
Plant Biomass	Cotton trash	18.0		
Gaseous Fuel		MJ/m <sup>3</sup>		
Natural Gas		39.0		
Ethane		66.0		
LPG	Propane	93.3		
LPG	Butane	124.0		
Town Gas	Reformed gas	20.0		
Gas	Coke oven	18.1		
Gas	Blast furnace	4.0		
Liquid Fuel		MJ/litre	Litre/Tonne	GJ/tonne
LPG	Propane	25.3	1960	49.6
LPG	Butane	27.7	1750	49.1
LPG	Mixture	25.7	1928	49.6
Gasoline	Aviation	33.0	1412	49.6
Gasoline	Automotive	34.2	1360	46.4
Kerosene	Power	37.5	1230	46.1
Kerosene	Turbine fuel	36.8	1261	46.4
Kerosene	Lighting	36.6	1270	46.5
Heating Oil		37.3	1238	46.2
Diesel Oil	Automotive	38.6	1182	45.6
Diesel Oil	Industrial	39.6	1135	44.9
Fuel Oil	Low sulphur	39.7	1110	44.1
Fuel Oil	High sulphur	40.8	1050	42.9
Refinery Fuel		40.9	1050	42.9
Naphtha		31.4	1534	48.1
Lubricants		38.8	1120	43.4
Bitumen		44.0	981	42.7
Solvents		34.4	1229	44.0
Waxes		38.8	1180	45.8
Crude Oil		38.7	1160	44.9
Ethanol		23.4	1266	29.6
LNG	-160C & 300kPa	25.0	2174	54.4
Uranium		GJ/tonne		
Uranium	Metal (U)	560,000		
Uranium	Oxide (U <sub>3</sub> O <sub>8</sub> )	470,000		

## Appendix K: CO<sub>2</sub> Emission Factors

The tables below show the heating value and standard CO<sub>2</sub> emission factors of fuels used in The Netherlands (Senternovem, edition April 2009).

Main group (Dutch language)	Main group (English) IPCC (supplemented)	Unit	HV (MJ/unit)	CO <sub>2</sub> EF (kg/GJ)
	<b>A. Liquid Fossil, Primary Fuels</b>			
Ruwe aardolie	Crude oil	Kg	42.7	73.3
Orimulsion	Orimulsion	Kg	27.5	80.7
Aardgascondensaat	Natural Gas Liquids	Kg	44.0	63.1
	<b>Liquid Fossil, Secondary Fuels/ Products</b>			
Motorbenzine	Petrol/gasoline	Kg	44.0	72.0
Kerosine luchtvaart	Jet Kerosene	Kg	43.5	71.5
Petroleum	Other Kerosene	Kg	43.1	71.9
Leisteenolie	Shale oil	Kg	36.0	73.3
Gas-/dieselolie	Gas/ Diesel oil	Kg	42.7	74.3
Zware stookolie	Residual Fuel oil	Kg	41.0	77.4
LPG	LPG	Kg	45.2	66.7
Ethaan	Ethane	Kg	45.2	61.6
Nafta's	Naphtha	Kg	44.0	73.3
Bitumen	Bitumen	Kg	41.9	80.7
Smeeroliën	Lubricants	Kg	41.4	73.3
Petroleumcokes	Petroleum Coke	Kg	35.2	100.8
Raffinaderij grondstoffen	Refinery Feedstocks	Kg	44.8	73.3
Raffinaderijgas	Refinery Gas	Kg	45.2	66.7
Chemisch restgas	Chemical Waste Gas	Kg	45.2	66.7
Overige oliën	Other Oil	Kg	40.2	73.3
	<b>B. Solid Fossil, Primary Fuels</b>			
Antraciet	Anthracite	Kg	26.6	98.3
Cokeskolen	Coking Coal	Kg	28.7	94.0
Cokeskolen (cokeovens)	Coking Coal (used in coke oven)	Kg	28.7	95.4
Cokeskolen (basismetaal)	Coking Coal (used in blast furnaces)	Kg	28.7	89.8
(Overige bitumineuze) steenkool	Other Bituminous Coal	Kg	24.5	94.7
Sub-bitumineuze kool	Sub-bituminous Coal	Kg	20.7	96.1
Bruinkool	Lignite	Kg	20.0	101.2
Bitumineuze Leisteen	Oil Shale	Kg	9.4	106.7
Turf	Peat	Kg	10.8	106.0
	<b>Solid Fossil, Secondary Fuels</b>			
Steenkool- en bruinkoolbriketten	BKB & Patent Fuel	Kg	23.5	94.6
Cokesoven/ gascokes Coke	Oven/Gas Coke	Kg	28.5	111.9
Cokesovengas Coke	Oven gas	MJ	1.0	41.2
Hoogovengas	Blast Furnace Gas	MJ	1.0	247.4
Oxystaalovengas	Oxy Gas	MJ	1.0	191.9
Fosforovengas	Phosphor Gas	Nm <sup>3</sup>	11.6	149.5

Main group (Dutch language)	Main group (English) IPCC (supplemented)	Unit	HV (MJ/unit)	CO <sub>2</sub> EF (kg/GJ)
	<b>C. Gaseous Fossil Fuels</b>			
Aardgas	Natural Gas (dry)	Nm <sup>3</sup>	31.65	56.7 *)
Koolmonoxide	Carbon Monoxide	Nm <sup>3</sup>	12.6	155.2
Methaan	Methane	Nm <sup>3</sup>	35.9	54.9
Waterstof	Hydrogen	Nm <sup>3</sup>	10.8	0.0
	<b>Biomass **)</b>			
Biomassa vast	Solid Biomass	Kg	15.1	109.6
Biomassa vloeibaar	Liquid Biomass	Kg	39.4	71.2
Biomassa gasvormig	Gas Biomass	Nm <sup>3</sup>	21.8	90.8
RWZI biogas	Wastewater biogas	Nm <sup>3</sup>	23.3	84.2
Stortgas	Landfill gas	Nm <sup>3</sup>	19.5	100.7
Industrieel fermentatiegas	Industrial organic waste gas	Nm <sup>3</sup>	23.3	84.2
	<b>D. Other fuels</b>			
Afval (niet biogeen)	Waste (not biogenic)	Kg	34.4	73.6

## Appendix L: Electricity Emission Factors

The table below shows the electricity emission factors of different countries. This page is copy from U.S. Department of Energy, Energy Information Administration (2007).

U.S. Department of Energy  
Energy Information Administration  
Form EIA-1605 (2007)

Voluntary Reporting of Greenhouse Gases

Form Approved  
OMB No. 1905-0194  
Expiration Date: 07/31/2010

### F.3 Foreign Electricity Emission Factors, 1999-2002

Region/Country	Emission Inventory <sup>a</sup>			Emission Reductions	
	Carbon Dioxide (Metric tons/ MWh)	Methane (kg/ MWh)	Nitrous Oxide (kg/ MWh)	Avoided Emissions <sup>b</sup> (Metric tons CO <sub>2</sub> e/MWh)	Indirect Emissions <sup>c</sup> (Metric tons CO <sub>2</sub> e/MWh)
<b>OECD North America</b>					
Canada	0.223	0.00390	0.00351	0.802	0.876
Mexico	0.593	0.01676	0.00230	0.763	0.899
<b>OECD Europe<sup>d</sup></b>	<b>0.387</b>	<b>0.00694</b>	<b>0.00505</b>	<b>0.694</b>	<b>0.749</b>
Austria	0.197	0.00377	0.00207	0.558	0.594
Belgium	0.289	0.00420	0.00275	0.682	0.716
Czech Republic	0.604	0.00783	0.01074	0.782	0.854
Denmark	0.358	0.01181	0.00831	0.475	0.506
Finland	0.239	0.00395	0.00348	0.451	0.468
France	0.083	0.00136	0.00093	0.849	0.912
Germany	0.539	0.00637	0.00779	0.829	0.869
Greece	0.887	0.01453	0.01141	0.900	1.044
Hungary	0.437	0.01009	0.00540	0.673	0.773
Iceland	0.001	0.00003	0.00001	0.315	0.331
Ireland	0.699	0.01623	0.00765	0.738	0.807
Italy	0.525	0.01773	0.00482	0.649	0.693
Luxembourg <sup>e</sup>	0.387	0.00694	0.00505	0.694	0.749
Netherlands	0.479	0.00998	0.00492	0.545	0.568
Norway	0.005	0.00003	0.00001	0.410	0.442
Poland	0.730	0.01084	0.01528	0.749	0.848
Portugal	0.511	0.01459	0.00711	0.690	0.755
Slovak Republic	0.297	0.00357	0.00324	0.706	0.750
Spain	0.443	0.00923	0.00631	0.790	0.865
Sweden	0.048	0.00092	0.00046	0.495	0.537
Switzerland	0.022	0.00030	0.00005	0.379	0.408
Turkey	0.584	0.01135	0.00628	0.786	0.973
United Kingdom	0.475	0.00793	0.00549	0.643	0.701
<b>OECD Asia</b>	<b>0.511</b>	<b>0.00787</b>	<b>0.00679</b>	<b>0.808</b>	<b>0.963</b>
Australia	0.924	0.01008	0.01290	0.900	1.096
Japan	0.417	0.00839	0.00465	0.696	0.730
Korea	0.493	0.00758	0.00672	0.842	0.892
New Zealand	0.159	0.00307	0.00084	0.526	0.595
<b>Non-OECD Europe and Eurasia</b>	<b>0.513</b>	<b>0.01300</b>	<b>0.01309</b>	<b>0.900</b>	<b>1.077</b>
Albania	0.051	0.00251	0.00050	0.685	1.025
Armenia	0.230	0.00950	0.00095	0.490	0.693
Azerbaijan	0.613	0.03937	0.00710	0.664	0.790
Belarus	0.326	0.02441	0.00335	0.328	0.369
Bosnia-Herzegovina	0.770	0.01074	0.01544	0.900	2.145
Bulgaria	0.492	0.01087	0.01351	0.900	1.124
Croatia <sup>e</sup>	0.513	0.01300	0.01309	0.900	1.077
Estonia	0.774	0.02085	0.02810	0.900	1.300
FYR of Macedonia	0.773	0.01810	0.02453	0.900	1.255
Georgia	0.137	0.00392	0.00052	0.853	1.007
Gibraltar	0.870	0.05168	0.01034	0.874	0.874
Kazakhstan	1.293	0.01888	0.02150	0.900	1.814
Kyrgyzstan	0.102	0.00209	0.00168	0.407	0.605
Latvia <sup>e</sup>	0.513	0.01300	0.01309	0.900	1.077
Lithuania	0.165	0.00629	0.00103	0.343	0.407
Malta	0.904	0.05977	0.01195	0.900	1.051
Republic of Moldova <sup>e</sup>	0.513	0.01300	0.01309	0.900	1.077
Romania	0.426	0.01443	0.01135	0.676	0.785
Russia	0.351	0.01379	0.00668	0.403	0.463
Serbia and Montenegro	0.786	0.01291	0.01828	0.900	1.595
Slovenia	0.369	0.00674	0.00915	0.861	0.918
Tajikistan	0.038	0.00044	0.00004	0.475	0.554



## Appendix N: Calculation of the wall thickness of the pipe

The formula's used in this appendix are from paper of Pochodaj (2005). To calculate the amount of steel needed to produce the pipeline which is needed for the transportation of CO<sub>2</sub> from a large point-source to a storage point a lot of information is needed. In the previous paragraphs the length and diameter of the pipeline is calculated. But a third parameter is needed to calculate the amount of steel namely the thickness of the wall. The thickness of the wall depends the stress and pressure on the pipeline. To calculate the thickness of the wall, formulas for thick cylinders are used for this calculation because the theoretical treatment of thin cylinders assumes that the hoop stress is constant across the thickness of the cylinder wall, and also that there is no pressure gradient across the wall. Neither of these assumptions can be used for thick cylinders. Lamé equation is used to calculate the hoop and radial stresses:

$$\text{Hoop stress: } \sigma_H = A + \frac{B}{r^2} \quad (1)$$

$$\text{Radial stress: } \sigma_r = A - \frac{B}{r^2} \quad (2)$$

Figure 9.12 shows an intersection of a thick cylinder with P for pressure and r for radius.

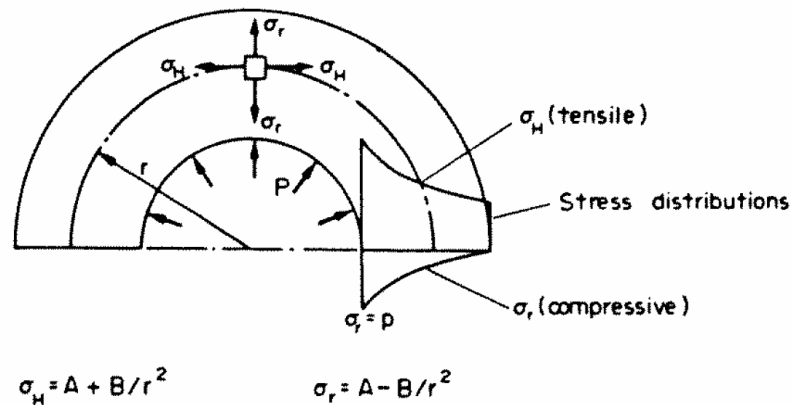


Figure 9.12: Intersection of cylinder (Pochodaj, 2005)

For the internal pressure  $P_1$  is used and for the external pressure  $P_2$  and the internal and external radii  $R_1$  and  $R_2$  are used respectively. The longitudinal stress in a cylinder with closed ends the following formula is used:

$$\sigma_L = \frac{P_1 R_1^2 - P_2 R_2^2}{R_2^2 - R_1^2} = \text{Lamé constant } A \quad (3)$$

$$B = \frac{(P_1 - P_2) R_1^2 R_2^2}{R_2^2 - R_1^2} \quad (4)$$

To calculate the maximum shear stress at any point of the cylinder the following equation is used:

$$\tau_{\max} = \frac{\sigma_H - \sigma_r}{2} \quad (5)$$

since  $\sigma_H$  is normally tensile, whilst  $\sigma_r$  is compressive and both exceed  $\sigma_L$  in magnitude

$$\tau_{\max} = \frac{1}{2} \left[ \left( A - \frac{B}{r^2} \right) - \left( A - \frac{B}{r^2} \right) \right] \quad (6)$$

$$\tau_{\max} = \frac{B}{r^2} \quad (7)$$

The greatest value of  $\tau_{\max}$  thus normally occurs at the inside radius where  $r = R_1$ .

Substituting equation X and X can be written as:

$$\tau_{\max} = \frac{(P_1 - P_2)R_1^2 R_2^2}{R_2^2 (R_2^2 - R_1^2)} \quad (8)$$

Where  $R_2 = R_1 - t$  and  $R_1 = \frac{D}{2}$ , putting in to equation:

$$\tau_{\max} = \frac{(P_1 - P_2) \left( \frac{D^2}{4} + 2 \frac{D}{2} t + t^2 \right)}{2 \frac{D}{2} t + t^2} \quad (9)$$

Transformation with regard on t:

$$\left[ \tau_{\max} - (P_1 - P_2) \right] \cdot t^2 + \left[ \tau_{\max} D - (P_1 - P_2) D \right] \cdot t - \frac{(P_1 - P_2)}{4} D^2 = 0 \quad (10)$$

Simplifying equation by dividing it into 3 parts:

$$1: \left[ \tau_{\max} - (P_1 - P_2) \right] \quad (11)$$

$$2: \left[ \tau_{\max} D - (P_1 - P_2) D \right] \quad (12)$$

$$3: \frac{(P_1 - P_2)}{4} D^2 \quad (13)$$

Substituting into equation:

$$\Delta = \quad (14)$$

$$\sqrt{\Delta} = \quad (15)$$

$$t = \frac{D - 4ac}{2b} = \quad (16)$$

## Appendix 0: Drilling formulas

The formula's used in this appendix are from a SPE (Society of Petroleum Engineers) paper by Samuel G. R. and McColpin G., 2001. The table shows the parameters used in this appendix.

<b>Symbol</b>	<b>Name</b>
$W^x$	Bit diameter
$i$	
$D_h$	Diameter of the housing
	Diameter of the shaft
$p_h$	Pitch of the motor
$N$	Rotational Speed per minute (rpm)
$ROP$	Rate of penetration (ft / hr)
$WOP$	Weight on bit (klbs)
$HP$	Maximal Horse Power
$a_1$	
$a_2$	
$d_b$	
$K_f$	Formation drillability factor (ft / hr)
$K_x$	Constant
$K_y$	Constant
$K_b$	Formation hardness, teeth, bearing, mud coefficient
$K_i$	Winding ration coefficient
$K_{rc}$	Pressure drop coefficient
$\eta$	Overall efficiency

The relationship between the pressure drop across the motor in terms of the WOB (weight on bit) can be given as:

$$\Delta p_{mot} = K_{rc} \left( \frac{W^x d_b^y}{D_h^2 p_h \eta} \right) \quad (1)$$

where,

$$K_{RC} = \left( \frac{K_x K_b}{K_y K_i} \right) \quad (2)$$

and,

$$K_i = i \left( \frac{1+i}{(2-i)^2} \right) \quad (3)$$

Combine Eq. 1 and Eq. 2 and fill in

$$\Delta p_{mot} = \left( \frac{K_x K_b}{K_y K_i} \right) \cdot \left( \frac{W^x d_b^y}{D_h^2 p_h \eta} \right) = \quad (4)$$

A relation for torque is:

$$T = 0,01 \Delta p_{mot} i \left( \frac{1+i}{(2-i)^2} \right) D_h^2 p_h \eta \quad (5)$$

The average rate of penetration as a function of weight on bit and bit rotational speed is given by,

$$ROP = K_f \left( \frac{W}{4d_b} \right)^{a_1} \left( \frac{N}{100} \right)^{a_2} \quad (6)$$

where  $K_f = X$ ,  $W = X$ ,  $N = X$ ,  $d_b = X$

$$N = \left( \frac{HP}{\frac{T}{550} \frac{2\pi}{60}} \right) \quad (7)$$

The power required for drilling can be calculated by the following formula

$$HP_b = K_f W^x N d_b^y \quad (8)$$

When the rate of penetration (ROP) is known, the drilling time can be calculated by dividing the required drilling depth by the ROP.

$$Drilling\ Time = \frac{Depth}{ROP} \quad (9)$$

With the use of Eq. 9 the drilling time can be calculated. Example: When a well with a depth of 3200 meter has to drilled and the ROP is 80 meters/day, it will take 40 days of non-stop drilling. When the drilling time is known it is very easy to calculated the energy needed to drill the hole, by using the following formula:

$$Drilling\ Energy = Drilling\ Time \cdot Moter\ Power \quad (10)$$

## Appendix P: Complete Exergy Table

This table shows the exergy production, power loss in the wells, power loss in the reservoir and the available exergy at different flow rates.

Flow rate [m <sup>3</sup> ]	Exergy Production [MW]	Power loss in wells (Exergy) [MW]	Power loss in reservoir (Exergy) [MW]	Available Exergy [MW]
0	0.00	0.00	0.00	0.00
10	0.06	0.00	0.00	0.06
20	0.12	0.00	0.00	0.12
30	0.19	0.00	0.01	0.18
40	0.25	0.00	0.01	0.23
50	0.31	0.00	0.02	0.29
60	0.37	0.01	0.03	0.33
70	0.44	0.01	0.04	0.38
80	0.50	0.01	0.06	0.43
90	0.56	0.02	0.07	0.47
100	0.62	0.03	0.09	0.50
110	0.69	0.04	0.11	0.54
120	0.75	0.05	0.13	0.57
130	0.81	0.06	0.15	0.59
140	0.87	0.08	0.18	0.62
150	0.93	0.09	0.21	0.63
160	1.00	0.11	0.23	0.65
170	1.06	0.14	0.26	0.66
180	1.12	0.16	0.30	0.66
190	1.18	0.19	0.33	0.66
200	1.25	0.22	0.36	0.66
210	1.31	0.26	0.40	0.65
220	1.37	0.30	0.44	0.63
230	1.43	0.34	0.48	0.61
240	1.50	0.39	0.53	0.58
250	1.56	0.44	0.57	0.55
260	1.62	0.49	0.62	0.51
270	1.68	0.55	0.66	0.47
280	1.74	0.62	0.71	0.41
290	1.81	0.68	0.77	0.36
300	1.87	0.76	0.82	0.29

Flow rate [m <sup>3</sup> ]	Exergy Production [MW]	Power loss in wells (Exergy) [MW]	Power loss in reservoir (Exergy) [MW]	Available Exergy [MW]
310	1.93	0.83	0.88	0.22
320	1.99	0.92	0.93	0.14
330	2.06	1.01	0.99	0.06
340	2.12	1.10	1.05	-0.04
350	2.18	1.20	1.12	-0.14
360	2.24	1.31	1.18	-0.25
370	2.31	1.42	1.25	-0.36
380	2.37	1.54	1.32	-0.49
390	2.43	1.66	1.39	-0.62
400	2.49	1.79	1.46	-0.76
410	2.55	1.93	1.53	-0.91
420	2.62	2.08	1.61	-1.07
430	2.68	2.23	1.69	-1.23
440	2.74	2.39	1.76	-1.41
450	2.80	2.55	1.85	-1.60
460	2.87	2.73	1.93	-1.79
470	2.93	2.91	2.01	-1.99
480	2.99	3.10	2.10	-2.21
490	3.05	3.30	2.19	-2.43
500	3.12	3.50	2.28	-2.67
510	3.18	3.72	2.37	-2.91
520	3.24	3.94	2.46	-3.16
530	3.30	4.17	2.56	-3.43
540	3.36	4.41	2.66	-3.71
550	3.43	4.66	2.76	-3.99
560	3.49	4.92	2.86	-4.29
570	3.55	5.19	2.96	-4.60
580	3.61	5.47	3.07	-4.92
590	3.68	5.75	3.17	-5.25
600	3.74	6.05	3.28	-5.59

## Appendix Q: Flow Chart

